ABSTRACT

Title of Thesis:	EVALUATING ENVIRONMENTAL DRIVERS OF SOIL REDUCTION USING IRIS IN FIELD AND LABORATORY SETTINGS
	Grace Michiko Bodine, Master of Science, 2025
Thesis Directed By:	Professor Martin C. Rabenhorst Department of Environmental Science and Technology

Providing evidence of anaerobic conditions is critical to identify hydric soils for wetland research and mitigation efforts. Indicator of Reduction in Soils (IRIS) devices utilize the reduction of iron (Fe) oxides and manganese (Mn) oxides to document anaerobic conditions. Currently, only Fe IRIS devices are incorporated into the guidelines of the Hydric Soil Technical Standard (HSTS). Even though Fe IRIS have been used for the past two decades, there is a growing need to clarify and compare the effect of early growing season conditions on the performance of Fe and Mn IRIS. In this study, we set out to explore the influence of saturation, temperature, and soil organic carbon content on IRIS performance in 11 mitigation wetland sites as well as in two laboratory microcosm experiments. In addition, the suppressive effect of Mn oxide on Fe reduction was demonstrated in a third microcosm experiment. We observed that increasing the temperature, duration of saturation, and soil organic carbon content all significantly increased the amount of Fe and Mn oxides removed from IRIS films and promoted the mobilization of these metals into microcosm porewater. Furthermore, we demonstrated that the current HSTS threshold for Fe IRIS paint removal of ≥30% adequately identifies anaerobic conditions in warm (≥11 °C) conditions, but it is too conservative in cool conditions (<11 °C) and lowering the threshold to ≥15% minimizes the possibility of false negative results. In contrast, Mn IRIS paint removal is more sensitive than Fe IRIS paint removal. While no HSTS guidelines exist for Mn IRIS, we found a threshold of ≥30% Mn removal best documented anaerobic conditions in cool conditions. However, no Mn IRIS threshold was deemed informative in warm conditions due to the greater reactivity of Mn oxides. This study presents insights into the environmental drivers of soil reduction and provides a more nuanced understanding of the application and interpretation of IRIS films in seasonal conditions and restored wetlands.

EVALUATING ENVIRONMENTAL DRIVERS OF SOIL REDUCTION USING IRIS IN FIELD AND LABORATORY SETTINGS

by

Grace Michiko Bodine

Thesis submitted to the Faculty of the Graduate School of the
University of Maryland, College Park, in partial fulfillment
of the requirements for the degree of
Master of Science
2025

Advisory Committee:
Professor Martin C. Rabenhorst, Chair
Assistant Professor Jared Wilmoth
Dr. Matthew Fischel

Acknowledgements

First and foremost, I would like to thank my supervisor, Dr. Martin Rabenhorst, for your caring and patient mentorship. Witnessing your knowledge, passion, and dedication to pedology and research has inspired my own devotion to a career in soil science research. Your guidance over these three years has taught me to be a more thoughtful and well-rounded soil scientist and individual.

To my committee, Drs. Jared Wilmoth and Matt Fischel, thank you for providing your expertise and guidance throughout my program. I value the many insightful discussions I have shared with each of you during formal meetings and informal chats after class or in the lab. I would also like to thank Dr. Brian Needelman for your early involvement and feedback on my research.

To the Maryland Department of Transportation State Highway Administration, specifically Kristen Rigney and Johnathan Coplin, thank you for granting me access to and providing information on MDOT mitigation wetland sites. This research would not have been possible without this cooperation. I also must express my sincere appreciation to Bill Buettner, Gary Jellick, and Dave Smith for sharing your knowledge about Maryland wetland mitigation and providing feedback during the site selection process for my field study.

To my fellow lab mates in the UMD Pedology Lab (graduate and undergraduate), Jocelyn Wardrup, Patrick Burke, Jordan Kim, David Hutch, Alex Quigley, Kelsey Genovese, and Violet O'Neill, thank you for your support and friendship in the field, lab, classroom, and daily life. I would like to extend a special thank you to David for making a whole spring semester of weekend field work more enjoyable and helping set up my laboratory experiment for success.

To the Department of Environmental Science and Technology as a whole, thank you for providing a welcoming and interdisciplinary space to learn and grow as a student and researcher.

To my friends, peers, and mentors (both near and far), I am so grateful to have surrounded myself with such an extensive and supportive village. My warmest thanks go to Daniel Sanchez and Isabelle Van Benschoten for your never-ending kindness, humor, and friendship since we first met three years ago. I am also very thankful to the many other graduate and undergraduate students who have enriched my master's experience, especially those in the same courses, the members of GATES, and the members of the UMD Soil Judging Team.

To my family, I am here today because of your unconditional love and unwavering support. Thank you for always believing in me and helping me pursue my most ambitious desires, even when they take me far from home.

This work was made possible through the Ray Weil E-Nnovate Professorship Endowment.

Table of Contents

List of Tables

List of Figures

Introduction

The anaerobic state of wetland and other inundated soils chemically sets these soils apart from better-drained upland soils. Electron transfers during oxidation-reduction (redox) reactions in anaerobic soil conditions influence the formation and identification of hydric soils as well as the cycling, availability, and transport of nutrients, contaminants, and many other compounds (Essington, 2015; Reddy et al., 2022).

In prolonged saturation, aerobic microbial respiration quickly depletes oxygen levels in the soil as the diffusion of atmospheric O_2 into water is extremely slow. In turn, this promotes the activity of anaerobic microorganisms and the decrease in redox (Eh) potential (McBride, 1994). In the process of oxidizing organic matter during anaerobic respiration, inorganic compounds are utilized as alternative terminal electron acceptors due to the lack of O_2. Listed here in order of decreasing Eh and energetic favorability, the alternative electron acceptors include NO_3^-, Mn oxides, Fe oxides, SO_4^{2-}, and CO_2 (Ponnamperuma, 1972). While some of these compounds can be reduced abiotically, insoluble Mn and Fe oxides are primarily reduced to soluble Mn^{2+} and Fe^{2+} by metal-reducing bacteria (e.g., *Geobacter* or *Shewanella*) (Ehrlich et al., 2016; Lovley, 1991; Lovley et al., 2004). Mn oxides generally reduce before Fe oxides at higher redox potentials, and therefore Mn reduction has been considered representative of "weakly" reducing conditions, while Fe reduction represents "moderately" reducing conditions (Dorau et al., 2016).

The redox dynamics of Fe oxides, and to a lesser extent Mn oxides, are used to help document the presence of anaerobic conditions and hydric soils. These common soil minerals are strong pigmenting agents in the soil, but when reduced, they turn into colorless soluble ions in solution. This can result in colorful Fe and Mn redoximorphic features (i.e., concentrations and depletions) or the development of gray horizons characteristic of wetland soils (Schwertmann, 1993). As these features provide insight into the long-term hydrology and drainage conditions of a given soil, Fe and Mn redoximorphic features, as well as other morphological features, are incorporated into the Field Indicators of Hydric Soils (USDA-NRCS, 2024). These field indicators are designed to identify soils formed under long-term conditions of saturation and anaerobic conditions and are not always reliable in systems that have highly altered soils or have experienced anthropogenic drainage, like those commonly found in restored wetlands.

As morphology cannot be used in all cases, the Hydric Soil Technical Standard (HSTS), created by the National Technical Committee for Hydric Soils, outlines other field methods and criteria to document anaerobic conditions (Berkowitz et al., 2021). One approved method includes Indicator of Reduction in Soils (IRIS) devices, which were first developed by Jenkinson (2002) as a tool to visually capture Fe reduction (Jenkinson & Franzmeier, 2006; Sapkota et al., 2022). IRIS consists of a white plastic substrate coated with either orange Fe oxide paint or dark brown Mn oxide paint, which is “removed” via reductive dissolution. Currently, the HSTS only has guidelines for Fe IRIS, as some feel that further testing is needed to verify that Mn IRIS oxide paint can provide certain evidence of anaerobic conditions and does not remove too easily.

The rate and degree of soil reduction, especially in terms of Mn and Fe reduction, are known to be controlled by various environmental and soil factors, including the duration of saturation, temperature, organic carbon, pH, and the availability of terminal electron acceptors (Ponnamperuma, 1972). Mn IRIS were first used by Stiles et al. (2010) to help identify anaerobic conditions and hydric soils in alkaline Alaskan soils that did not favor Fe reduction. More recently, Rabenhorst et al. (2021) found that Mn IRIS removal was more informative and indicative of anaerobic conditions than Fe IRIS removal under cooler soil temperatures (5–11°C) in natural wetlands. They suggested that Mn IRIS may better capture reducing soil conditions in the early growing season. This may be especially useful in Maryland as there are many seasonally saturated wetlands or recently mitigated wetlands which are wettest in the early growing season (Rabenhorst et al., 2021).

Objectives

The overall objective of this research is to better understand how key environmental drivers of soil reduction impact the performance and interpretation of Fe and Mn IRIS films through field and laboratory investigations.

The specific objectives of this research are to:

1. Evaluate and compare the performance of Fe and Mn IRIS films in restored, seasonal nontidal wetland systems from early to mid-growing season in Maryland,
2. Quantify and compare Fe and Mn mobilization in soils to drivers of soil reduction, namely duration of saturation, soil temperature, soil organic carbon content, and Mn oxide concentration,
3. Assess current and alternative IRIS removal thresholds for Fe and Mn IRIS films, and
4. Compare the mobilization of reduced Mn and Fe into soil porewater with the removal of Mn and Fe oxide IRIS paint.

Chapter 1: Background

1.1 WETLANDS

Wetlands are estimated to cover only 5–8% of the global land (Mitsch & Gosselink, 2015), but they play a key role in many local and global environmental processes. Wetlands provide a wide array of ecosystem functions and services, including terrestrial and aquatic habitat, water quality management, flooding and erosion control, and climate change mitigation (Mitsch & Gosselink, 2015). Ambitious attempts to quantify the monetary value of wetlands have estimated that global wetlands are valued at upward of $47.4 trillion per year at 2011 values (Davidson et al., 2019). While wetlands can be defined and classified in multiple ways, wetlands are all fundamentally characterized by the presence of hydrophytic vegetation, hydric soils, and wetland hydrology, indicating periodic or permanent saturation or inundation (National Research Council, 1995).

Humanity has a long history of draining and degrading wetlands for cultivation and urbanization around the world. In the United States, 22 states (including Maryland) have lost at least 50% of their original wetlands from the 1780s to the mid-1980s, and another six states have lost more than 85% (Dahl & Allord, 1996). Recently, Fluet-Chouinard et al. (2023) found that the United States, Europe, and Asia are regional hotspots of wetland loss with more than 50% of wetlands lost between the 1700s and 2020.

1.1.1 Rise of wetland policy in the USA

For much of the country's history, wetland policy in the US was largely characterized by the promotion of draining and converting wetlands to other land uses. The Swampland Acts of 1849, 1850, and 1860 saw more than 26 million ha (64 million acres) of wetlands converted across 15 states (Heimlich et al., 1998; Mitsch & Gosselink, 2015). Many agricultural subsidies and other federal programs provided direct and indirect incentives to convert wetlands to support agricultural activities, flood control, hydroelectric power, highway construction, forestry, and grazing (Heimlich et al., 1998).

The rise in environmental activism and awareness in the 1960s and 70s followed the increase in visible pollution as well as the influential events of Rachel Carson's publication of *Silent Spring* in 1962 and the 1969 Cuyahoga River fire in Cleveland, Ohio. This awareness resulted in the establishment of the Environmental Protection Agency, along with new programs and policies, including the Federal Water Pollution Control Act Amendments in 1972 (US EPA, 2013). Now known as the Clean Water Act (CWA) after the 1977 amendments, this law aimed to restore and maintain US water bodies by controlling water pollution and associated activities. Under Section 404 of the CWA, the US Army Corps of Engineers has the power to permit "the discharge of dredged or fill material into the navigable waters," including wetlands (National Research Council, 1995). Additionally, the Food Security Act (1985, i.e., "Farm Bill") includes the "swampbuster" provision, which focused on protecting wetlands on agricultural land. Under this provision, a producer would be ineligible to receive USDA benefits if they drained and farmed any wetlands after December 23, 1985 (Vepraskas, 2016). However, it should be noted that presently, there are no federal laws dedicated solely to wetlands; the regulation of wetlands is managed by multiple groups and is tied to water quality and land use policies (Mitsch & Gosselink, 2015).

The CWA, Farm Bill, and subsequent state-level legislation all recognized a need to develop and revise the definition and identification of hydric soils to delineate wetlands. The National Technical Committee for Hydric Soils (NTCHS) was established by the USDA in 1981 to formalize the hydric soil definition and the strategies to document them in the field. This group originally consisted of USDA soil scientists and a biologist, a US Fish and Wildlife biologist, and university wetland soil scientists (Vepraskas, 2016). Since identifying hydric soils is required to enforce the CWA, representatives from the US Army Corps of Engineers joined the NTCHS, as well as representatives from other federal agencies (US Bureau of Land Management, US Environmental Protection Agency, and US Forest Service) (Berkowitz et al., 2021; Vepraskas, 2016).

1.1.2 Wetland mitigation

Since the late 1980s, US wetland conservation efforts have operated on the premises of the "no net loss" policy (National Research Council, 1995). The goal of maintaining, and in the long-term increasing, the quality and quantity of the wetlands of the US require wetland creation and restoration activities alongside conservation. Thus, the "no net loss" policy spurred the development of the wetland mitigation industry. This policy is highlighted in federal and several state-level legislations, which require compensation for wetland loss due to permitted development by creating, restoring, or enhancing replacement wetlands (Mitsch & Gosselink, 2015). This practice is often called *wetland (compensatory) mitigation*, and the resulting wetland is often called either a *mitigation* or *replacement wetland*. Mitsch & Gosselink (2015) identifies other common terms used to describe the types of mitigation wetlands, including *restored*, *enhanced*, or *created wetlands.* Former wetlands, which have been disturbed/degraded by human activity, that are then returned to pre-existing, natural conditions are referred to as *restored wetlands*. When people work to increase one or more functions of an existing wetland, this is usually considered *wetland enhancement.* Engineering areas of land not originally considered a wetland (upland or even shallow water areas) into one is usually called a *created wetland*.

Constructed or *treatment wetlands* generally refer to a type of created wetland designed to improve water quality by removing contaminants/pollutants from wastewater or runoff.

The overall goal for these mitigation projects is to gain back the area, function, and ecology of the lost wetland by mimicking natural wetland systems. In Maryland, there are specified acreage replacement ratios depending on the type of wetland lost to determine the area of the mitigation required. For example, the Maryland Department of Environment requires for every one acre of forested, non-tidal wetland impacted, two acres must be mitigated (2:1) (Walbeck et al., 2011). However, recovering the acreage of the original wetland lost is only beneficial if the replacement wetland is successfully established and functions similarly to a natural wetland. Thus, mitigation sites are monitored and evaluated using performance standards, which list legal and ecological criteria used to assess the overall success of a wetland mitigation project. These standards are based on the presence of the three defining parameters of a wetland: wetland hydrology, hydrophytic vegetation, and hydric soils. For non-tidal wetland mitigation sites in Maryland, ecological standards include, but are not limited to, assessing the vegetation community (the type, cover, density, and richness), the hydrology (depth, degree, duration, and periodicity), and soils (anaerobic conditions, bulk density, topsoil replacement, and microtopography) (USACE & MDE, 2023).

1.2 HYDRIC SOILS

Finding the presence of hydric soils is key in delineating natural wetlands as well as demonstrating the success of a created or restored wetland. The current definition used by the NTCHS states a hydric soil is “a soil that formed under conditions of saturation, flooding, or ponding long enough during the growing season to develop anaerobic conditions in the upper part” (Federal Register, 1994). This reflects the saturated conditions characteristic of wetlands.

Additionally, this definition differentiates between the conditions when the soil developed and the current conditions. Alteration to contemporary hydrologic conditions, such as drainage, of a hydric soil does not change its status as a hydric soil if it was formed as one.

The development of anaerobic conditions occurs when a soil is saturated for enough time that oxygen is diminished due to microbial respiration outpacing the slow diffusion of oxygen in water (McBride, 1994). This causes the oxidation-reduction (redox) potential (Eh) and aerobic microorganism population to decrease, resulting in anaerobic microorganisms utilizing terminal electron acceptors other than O_2 (Ponnamperuma, 1972). These alternative terminal electron acceptors are common redox-active elements or compounds in soils and include nitrogen (NO_3^-), manganese (Mn[III/IV] oxides), iron (Fe[III] oxides), sulfur (SO_4^{2-}), and carbon (CO_2). The compounds are listed in the order of the “redox ladder” model (Figure 1), which represents the

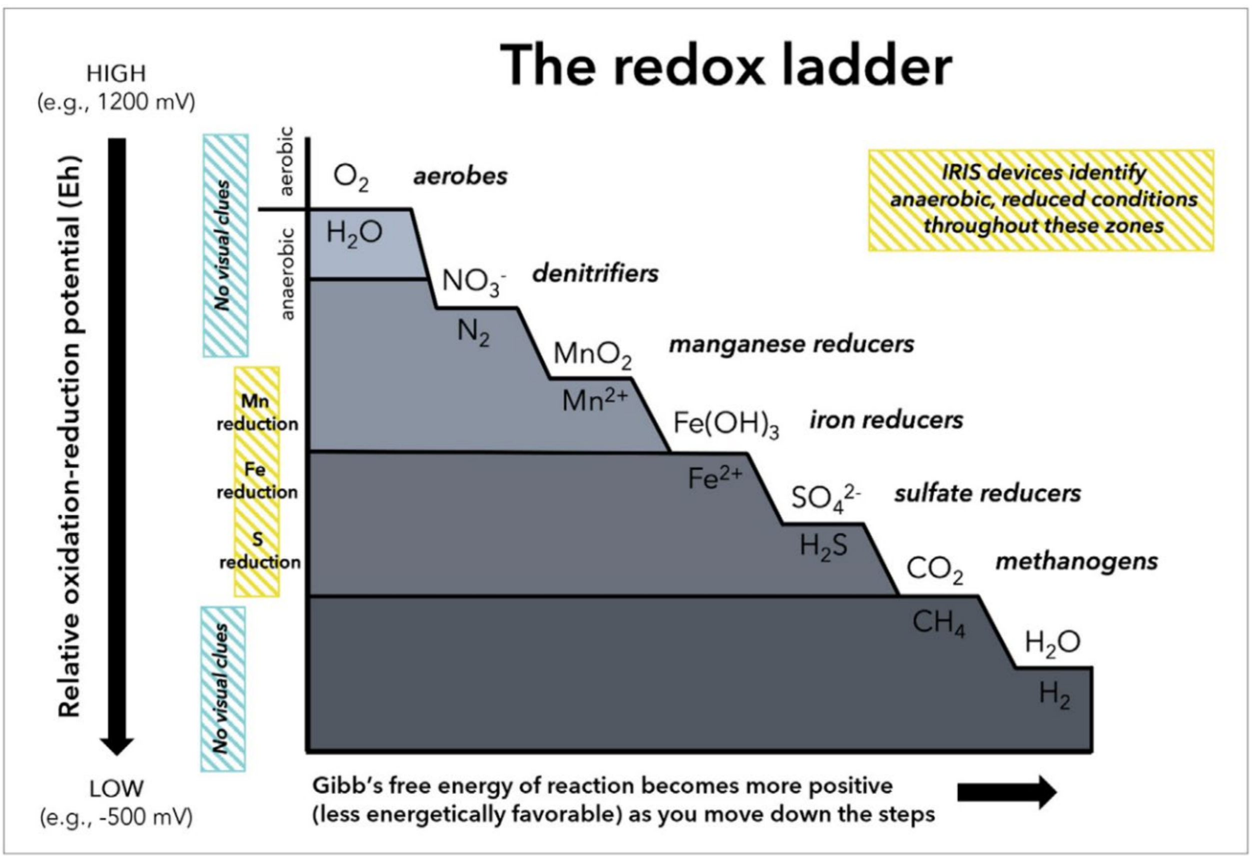

Figure 1-1. Illustration of the redox ladder as seen in Sapkota et al. (2022).

progressive reduction of these compounds as Eh declines and Gibb's free energy of reaction increases (McBride, 1994; Sapkota et al., 2022).

As stated in the hydric soil definition, the development of anaerobic conditions must occur during the growing season. According to the NTCHS, the "growing season" for hydric soils is determined by sufficient microbial activity to induce anaerobic conditions in the soils rather than vegetative productivity or a specific temperature (Berkowitz et al., 2021). Traditionally, 5 °C is considered the temperature threshold at which microbial activity is negligible, referred to as "biological zero" (Rabenhorst, 2005). However, it is recognized that this is a somewhat simplistic benchmark as it was established in the context of agricultural productivity (Rabenhorst, 2005). Field studies in southern or coastal areas of the US found that the "microbially active season" persisted the entire calendar year, as soil temperatures rarely drop below 5 °C (Burdt et al., 2005; Megonigal et al., 1996; Seybold et al., 2002). Furthermore, there are multiple studies which provide evidence of microbial activity and anaerobic conditions present below 5 °C, especially in permafrost soils and wetlands (National Research Council, 1995). Wetland scientists and practitioners operate under the assumption that the microbial activity occurs year-round and do not take the "growing season" into account when evaluating hydric soils (Rabenhorst, 2005).

1.2.1 Hydric Soil Technical Standard

To identify hydric soils, the presence of anaerobic conditions and saturation must be documented according to guidelines approved by the NTCHS. If a soil meets the requirements provided by the NTCHS, then the soil has met the definition of a hydric soil and is treated as such. One set of guidelines used, "Field Indicators of Hydric Soils in the United States," is based on the morphology of the soil, such as color, texture, and other physical features. These field indicators are designed to be "proof positive," so if a soil meets a field indicator, then it is confirmed to be a hydric soil. However, if no field indicator is present in the soil, that does not necessarily mean the soil is not a hydric soil. The absence of a field indicator can occur in a variety of problematic soil situations, including soils derived from red parent materials (Rabenhorst et al., 2020) or those with high pH (>8.0) which inhibit the formation of redoximorphic features (i.e. concentrations and depletions) (King et al., 2019). More notably, field indicators are not dependable at sites that have been highly disturbed by human activity, such as in restored or created wetlands. Soils at these sites may experience a high degree of compaction, mixing, removal, and additions of transported materials. Additionally, wetland restorations are ideally located on a former wetland that has been drained. Thus, these drained soils often retain morphological features indicative of hydric soils even though they are not functioning as such. While these soils are hydric, the presence of retained or "relict" features can cause uncertainty when evaluating the functional performance of a wetland mitigation project. When these challenges and problematic situations arise, we must use the Hydric Soil Technical Standard (HSTS), the other set of NTCHS guidelines, to see if additional evidence of saturation and anaerobic conditions is present.

Unlike the field indicators, the HSTS evaluates the biogeochemistry of a soil to address if the soil conditions are currently functioning as a hydric soil rather than if it was formed under such conditions (Berkowitz et al., 2021). The HSTS is used to identify hydric soils in the absence of a field indicator and when testing or developing new field indicators. The HSTS has three main requirements: (a) saturation in the upper 25 cm of soil profile for a minimum of 14 consecutive days (slightly different criteria for Vertisols in Louisiana and Texas); (b) anaerobic conditions; and (c) the previous criteria must occur during a period when the precipitation is normal or drier than normal and the soil is microbially active (Berkowitz et al., 2021).

These three requirements are based on the definition that a hydric soil is "formed under conditions of saturation, flooding, or ponding long enough during the growing season to develop anaerobic conditions in the upper part" (Federal Register, 1994). Saturation in the soil is measured using piezometers or water table wells. Analyzing the normality of precipitation during the measurement period is key to preventing a soil from being misidentified as hydric or nonhydric due to wetter or drier than normal conditions. The recommended methods outlined in the HSTS include the Direct Antecedent Rainfall Evaluation Method (DAREM), the Moving Total Antecedent Rainfall Method, and the Adjusted Moving Total Antecedent Rainfall Method (Berkowitz et al., 2021). Lastly, there are three approved methods to document anaerobic conditions in the soil: (a) Indicator of Reduction in Soils (IRIS) devices; (b) α,α'-dipyridyl dye; and (c) platinum-tipped electrodes to measure redox potential (Eh). In this chapter, the IRIS device method will be described in depth. More details on the other methods can be found in Berkowitz et al. (2021).

1.2.2 Indicator of Reduction in Soils (IRIS) devices

IRIS devices are used to visually document the reduction of Fe or Mn oxides in a soil as a proxy measurement of anaerobic soil conditions. This relatively new technique was first developed in 2002 and has become increasingly utilized in wetland and hydric soils research (Jenkinson, 2002; Jenkinson & Franzmeier, 2006). Sapkota et al. (2022) recently reviewed the history of this technology and described the application and interpretation of IRIS devices. Briefly, an IRIS device is composed of either synthetic Fe or Mn oxide mineral paint applied to a plastic substrate, often polyvinyl chloride (PVC), which is deployed directly into the soil. If the soil is anaerobic, anaerobic microorganisms will reduce the Fe or Mn oxides in the paint as they utilize them as electron acceptors, and the reduced species will solubilize into the soil solution. This results in the removal of the paint from the plastic substrate, which exposes the white color of the substrate and creates a pattern of depleted areas (either lighter in color or white).

Currently, only Fe IRIS devices are approved in the HSTS. To verify anaerobic conditions according to the HSTS, a majority (at least three of five) of the IRIS devices deployed must have ≥30% of the Fe paint removed within a contiguous 15 cm zone that is entirely within the upper 30 cm of the soil. The percentage of paint removed from the device is determined through visual estimation, counting using a grid technique, or (preferably) by scanning the device to accurately measure the stripped area. Image analysis is further discussed in Chapter 2. While there is no official standard specified in the HSTS for the duration of IRIS deployment (Berkowitz et al., 2021), Rabenhorst (2008, 2018) recommends that the devices be deployed for one month (28 days) when evaluating Fe and Mn reduction. Shorter deployment periods (minutes or hours) can be used to investigate other processes, like sulfate reduction, as iron monosulfides rapidly form on the Fe coating when soluble sulfides are present in solution (Duball et al., 2020; Rabenhorst et al., 2010, 2025; Vaughan et al., 2016).

The initial IRIS devices used an Fe oxide paint (ferrihydrite-goethite suspension) (Rabenhorst & Burch, 2006) and PVC tubing (Jenkinson & Franzmeier, 2006), but improvements over the years have introduced the use of PVC films (Rabenhorst, 2018) and Mn oxide paint (birnessite, $[Na,Ca,K]_{0.5}Mn_2O_4.1.5H_2O$) (Rabenhorst & Persing, 2017). Replacing the IRIS tubes with a thin, flexible PVC film alleviates multiple challenges associated with rigid PVC tubes, including (but not limited to) issues with capturing a 2D image from a 3D cylindrical tube and abrasion of oxide paint during installation and transportation (Rabenhorst, 2018; Sapkota et al., 2022).

The development of Mn oxide paint was a critical advancement for this technique as it expands the potential applications of IRIS devices (Sapkota et al., 2022; Stiles et al., 2010). Mn oxides have long been recognized to reduce before Fe oxides due to the thermodynamics of the reactions (McBride, 1994; Ponnamperuma, 1972). Mn oxide removal has been shown to be 2 to 5 times greater than Fe oxide removal (Dorau et al., 2016). Mn oxides reduce to Mn^{2+} at higher redox potentials, similar to the Eh ranges of other significant biogeochemical processes such as oxygen depletion and denitrification. A potential, but understudied, application of Mn IRIS includes using Mn IRIS as a proxy measurement of denitrification and element mobilization that occur at redox potentials that overlap with Mn reduction (Romero et al., 2021; Sapkota et al., 2022).

1.3 IRON AND MANGANESE IN SOIL

Fe and Mn oxides, hydroxides, and oxyhydroxides (referred to as "oxides" for the remainder of the chapter) are ubiquitous soil minerals. Fe is a much more abundant (2–550 g kg^{-1} of soil) element in the soil than Mn (0.02–10 g kg^{-1}) (Essington, 2015), but Mn oxides usually occur in association with Fe oxides (Sparks et al., 2022). In soils, Fe is found in two oxidation states (+2 and +3) while Mn is found in three (+2, +3, and +4). In aerobic soils, Fe and Mn oxides largely exist in the Fe^{3+} and Mn^{4+} states, but these oxides can be chemically complex as the substitution of forms between oxidation states and between these two elements can occur (Sparks et al., 2022). As there are smaller concentrations of pedogenic Mn oxides in soils than Fe oxides, and Mn oxides are generally fine-grained and poorly crystalline, they are notoriously difficult to identify and study (Dixon & White, 2002; Post, 1999).

Fe and Mn oxides can exist as discrete crystals within the soil and are recognized as strong pigmenting agents. Fe oxides typically contribute yellow, orange, red, and brown colors, and Mn oxides, especially when concentrated, contribute dark brown or black colors to soils (Schwertmann, 1993). Both Fe and Mn oxides commonly occur in soil as redoximorphic concentrations, including masses, coatings, concretions, or nodules. Under anaerobic conditions, insoluble Fe and Mn oxides may become reduced and solubilized as colorless Fe^{2+} and Mn^{2+} ions. With enough time, the reductive dissolution of Fe and Mn oxides can sufficiently remove coatings of Mn and Fe oxides, resulting in the formation of gray depletions or horizons as the underlying silicate minerals are exposed. The influence of these oxides, especially Fe, on the distribution and changes in soil color has long been used to determine soil drainage and landscape hydrology (Bigham et al., 2002). Therefore, these features have been incorporated into the hydric soils field indicators, and the visible color change caused by reduction is the basis of the IRIS method (see previous "Hydric Soil Technical Standard" and "Indicator of Reduction in Soils (IRIS) Devices" sections).

1.4 ENVIRONMENTAL DRIVERS OF SOIL REDUCTION

An oxygen-deficient environment with oxidizable organic carbon and anaerobic microorganisms is the prerequisite for soil reduction. The intensity and rate of soil reduction are controlled by the depth and duration of soil saturation, temperature, the nature and quantity of organic carbon, pH, and the nature and quantity of redox-sensitive chemical species (Ponnamperuma, 1972).

1.4.1 Saturation

It is well understood that saturation dramatically lowers O_2 diffusion into the soil. Soils can become anoxic within hours to days of saturation (Ponnamperuma, 1972), but the period of saturation required for specific alternate terminal electron acceptors to become reduced depends greatly on the physiochemical conditions of the soil, especially soil temperature and organic matter content (Vepraskas & Vaughan, 2016). In soil core experiments, Cogger & Kennedy (1992) show that Fe reduction and the development of redoximorphic depletions occurred faster in soils with higher organic carbon content and at warmer temperatures. Vaughan et al. (2009) similarly found that the lag time to induce Fe reducing conditions (with respect to ferrihydrite) decreased with increased temperature (20 days at 3 °C and 2 days at >9 °C).

1.4.2 Organic carbon

Organic matter, as the primary energy source for microbial respiration and thus the electron source in biogeochemical redox reactions, is critical to establishing soil reducing conditions (Lovley, 1991; Lovley et al., 2004). The rate of Fe and Mn reduction has been shown to typically increase when there is more organic carbon present (Cogger & Kennedy, 1992; Glinski et al., 1996; Magen et al., 2011; Ponnamperuma, 1972; Reddy et al., 2022; Roden & Wetzel, 2002). Soil organic carbon encompasses a complex and heterogeneous group of compounds derived from organic (mostly plant) residues. Organic carbon is preferentially decomposed and metabolized by microorganisms based on the length of carbon chains, composition, and other physicochemical properties (Marschner & Kalbitz, 2003; Straathof et al., 2014; Xu et al., 2019). Thus, the nature and properties of the organic carbon that in turn affect the reactivity and biodegradability of the carbon in a soil may impact the rate of Fe and Mn reduction.

1.4.3 Temperature

As previously mentioned, the reduction of Fe and Mn oxides are primarily mediated by microorganisms. It has long been understood that microbial activity is temperature dependent and thus will impact microbially mediated biogeochemical processes (Davidson & Janssens, 2006; Van't Hoff, 1898). Cold temperatures have been found to decrease the reduction of Fe and Mn oxides in both laboratory and field studies. Vaughan et al. (2009) showed that the duration of saturation required to reduce ferrihydrite increased as soil temperature decreased due to lower rates of microbial activity. Using a soil column experiment and coated redox bars, Dorau et al. (2018) highlighted the importance of temperature and organic carbon on the reduction and removal of Mn oxides. When evaluating the performance of Mn IRIS in natural wetlands across eight US states, Rabenhorst et al. (2021) found that Mn IRIS is more sensitive and informative in cooler soil conditions (5–11°C) compared to Fe IRIS due to the significant inhibition of Fe reduction and coating removal at lower soil temperatures. When examining the effect of temperature on Fe and/or Mn reduction in soil microcosm experiments, porewater concentrations of aqueous Fe and Mn were typically significantly diminished in colder conditions (Hofacker et al., 2013; Ponnamperuma, 1984, as cited in Reddy et al., 2022; Sparrow & Uren, 2014; Weber et al., 2010).

1.4.4 Presence of alternate electron acceptors

Facultative and obligate anaerobic heterotrophic microorganisms can often utilize multiple terminal electron acceptors. Microorganisms that utilize nitrate and manganese may have a competitive advantage over those that utilize ferric iron and sulfate, as they are more energetically favorable (Hansel, 2017). Large quantities of more easily reducible compounds have been shown to inhibit the decrease in Eh and the production of subsequent reduction products (Hansel, 2017; Kappler et al., 2021; McBride, 1994; Ponnamperuma, 1972). In addition to quantity, the form (mineralogy, crystallinity, and stability) of Mn and Fe oxides likely contributes to the rate of reduction (Hansel, 2017; Kappler et al., 2021; Li et al., 2021; Mack et al., 2019).

Even though Fe is much more abundant than Mn in the soil, elevated amounts of Mn oxides have been shown to impede the reduction of Fe oxides (Ponnamperuma, 1972). Additions of Mn oxides were used as a potential remedy for physiologic disorders in rice caused by lower Eh and ferrous iron (Ponnamperuma et al., 1965; Yuan & Ponnamperuma, 1966). The inhibitory effect of Mn oxides on Fe reduction has also been studied to moderate the release of heavy metals and contaminants such as arsenic (As), which are generally sorbed by Fe oxides (Ehlert et al., 2014, 2016). Lovley and Phillips (1988) found the addition of Mn oxides to microcosms of freshwater sediments removed all porewater Fe^{2+}, inhibited net Fe reduction, and prompted Mn reduction. But they found that the preferential reduction of Mn to Fe by bacteria does not fully account for the lack of reduced Fe, and cited the Mn(IV) oxidation of Fe^{2+} as an important abiotic mechanism (Lovley & Phillips, 1988).

As previously discussed, the amount of Mn oxides in most soils is naturally low. According to Rabenhorst & Wardrup (2024), over 80% of surface soil samples have less than 0.10% Mn, with the mean and median content being 0.066% and 0.041%, respectively. Thus, the potential competition between Mn and Fe as a terminal electron acceptor is not a common concern when using IRIS devices to determine the presence of anaerobic conditions in the field. However, no studies have yet to look at the effect of higher soil concentrations of Mn oxides on the removal of Fe or Mn IRIS paint.

Chapter 2: Performance of IRIS Films for Evaluating Wetland Restoration during the Early-Growing Season

2.1 INTRODUCTION

Wetlands are a key ecosystem broadly defined by the presence of wetness, hydrophytic vegetation, and hydric soils (National Research Council, 1995). All over the world, humans have a long history of destroying and converting wetlands to other land uses. The United States has lost over 50% of its wetlands and accounts for an estimated 15.6% of global wetland losses (Fluet-Chouinard et al., 2023). With increased public awareness and scientific understanding of the value of wetlands, US regulations and policies in the 1970s and '80s began to support the conservation, creation, and restoration of wetlands (Mitsch & Gosselink, 2015). To ensure the ecological success of such efforts, wetland scientists and practitioners must measure various indicators related to the three-parameter definition of a wetland, including hydric soils.

Hydric soils are "formed under conditions of saturation, flooding, or ponding long enough during the growing season to develop anaerobic conditions in the upper part" (Federal Register, 1994). Generally, hydric soils can be identified with soil morphological investigations and the application of the Field Indicators of Hydric Soils (USDA-NRCS, 2024). However, these indicators are unreliable in highly altered soils such as those in recently restored and created wetlands. The presence of a field indicator can represent current or former conditions of saturation and reduction (USDA-NRCS, 2024). Wetland mitigation projects (which either enhance, restore, create, or preserve wetlands) often occur where hydric soils have been formerly drained, so the soil may still retain features that indicate anaerobic conditions of the past. In this case, it is difficult to assess whether the morphology is indicative of current or past conditions.

When morphology cannot be used, the reduction-oxidation (redox) biogeochemistry of wetland soils is utilized. The National Technical Committee for Hydric Soils (NTCHS) created the Hydric Soil Technical Standard (HSTS) to provide the criteria and guidance to document the required evidence of saturation and anaerobic conditions to identify hydric soils (Berkowitz et al., 2021). Saturation is routinely determined by finding the shallow groundwater (water table) using wells or piezometers. Determining anaerobic conditions in soils requires more specialized methods. The HSTS approved methods include α,α′-dipyridyl indicator dye (Berkowitz et al., 2017), Pt-tipped electrodes to measure redox potential (Eh) (Rabenhorst et al., 2009), and Indicator of Reduction in Soils (IRIS) devices (Berkowitz et al., 2021; Sapkota et al., 2022).

Anaerobic (reducing) conditions develop when there is saturation for an extended period, so that dissolved oxygen (O_2) is depleted from the soil due to microbial respiration far outpacing the slow diffusion of oxygen in water (McBride, 1994). This saturation causes a gradient of redox potential to form as soil microbial respiration shifts from aerobic to anaerobic, or, in other words, shifts from using O_2 as a terminal electron acceptor to alternative ones. These redox active compounds, listed in the idealized order of reduction based on declining redox potentials and increasing Gibb's free energy of reaction, include nitrogen (NO_3^-), manganese (Mn[III, IV] oxides), iron (Fe[III] oxides), sulfur (SO_4^{2-}), and carbon (CO_2) (Ponnamperuma, 1972). While some of these reactions can occur abiotically, facultative and obligate anaerobic microorganisms can be thought of as the primary "actors" behind soil reduction with prolonged saturation as the "setting" and oxidizable organic carbon as the "fuel." The intensity and rate of reduction in soil is influenced by many factors, but this study focuses on three key environmental drivers: the duration of saturation, soil temperature, and the quantity of soil organic carbon (SOC).

According to thermodynamics, Mn reduction occurs more easily at higher redox potentials under weakly to moderately reducing conditions, and thus typically sooner than Fe. Reduction of Fe occurs at much lower redox potentials and is indicative of stronger reducing conditions, which commonly take longer to develop. The HSTS approved methods for documenting anaerobic conditions are based on Fe reduction to ensure confidence that oxygen is essentially absent from the soil, including IRIS (Berkowitz et al., 2021).

IRIS devices usually consist of a plastic substrate (such as PVC tube or film) and either iron (Fe) or manganese (Mn) oxide "paint" which coats the substrate. When deployed in the soil (typically for 4 weeks) where reduction of Fe or Mn occurs, the oxide paint is solubilized and "removed," revealing the original white PVC substrate. The original Fe-coated IRIS tubes were first developed over 20 years ago by Jenkinson (2002), and the use of IRIS technology, especially amongst wetland researchers and practitioners, has steadily increased since then (Sapkota et al., 2022). When used according to the HSTS, at least 3 of 5 IRIS devices must have ≥30% Fe oxide paint removed from a contiguous 15 cm zone within the upper 30 cm of soil (Berkowitz et al., 2021). Sapkota et al. (2022) recently reviewed the history and application of IRIS devices.

The more recent advancement of using Mn oxide paint (Stiles et al., 2010; Coffin, 2012) has been a topic of interest for IRIS researchers. A growing body of research has focused on the construction (Dorau & Mansfeldt, 2015; Rabenhorst & Persing, 2017; Rabenhorst, 2018) and interpretive applications of Mn IRIS (Dorau et al., 2016, 2018; Rabenhorst et al., 2021; Evans et al., 2021; Hino et al., 2023; Limmer et al., 2023; Loffredo et al., 2023a; Dorau et al., 2024). Currently, the HSTS only approves using the original Fe-coated IRIS devices (referred to as Fe IRIS for the remainder of the writing) to recognize reducing conditions in hydric soils. Since Mn reduction can occur under more weakly reducing soil conditions than Fe (McBride, 1994), there may be concern by some that Mn-coated IRIS (Mn IRIS) paint removal may occur too rapidly or too easily to use as evidence of anaerobic conditions when identifying or delineating hydric soils.

On the other hand, challenges have been recognized when utilizing Fe IRIS and other Fe-reduction-based methods. Some saturated soil conditions do not favor Fe reduction (i.e., Fe IRIS paint removal), including soils with high pH or cold soil temperatures (Stiles et al., 2010). Additionally, in formal discussions amongst IRIS researchers and practitioners, concerns have been expressed regarding how difficult it can be to meet the 30% Fe IRIS threshold in natural and mitigated wetlands that experience seasonal hydrology and are wettest in the early growing season. When investigating the performance of Mn IRIS films in natural wetlands, Rabenhorst et al. (2021) found that Mn IRIS might better capture saturation and anaerobic conditions in the early growing season. Mn IRIS was found to be more sensitive and informative in cooler soil temperatures (5–11 °C), while Fe IRIS was better utilized in warmer soil temperatures (≥11 °C). The influence of soil temperature on controlling the rate of reduction and IRIS paint removal is also well documented in other studies (Cogger & Kennedy, 1992; Dorau et al., 2018; Rabenhorst & Castenson, 2005; Vaughan et al., 2009).

This study seeks to 1) evaluate the performance of IRIS films in seasonally saturated mitigation wetland systems in Maryland, US during early to mid-growing season conditions; 2) compare Fe and Mn IRIS paint removal as related to duration of saturation, soil temperature, and SOC content; 3) test current and alternative IRIS oxide coating removal thresholds for both Fe and Mn IRIS; and 4) explore the impact of HSTS hydrology requirement on IRIS interpretations. We believe the application of both Fe and Mn IRIS films in mitigation wetlands will yield similar results as those found in natural wetlands, and that there may be a need to incorporate soil temperature into the guidance for interpreting IRIS paint removal data.

2.2 MATERIALS AND METHODS

2.2.1 Study location and site selection

This field study was conducted at 11 wetland mitigation sites in Maryland, USA. The 11 sites span two Mid-Atlantic physiographic provinces: Piedmont Plateau and Atlantic Coastal Plain, which was further split into Inner Coastal Plain and Outer Coastal Plain (Figure 2-1). Ten sites are compensatory mitigation sites for the Maryland Department of Transportation State Highway Administration (Appendix A). One site is a private compensatory restoration project for local commercial development. Site selection was based on the criteria that the site 1) has an area of two or more acres, 2) has hydric soils mapped in the immediate vicinity, 3) was not designed as a water retention pond, and 4) construction was completed between 5 and 30 years prior to this study. At each of the 11 sites, a single plot (approximately 9 m^2) was set up in a marginally wet area of the site (i.e., not in areas of ponded water). Plot location at each site was determined based on personal communication with soil consultants, who engaged in the original restoration projects, and field investigations in December 2022.

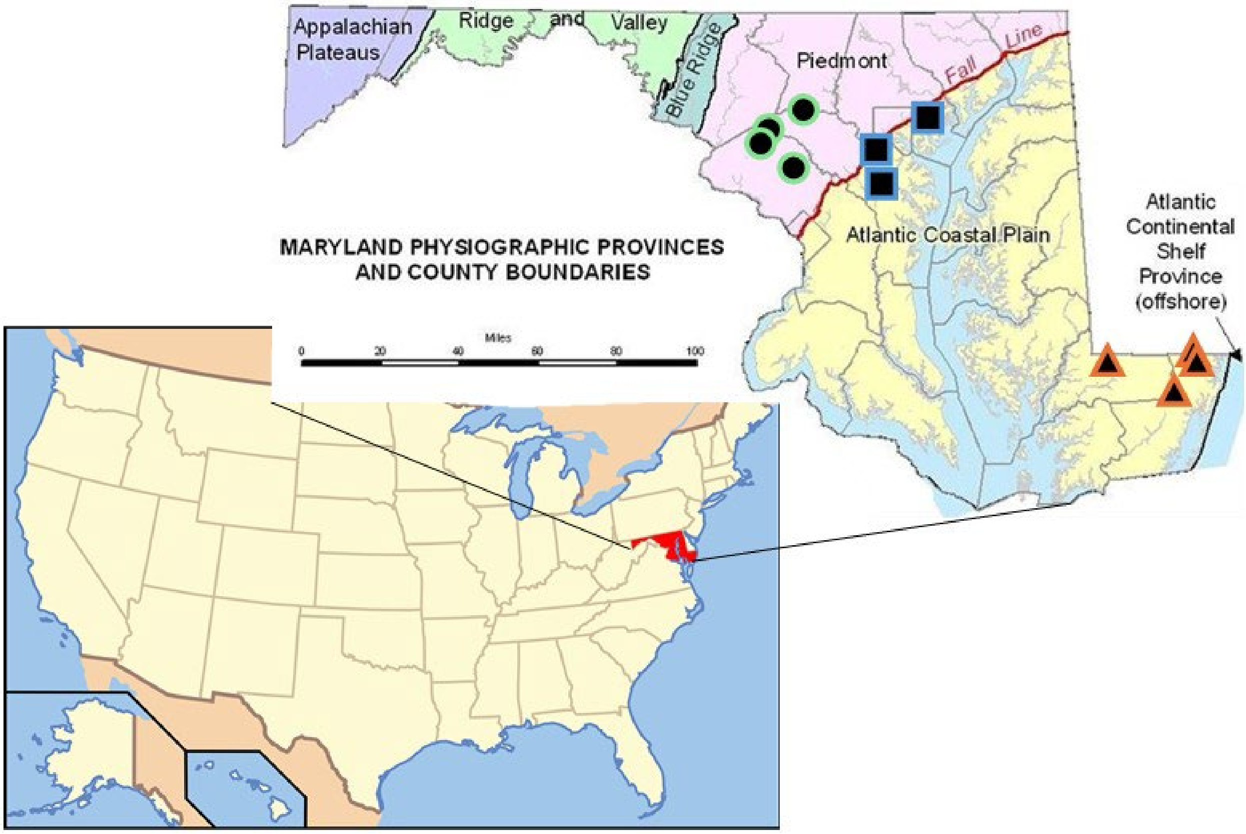

Figure 2-1. Approximate location of Indicator of Reduction in Soils (IRIS) field study sites (11) in Maryland, USA. Sites are grouped into three regions: Piedmont (green circle), Inner Coastal Plain (blue square), and Outer Coastal Plain (orange triangle). Maps modified from Campbell et al., 2018 and Musser & Pierce, 2012.

2.2.2 Site instrumentation

At the center of each study plot, a 1 m well was installed (Figure 2-2) equipped with an automated sensor and logger (HOBO MX2001 Water Level Data Logger, Onset Computer Corp., Bourne, MA) that recorded water table depth at 6-hour intervals. An open borehole was maintained to a depth of 35 cm adjacent to the well, which allowed for a secondary measurement of the site's water table every two weeks, corresponding to the IRIS deployment schedule (Table 1). A soil temperature probe (HOBO 64K Pendant Temperature Data Logger, Onset Computer Corp., Bourne, MA) was installed at 25 cm depth and recorded temperatures every two hours.

Figure 2-2. (Left) Conceptual diagram of study plot set up, and (Right) a photo of the study plot at the Northwest Branch (NW-128) site. White tops of IRIS films are visible above the soil surface.

2.2.3 Soil sampling and characterization

Soil morphological descriptions were made to a depth of approximately 1 m or to the depth of auger refusal. Pedon descriptions can be found in Appendix A. Samples were collected by horizon for further laboratory analysis. Total carbon was determined by high-temperature combustion using a LECO CN analyzer (Nelson & Sommers, 1996). As carbonate C is absent from these soils, total carbon was assumed to equal organic carbon. Soil pH was determined on a 1:1 soil and DI water slurry using a glass electrode.

2.2.4 IRIS

2.2.4.1 Field methods

The IRIS films consist of white PVC vinyl sheets coated with either Fe or Mn oxide paint and cut so the painted area is 7.62 cm (3 inches) wide and 35 cm (13.78 inches) long (Rabenhorst, 2018). An additional 10 cm area remained unpainted at the top of each film for labeling and ease of removal. The Fe oxide (ferrihydrite and goethite) and Mn oxide (birnessite) paints were synthesized following the protocols found in Rabenhorst and Burch (2006) and Rabenhorst and Persing (2017), respectively.

Batches of IRIS films were deployed every two weeks for a total of seven campaigns from February to June 2023 and were installed for a period of four weeks (Table 2-1). Five Fe IRIS films and five Mn IRIS films were deployed so as to be evenly distributed around the well, following the guidance of Rabenhorst (2018) (Figure 2-2). A total of 70 films were deployed at each site throughout the duration of the experiment, except on one date at one site (Firehouse) where some films could not be installed due to excessively dry field conditions (62 films deployed).

Table 2-1. Schedule of Indicator of Reduction in Soils (IRIS) film deployment batches and the associated number of films deployed during study.

	Installed	Retrieved	Fe Films	Mn Films
Batch 1	2/10/2023	3/10/2023	55	55
Batch 2	2/24/2023	3/24/2023	55	55
Batch 3	3/10/2023	4/7/2023	55	55
Batch 4	3/24/2023	4/21/2023	55	55
Batch 5	4/7/2023	5/5/2023	55	55
Batch 6	4/21/2023	5/19/2023	51*	51*
Batch 7	5/5/2023	6/2/2023	55	55
			381	381
			Total IRIS Films:	762

*Only one Fe and Mn film was deployed at the Firehouse site due to excessively dry soil conditions.

2.2.4.2 Image data processing

Retrieved IRIS films were gently washed with water to remove any soil residues and then air dried. Each film was scanned using a document scanner (ScanSnap iX1500, Fujitsu Inc., Tokyo, Japan) and saved as a JPEG (300 dpi) image. Using Adobe Photoshop (Adobe Photoshop Inc., San Jose, CA), the scanned JPEG images were cropped and transformed into binary images as described in Rabenhorst et al. (2021). Image cropping ensures the analysis was only completed on the portion of the film that was below the ground surface. The binary image processing displayed the areas of paint removal on the films as black pixels and remaining paint as white pixels.

The binary images were analyzed using a MATLAB (The MathWorks, Inc., Natick, MA) routine to calculate the percentage of paint removed for each 1 cm vertical increment along the 35 cm film. Data processing and visualization were completed in Excel to calculate the percentage of paint removal across the films at various depth intervals. Paint removal data from Fe IRIS was evaluated first using the criteria specified in the HSTS (Berkowitz et al., 2021; Sapkota et al., 2022). Further methods of evaluation are explained in the results and discussion section.

2.2.5 Analysis of precipitation normality

The HSTS requires an analysis of precipitation normality for any hydric soil investigation. For a soil to be hydric, the HSTS criteria for saturation and anaerobic conditions need to be met during periods of either normal or drier than normal precipitation (Berkowitz et al., 2021). However, our research objectives are not focused on making actual hydric soil determinations, but rather on comparing the performance of Mn and Fe IRIS. As such, the outcomes of the precipitation normality analysis do not directly impact our approach, but rather ensures that our results are interpreted in a climatic context (during a period of normal, wetter than normal, or drier than normal precipitation). We used a graphical averaging approach that compared the three-month weighted average precipitation data to long-term (WETS Tables) data during the study period (Appendix B). WETS Tables, published by the United States Department of Agriculture National Water and Climate Center, is a summary of the monthly precipitation for more than 8,000 National Weather Service (NWS) weather stations (Sprecher & Warne, 2000).

Normal rainfall is defined as falling between the 30th and 70th percentiles calculated from a 20 to 30 year period. Our graphical approach of comparing three-month weighted average data to long-term data is similar to the tabular approach of the Direct Antecedent Rainfall Evaluation Method (DAREM) (Sprecher & Warne, 2000; Sumner et al., 2009; Berkowitz et al., 2021). However, our graphical approach includes the precipitation total of the IRIS testing month, while the DAREM method looks at the three months prior. All precipitation data used were sourced from the NWS. Two representative stations (nearest to the sites) for each group of sites (Piedmont, Inner Coastal Plain, and Outer Coastal Plain) were selected for the analysis (Appendix B).

2.2.6 Statistical analysis

To measure the effects of duration of saturation, soil temperature, and SOC content on Fe and Mn IRIS paint removal, we used a restricted maximum likelihood (REML) mixed effects linear model. The three independent variables and their interactions were included as fixed effects, and the wetland study site was included as a random effect. Fe and Mn IRIS were analyzed separately. Prior to the statistical analysis, the mean oxide paint removal data were checked for normality, and data were normalized using a Johnson S_B transformation. Effects were considered significant at a p-value of <0.05. All statistical analyses were carried out using JMP Pro Version 17 (SAS Institute Inc., Cary, NC).

2.3 RESULTS AND DISCUSSION

2.3.1 Environmental conditions

Average deployment (4-week) temperatures across all sites ranged from 6.4 to 17.8 °C during the study period (Table 2-2). At some sites, the minimum and maximum daily temperatures were as low as 4 °C and as high as 23 °C, respectively. The analysis of precipitation normality based on the monthly data and the three-month weighted average precipitation data revealed the sites generally experienced drier than normal or normal conditions (Appendix B).

Table 2-2. Average soil temperatures (°C) at 25 cm depth for each IRIS deployment period (four weeks) at each site. Temperatures also averaged by region (gray) and for all sites combined (at bottom).

	IRIS Deployment Batch						
Sites	**1**	**2**	**3**	**4**	**5**	**6**	**7**
Piedmont	*6.7*	*7.0*	*9.0*	*12.6*	*14.0*	*15.0*	*15.0*
Nixon	6.9	7.0	8.9	12.5	13.6	14.1	14.1
NW-128	7.0	7.4	9.7	13.5	14.9	15.9	15.9
SC-02	6.6	7.0	8.9	12.4	14.0	15.4	15.4
SC-19	6.4	6.7	8.6	12.1	13.5	14.7	14.7
Inner Coastal Plain	*7.1*	*7.2*	*9.0*	*12.4*	*14.1*	*15.1*	*15.1*
Buckingham A	7.4	7.1	8.4	11.4	12.7	13.5	13.5
Churchview	7.2	7.5	9.3	12.8	14.6	15.7	15.7
Hollyneck	6.6	6.9	9.2	12.8	15.0	16.1	16.1
Outer Coastal Plain	*8.7*	*8.3*	*10.1*	*13.3*	*15.0*	*16.1*	*16.1*
Bishop	8.8	8.1	9.4	12.0	13.2	14.0	14.0
Bounds	8.6	7.9	9.2	11.9	13.3	14.2	14.2
Firehouse	9.3	9.1	11.4	15.4	17.3	18.3	18.3
Pilchard	8.3	8.0	10.2	14.1	16.2	17.8	17.8
Average	*7.5*	*7.5*	*9.4*	*12.8*	*14.4*	*15.4*	*15.4*
SD	*1.0*	*0.7*	*0.8*	*1.1*	*1.4*	*1.6*	*1.6*

Hydrographs (Figure 2-3) demonstrate that the water tables (WT) dropped as the spring season progressed with the occasional jump in WT level following precipitation events. The water levels in the Piedmont sites behaved similarly throughout the study period. In contrast, the WT levels at the Inner and Outer Coastal Plain sites were more variable between sites. The WT data show that not all sites met the HSTS saturation requirement throughout all IRIS deployment periods (Figure 2-4). Three of the 11 sites were never saturated within the upper 25 cm of the soil surface for ≥14 consecutive days during the study period. By the time of the last IRIS deployment (batch 7), only one of the sites met the HSTS hydrology requirement. The WT data also confirmed that these wetlands experience seasonal saturation. The wettest conditions occur in late winter and early spring (January to March), and then the wetlands quickly dry out during the spring, with warmer temperatures and vegetative growth increasing evapotranspiration (ET) rates (Hychka et al., 2013, Figure 4.2). This pattern of seasonal hydrology is also present in natural freshwater wetlands in Maryland and other areas of the Mid-Atlantic region (Rabenhorst et al., 2021; Hychka et al., 2013).

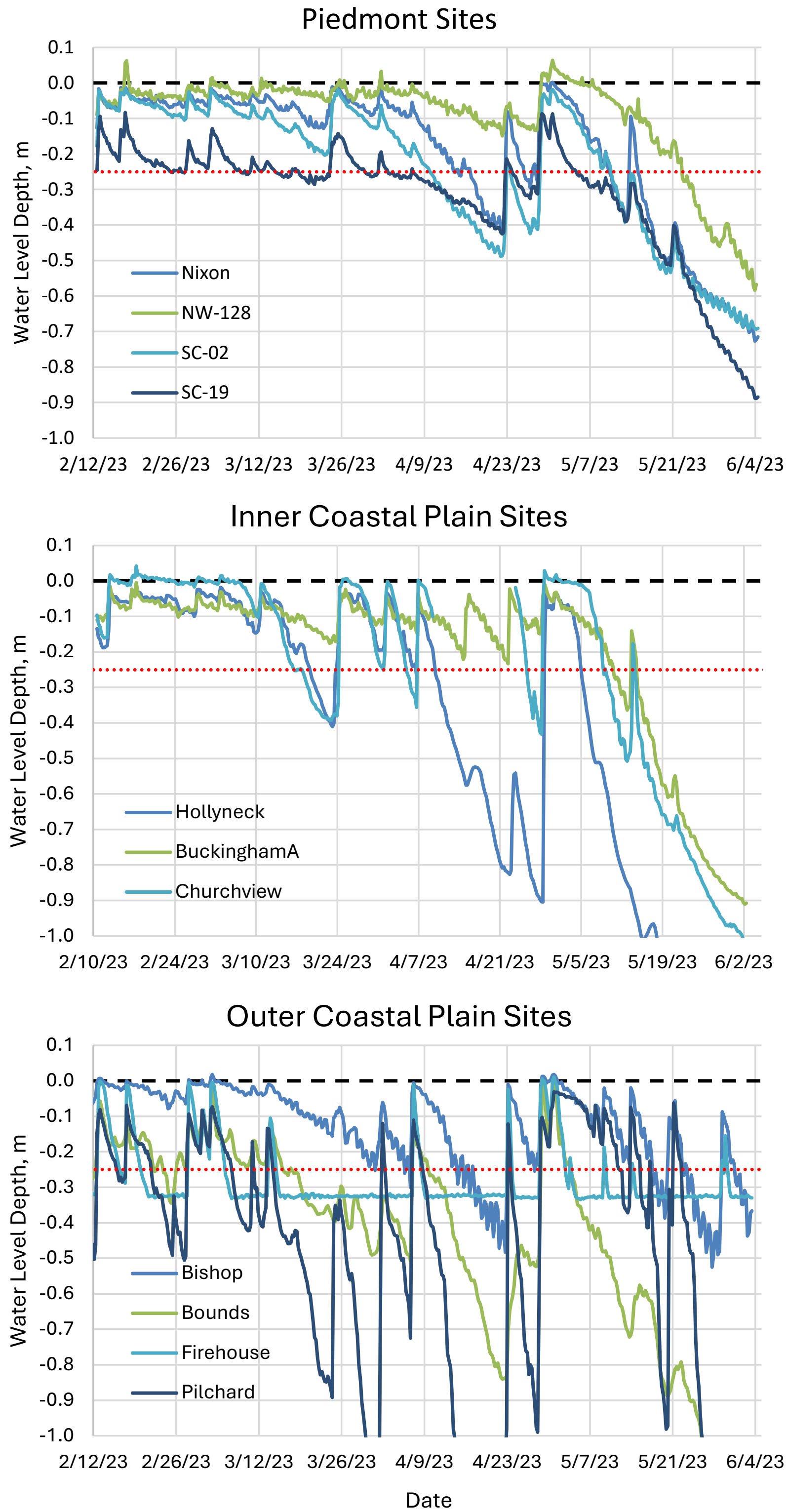

Figure 2-3. Hydrographs of water table (WT) levels (m) at study sites in the three physiographic regions. The black dashed line represents the soil surface. The red dotted line represents 25 cm below the soil surface. Note that the instrument at the Firehouse site (Outer Coast Plain) was only able to record WT levels greater than -0.33 m. *Missing data at the Churchview site (Inner Coastal Plain) in the month of April due to technical issues.

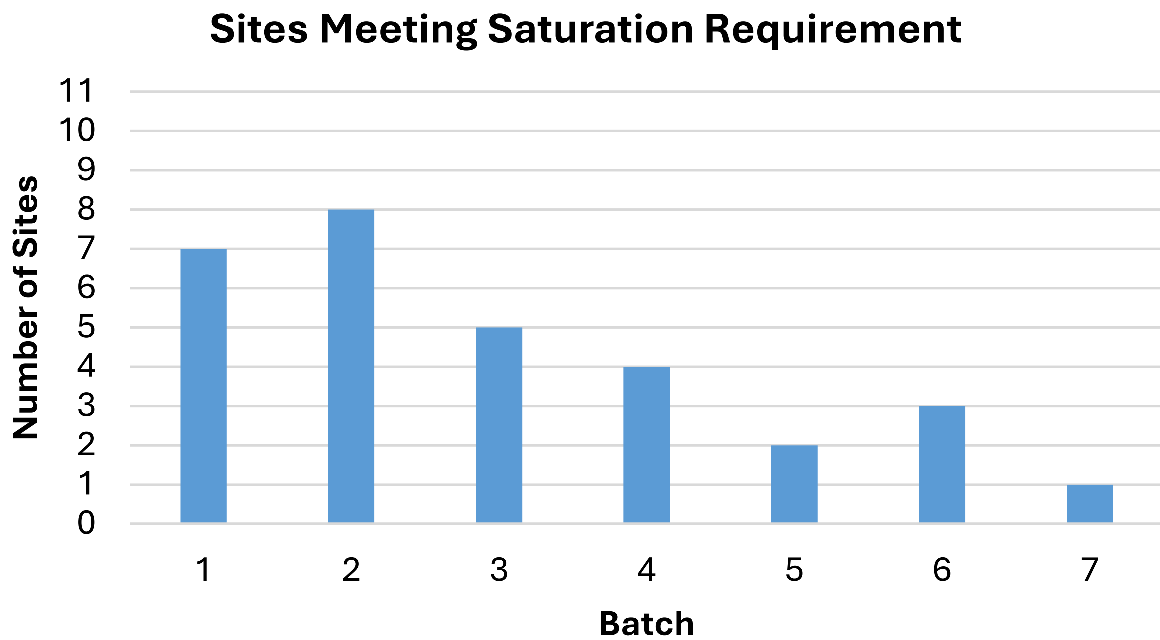

Figure 2-4. Number of study sites that meet the Hydric Soil Technical Standard (HSTS) criteria for saturation (water table within the upper 25 cm of the soil surface for ≥14 consecutive days) during each of the seven IRIS deployment periods.

2.3.2 Effects of key environmental drivers

A mixed effects model examining the magnitude of IRIS paint removal indicated that all three primary drivers of soil reduction (saturation, soil temperature, and SOC level) are statistically significant for both Fe and Mn oxide removal, with some of their interactions also being significant (Table 2-3). Consistent with our hypotheses and previous studies, we found that significantly more Mn oxide paint was removed from IRIS films than from Fe.

Table 2-3. A mixed effects linear model including all sites evaluating the impact of key environmental drivers of reduction on mean IRIS paint removal from 10 cm sections (0–10, 10–20, and 20–30 cm) of 5 replicate films. Key drivers include the impact of total days saturated during the deployment period, average soil temperature at 25 cm during the deployment period, and weighted average soil organic carbon (SOC). Study site was treated as a random effect in the model, and the random variance component was reported. Bolded p-values are significant at α=0.05.

Effect	df	**Fe** p-value	**Mn** P value
Total days saturated	1	**<.0001**	**<.0001**
Mean soil temperature (ST)	1	**<.0001**	**<.0001**
SOC%	1	**<.0001**	**<.0001**
Days saturated*Mean ST	1	**<.0001**	**<.0001**
Days saturated*SOC%	1	0.111	0.201
Mean ST*SOC%	1	**0.022**	0.068
Days saturated*Mean ST*SOC%	1	**0.026**	0.454
Site (random variance component)		43.6%	53.8%

Figure 2-5 demonstrates how Mn paint was removed from the films to a greater degree than Fe, similar to other reports (Rabenhorst and Persing, 2017; Rabenhorst et al, 2021). Up to the point of about 40% Fe removal, the removal of Mn was about two to three times more than Fe. However, the relationship plateaus when Fe removal is more than 40 to 50% because under those conditions, Mn removal is approaching 100%. The proportion of Mn to Fe removal is in the general range previously reported for field experiments (2 to 5 times) (Dorau et al., 2016, 2024).

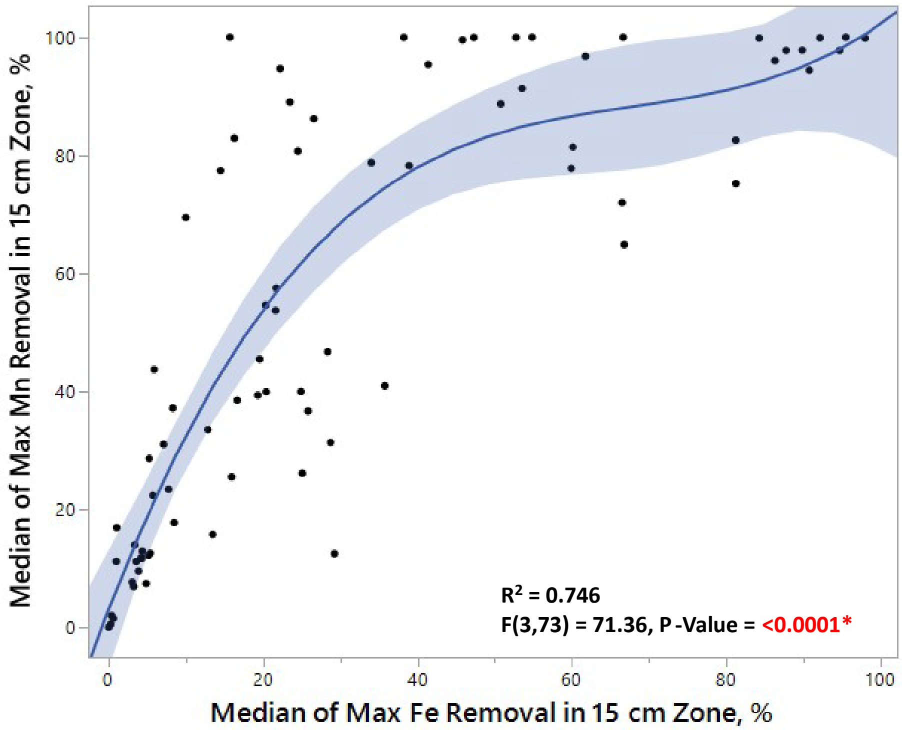

Figure 2-5. Relationship between the amount of Fe paint removed (x-axis) and Mn paint removed (y-axis). The data represent the median value (of 5 replicate films) derived from the HSTS IRIS analysis, which analyzes the 15 cm zone of maximum paint removal within the upper 30 cm.

2.3.2.1 Effect of saturation and temperature

Length of saturation and soil temperature both show a positive relationship with Fe and Mn paint removal from films, as predicted. To analyze the effect of temperature, each IRIS deployment was categorized as either "cool" (<11 °C) or "warm" (≥11 °C) based on the average soil temperature during the deployment period. Rabenhorst et al. (2021) identified 11 °C as a meaningful temperature threshold that corresponds to early (<11 °C) and later (≥11 °C) growing season conditions, and we adopted the same two temperature groups in this study. Out of all[1] the

---

[1] Our analysis included 76 batches instead of the original 77 batches. Batch six at one site (Firehouse) was not included in the analysis as not all five films were deployed as the soil was extremely dry and hard.

IRIS batches (site X deployment period) analyzed for this study, 32 batches (42%) experienced cold average deployment temperatures, and 44 batches (58%) were warm. Regarding saturation, 30 batches (39%) experienced sufficient saturation to meet the HSTS hydrology requirement (≥14 consecutive days of saturation within the upper 25 cm of soil), and the other 46 batches (61%) did not.

To further examine the effects of saturation and temperature, paint removal data along the films were split into three 10 cm zones (0–10, 10–20, 20–30 cm) (Figure 2-6). A 10 cm zone was considered saturated if the water table was present above the bottom depth of a given zone (i.e., shallower than 10, 20, or 30 cm, respectively). Analyzing the films in three 10 cm segments provides a finer resolution and a greater number of data points contributing to a more robust analysis.

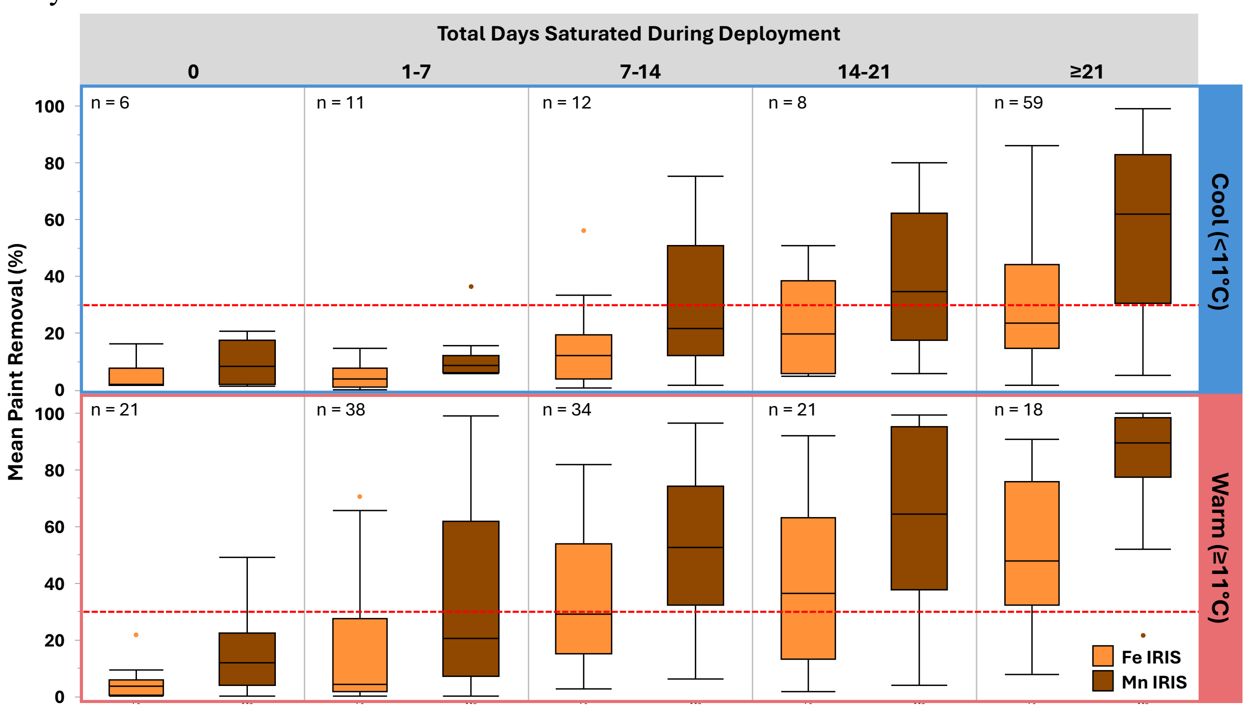

Figure 2-6. Boxplots represent the mean removal from 10 cm zones (0–10, 10–20, and 20–30 cm) of 5 replicate Fe (left, orange) or Mn (right, brown) IRIS films. Data are arranged by mean temperature during deployment (top and bottom rows) and the total number of days each 10 cm zone experienced saturation (increases left to right). The 30% removal threshold of the HSTS for Fe IRIS is represented as a dotted red line. Boxes represent the 25th and 75th percentiles, split by the median (50th percentile). The whiskers represent 1.5*IQR to determine outliers (dots).

Overall, under cool soil conditions (average soil temperature <11°C) there is less Mn and Fe IRIS paint removal compared to when temperatures are warmer (≥11°C). Under cool conditions, the majority of the Fe films (median value) did not have a mean removal of at least 30% from a 10 cm zone, even with 21 or more total days of saturation (Figure 2-6). By contrast, with at least 14 total days of saturation (or more), the majority of the Mn films exceed the 30% threshold. Under the warm conditions, there is an increase in removal, especially for Fe IRIS. When saturated for 14 or more total days, the majority of cases show average removal of Fe paint to be greater than 30%. Mn paint removal was also enhanced by the warmer temperatures, so much so that the mean removals were well above 30% with less saturation (7-14 days).

Our data confirm earlier reports of temperature effects on the removal of Fe and Mn IRIS paint in both lab (Dorau et al., 2018) and field settings (Rabenhorst et al., 2021; Rabenhorst & Castenson, 2005). In these mitigation wetlands, the Mn IRIS paint removal occurs at a meaningful rate under saturated and cool conditions during the early growing season, while Fe IRIS paint removal is inhibited. As temperatures increase into later parts of the growing season, Fe IRIS paint removal increases and can meet the HSTS threshold when there is sufficient saturation. Overall, these trends in IRIS performance in restored and created wetlands are similar to those found in natural wetlands (Rabenhorst et al., 2021). However, likely due to the seasonal nature of the hydrology at these mitigated wetlands and working with a smaller data set, there is more variability in the oxide paint removal data compared to Rabenhorst et al. (2021). Additionally, our results confirm the notion that under warm conditions Mn IRIS might be too sensitive and thus not as useful when documenting anaerobic conditions for hydric soil evaluations.

2.3.2.2 Effect of soil organic carbon

As with saturation and temperature, there was more oxide paint removal from zones with more SOC present in the profile. To analyze the effect of SOC on IRIS paint removal, mean paint removal data were split into three 10 cm zones as described in Section 2.3.2.1. The SOC content for each 10 cm zone was grouped into the two relative levels of "low" and "high" based on soil profile horizonation. The low level had a mean and median of 0.43% and 0.39% SOC, respectively, and ranged from 0.21 to 0.66% (Appendix D). The high level had a mean and median of 2.01% and 1.5% SOC, respectively, and ranged from 0.70 to 5.26%. The SOC content for each 10 cm zone (0–10, 10–20, and 20–30 cm) was determined by calculating a weighted average based on the SOC content (%) measured for each horizon and then arranged from highest to lowest. We considered A horizons to have "high" SOC content, so if the majority of a 10 cm zone corresponded to the depths of surface (A) horizons, then the SOC was designated as "high." However, there are a few deeper 10 cm zones (i.e. 10–20 and 20–30 cm) that were considered "high" because the weighted average SOC% ranked higher than the A horizon with the lowest SOC. While there are limitations with analyzing SOC as a categorical variable, we are still able to gain insight into the effect of SOC on IRIS paint removal in this study. This analysis only included data that had ≥14 total days of saturation within the corresponding 10 cm zone.

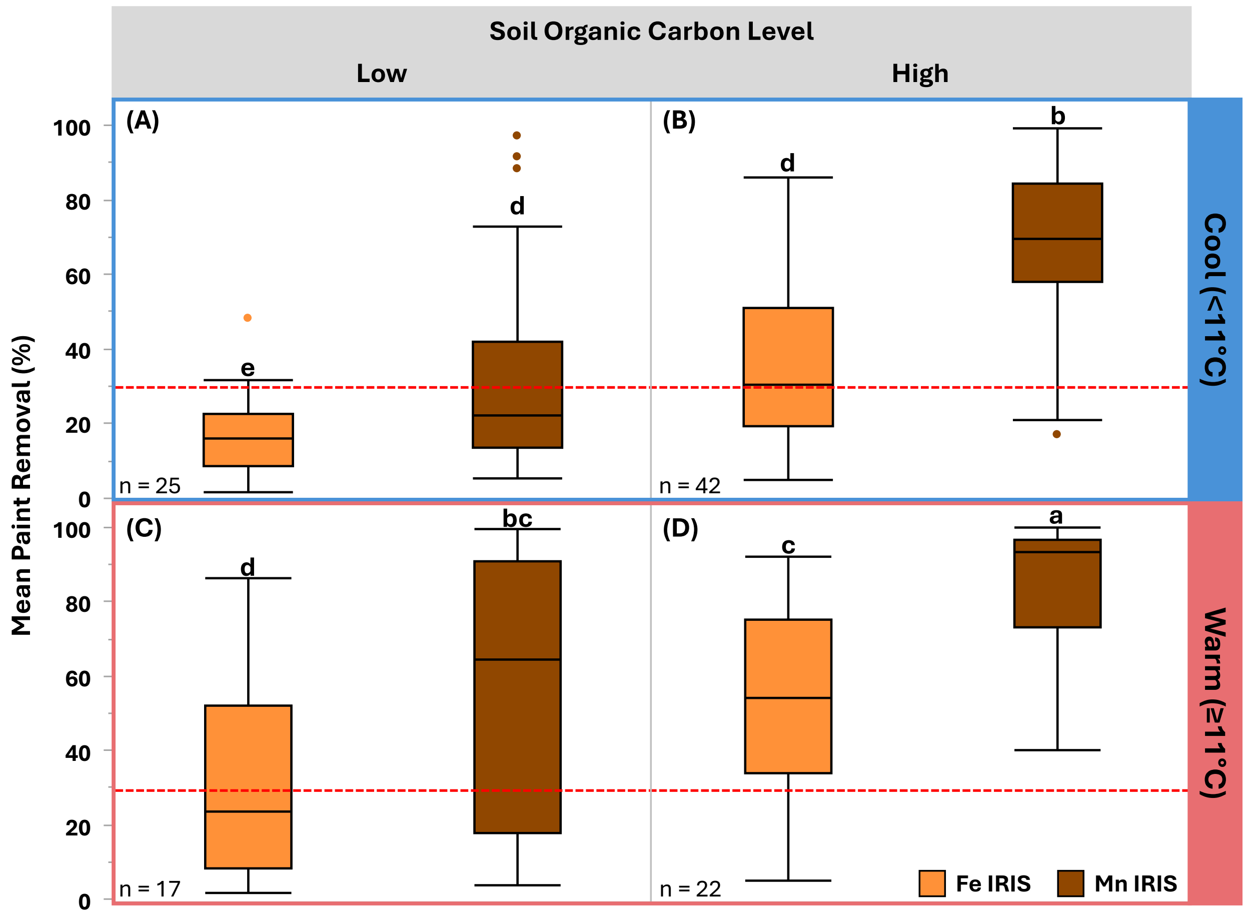

Figure 2-7. Boxplots represent the mean oxide paint removal from 10 cm zones (0–10, 10–20, and 20–30 cm) of 5 replicate Fe (left, orange) or Mn (right, brown) IRIS films. Data are arranged by soil organic carbon level (low or high) in the soil (columns) and mean soil temperature during deployment (rows). Zone depths that corresponded to majority topsoil (A horizons) were considered to have "high" SOC and zones that did not were considered to have "low." Data included in this analysis had ≥14 days of total saturation within the corresponding 10 cm zone. Data not sharing the same letter designation (lowercase) are significantly different based on LSD Student's t test at $\alpha = 0.05$. The 30% removal threshold of the HSTS for Fe IRIS is represented as a dotted red line. Boxes represent the 25th and 75th percentile, split by the median (50th percentile). The whiskers represent 1.5*IQR to determine outliers (dots).

When soils were saturated, more paint was removed for both Mn and Fe IRIS in zones where SOC was higher (Figure 2-7). The most paint removal occurred when there was the ideal combination of saturation, warm temperatures, and high SOC content (Figure 2-7D). As expected, Mn removal was higher than Fe removal under both low and high carbon scenarios, regardless of temperature. The availability of oxidizable SOC is thought to be a limiting control on Fe reduction when temperatures are warm (Rabenhorst & Castenson, 2005). Our results support this claim as there was significantly less Fe removal with low SOC (median removal = 23%, Figure 2-7C) compared to when SOC was high (median removal = 54%, Figure 2-7D) under warm conditions. Additionally, Fe removal significantly increased with more SOC under cool conditions (Figure 2-7A-B). Our results also suggest that Mn removal is significantly and positively affected by SOC content.

A common practice in wetland construction and restoration includes the addition of organic amendments (Richardson et al., 2016). These amendments—including stockpiled or imported topsoil, biosolids, manure, and composted plant materials—are intended to increase the organic matter/carbon content in the soil and may help to establish or recover wetland functions (Richardson et al., 2016). However, Scott et al. (2020) found the effectiveness of these amendments is not uniform. Many of our sites (7 out of 11) received additions of topsoil or other organic amendments, as it is required in Maryland nontidal wetland mitigation (Walbeck et al., 2011). This resulted in the upper 5 to 10 cm of soil having substantially elevated SOC content compared to lower horizons (Appendices A and D). In particular, IRIS films deployed at the Churchview site showed striking zonation in IRIS paint removal (Appendix E). As a result of scalping, land grading, and addition of amendments during construction, the SOC% was especially high in the upper 2 cm (5.39%), remained high (0.97% to 11 cm), and then quickly decreased to very low levels (0.25% and less) below this. The removal patterns on both Fe and Mn IRIS reflected the sudden drop in SOC in the subsoil.

While SOC is recognized as having an important influence on the development of reducing conditions in soil, SOC content is not formally addressed in the analysis and interpretation of IRIS. There is recent discussion on the impact of short-chain organic acids abiotically reducing both Fe and Mn paint off of IRIS films (Loffredo et al., 2023). However, paint removal occurred at the millimolar concentration level, which is one to two orders of magnitude above the usual concentrations these compounds are found in the soil solution (Loffredo et al., 2023; Sokolova, 2020). Paint removal is unlikely to be an issue in most use cases; however, recognizing the impact of SOC content may be useful when working in mitigated wetlands or other human-altered landscapes with unnatural or concentrated carbon distributions within the soil profile.

2.3.3 IRIS paint removal in the context of HSTS

2.3.3.1 Exploring optimal oxide removal thresholds

We evaluated the impact of the HSTS and other oxide removal thresholds on the interpretation of IRIS results (Figure 2-8). Following guidance from the HSTS, we calculated the maximum paint removal from a 15 cm contiguous zone within the upper 30 cm. To evaluate the effect of setting alternative thresholds (the % paint removal required to indicate reducing conditions), we used data calculated as specified in the HSTS. Additionally, we utilized the HSTS saturation requirement of 14 consecutive days within the upper 25 cm. For each possible IRIS paint removal threshold (x-axes in Figure 2-8A-D), the data were sorted into four categories based on whether the site met the saturation requirement ("wet" or "not wet") and whether or not the site met the IRIS paint removal threshold ("reducing" or "not reducing"). The four categories were: true positive (Wet-Reducing), true negative (Not Wet-Not Reducing), false positive (Not Wet-Reducing), and false negative (Wet-Not Reducing). The two combinations of true positive (Wet-Reducing) and true negative (Not Wet-Not Reducing) represent expected/desired outcomes where reduction by IRIS and the HSTS hydrology requirement were consistent (both are met, or neither are met). However, the combinations of false negative (Wet-Not Reducing) and false positive (Not Wet-Reducing) represent the potential problematic outcomes. Thus, the purpose of this analysis is to find the optimal IRIS threshold that minimizes the likelihood of problematic outcomes, especially false negative results. This approach assumes that if the HSTS saturation requirement is met then there should be adequate IRIS paint removal for a true positive result.

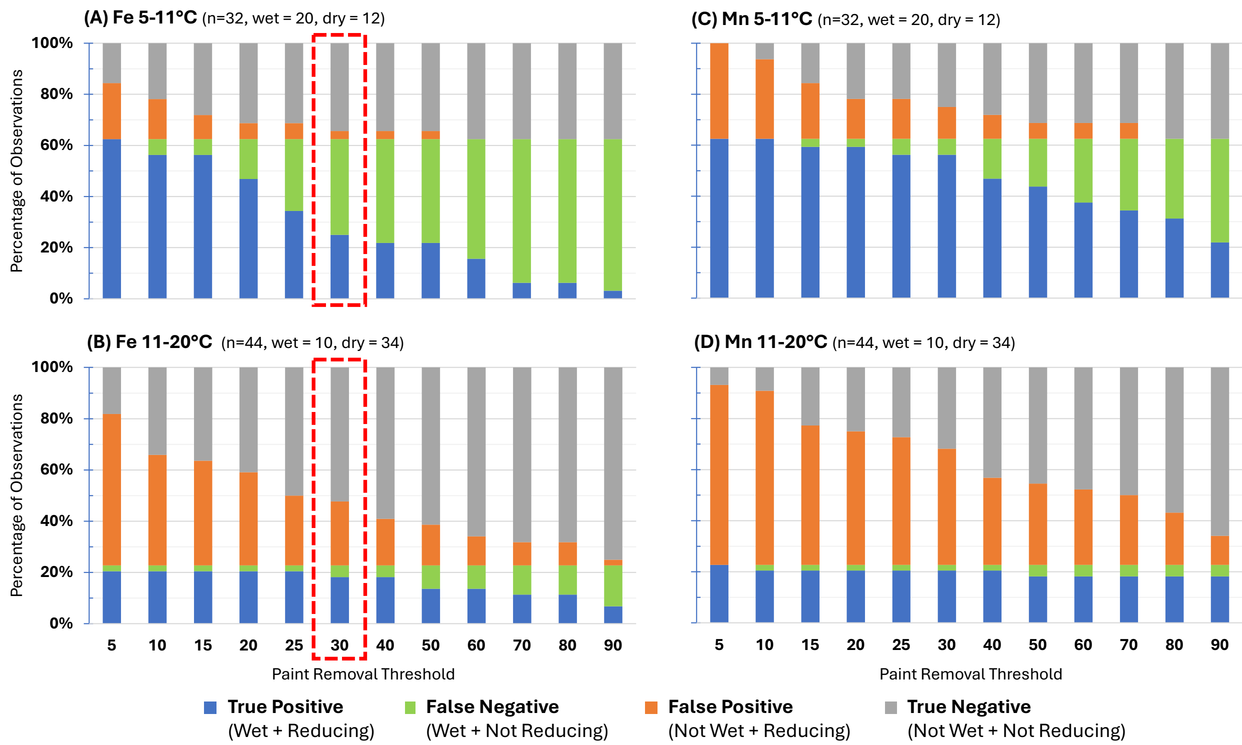

Figure 2-8. Bar graphs represent the percentage of observations among four possible combinations of outcomes, comparing saturation (based on WT levels) and reduction (based on IRIS paint removal). Sites were considered "wet" if the Hydric Soil Technical Standard (HSTS) saturation requirement of ≥14 days continuous saturation within upper 25 cm was met, and "not wet", otherwise. Sites were considered "reducing" when the IRIS paint removal met or exceeded a given threshold. Data during cool (5–11 °C) or warm (11–20 °C) periods are shown separately in A and C, B and D, respectively. Fe IRIS (A, B) and Mn IRIS (C, D) are also shown separately. True positive (wet-reducing) and True negative (not wet-not reducing) are the ideal, expected outcomes. False negative (wet-not reducing) and false positive (not wet-reducing) are problematic outcomes that should be minimized. Red dotted box represents the current HSTS threshold for Fe IRIS paint removal.

Under cool (5 to 11 °C) soil conditions, Fe IRIS paint removal is relatively low even when there is sufficient saturation (Figure 2-8A). In particular, when testing the current HSTS threshold (30% removal, red dotted box), our data indicate mostly problematic outcomes, specifically false negatives (graphed as green). Such a large proportion of false negative outcomes suggests that the current HSTS threshold is too conservative in cool conditions, since the majority (60%, or 12/20) of wet sites (graphed as blue and green) yield paint removal rates less than 30%. To decrease the number of problematic outcomes (graphed as green and orange) and to better capture anaerobic conditions, we suggest lowering the Fe IRIS paint removal threshold to 15% when the mean soil temperature is 11 °C or below. Using this threshold optimally increases the proportion of true positives, decreases the proportion of false negatives, and does not drastically increase the proportion of false positives (graphed as orange). A 15% threshold for Fe IRIS used in cool soil conditions is consistent with the previous findings in natural wetlands (Rabenhorst et al., 2021).

Under warm (11 to 20 °C) soil conditions, Fe oxide removal is substantially higher than in cool conditions (Figure 2-8B). At the current HSTS threshold of 30% (dotted red box), there are relatively few false negative outcomes (graphed as green). The 30% threshold has already been shown to be a conservative threshold for Fe oxide removal based on multiple IRIS studies (Berkowitz et al., 2021; Castenson & Rabenhorst, 2006; Sapkota et al., 2022). Thus, we suggest maintaining the HSTS 30% threshold for Fe, although we observed that using this threshold resulted in a number of false positive outcomes. These false positives (even at a threshold of 90%) likely occur due to high water tables that briefly drop below 25 cm at these restored and created wetlands (see Section 2.3.3.2 for more discussion).

Mn oxide removal occurs at much higher rates than Fe under cool (5 to 11 °C) soil conditions, indicated by the large portion of true positive outcomes (graphed as blue in Figure 2-8C). As previously mentioned, there is no current HSTS-approved threshold for Mn IRIS paint removal. The Mn thresholds with the smallest proportion of problematic outcomes (graphed as green and orange) range between 20 and 30%. In cool soil conditions, a Mn threshold of 20–30%

appears to optimize the desired outcomes, while the same range is too conservative for Fe IRIS in the early growing season. Rabenhorst et al. (2021) also found the same range of 20 to 30% to be optimal for Mn IRIS paint removal threshold in cool soil conditions in natural wetlands. Therefore, we suggest a 30% removal threshold for Mn IRIS in cool soil conditions. This suggestion conveniently aligns with the already established 30% Fe IRIS threshold and avoids the confusion of using too many different thresholds.

Mn removal dramatically increases under warm (11 to 20 °C) soil conditions (Figure 2-8D). This is exemplified by the large proportion of false positive outcomes (graphed as orange). The rapid/excessive removal of Mn oxide paint under warm temperatures makes it difficult to make confident interpretations about the anaerobic conditions of the soil. Thus, we do not recommend using Mn IRIS films alone as evidence of anaerobic conditions under warm conditions. Under such conditions, Mn IRIS could be used in tandem with Fe IRIS to provide additional insights about the redox conditions in the soil, such as denitrification.

In general, the optimal IRIS oxide removal thresholds, based upon deployments at restored and created wetlands, agree with those found for natural wetlands (Rabenhorst et al., 2021), although there are some minor differences. Most notably, our results show more false-positive outcomes for both Fe and Mn in both temperature categories. As previously mentioned, and further discussed in the next section, this may be due to the water tables at these sites briefly dropping below 25 cm (which resets the time clock for the 14-day continuous saturation) either due to regional hydrological dynamics or an artifact of the mitigation process. Additionally, these data are geographically constrained to Maryland, while Rabenhorst et al. (2021) considered sites across a much broader geographic area. Nevertheless, both studies recognize that the current HSTS criteria for Fe IRIS are too conservative when used early in the growing season.

2.3.3.2 Effect of HSTS saturation requirement on IRIS interpretation

Wetland sites with highly fluctuating water tables present challenges when trying to apply the HSTS. As currently stated, the HSTS requires ≥14 consecutive days of saturation in the upper 25 cm. This requirement is based on the findings National Research Council (1995) and is designed to ensure confidence that the soil is indeed sufficiently wet (Berkowitz et al., 2021). However, strict applications (i.e., excluding soils where the WT drops below 25 cm for 1 day or less) may force the conclusion that the soil is "not wet," although IRIS data might indicate that the soil is reducing, leading to a false positive interpretation.

As previously mentioned (Figures 2-8), we saw a high occurrence of false positive outcomes for both Fe and Mn IRIS throughout the study. These results often occurred in IRIS batches that had brief periods (a few hours to a few days) when the WT dropped below the depth of 25 cm (Figure 2-3). Further adding to the complexity, some of these sites exhibited evidence of perched saturation (not included in well data), likely due to soil compaction caused by the construction of these mitigation wetlands. These brief dips in the WT and the other complicated WT dynamics likely do not completely stop the development and maintenance of reducing conditions in the upper 25 cm soils, especially in the capillary fringe. In Fiola et al. (2020), the biogeochemistry of the capillary fringe was investigated in laboratory mesocosms, and various parameters suggested that the region just above the WT shared many characteristics with the saturated zone, including reducing conditions. Using PVC Fe IRIS tubes, they found more than 50% Fe removal in zones ranging from 2.5 to 12.5 cm above the WT (depending on soil texture) (Fiola et al., 2020, Figure 5). Jenkinson and Franzmeier (2006) also recognized that Fe IRIS paint removal can occur due to microsite reduction above the water table. This likely contributed to IRIS oxide removal from IRIS at our sites at times when the HSTS saturation requirement was not strictly met.

2.4 CONCLUSIONS

Prolonged saturation and the subsequent establishment of anaerobic conditions and biogeochemical reduction are the defining characteristics of hydric soils and wetlands. IRIS is an innovative tool that can be used to document the reduction of Fe and Mn and thus confirm anaerobic soil conditions. This study sought to investigate the performance of IRIS films in restored and created mitigation wetlands during the early to mid-growing season and to evaluate the impact of saturation, soil temperature, and SOC content on Fe and Mn IRIS paint removal. All three key environmental drivers of soil reduction significantly and positively affect Fe and Mn IRIS oxide removal. Consistent with previous studies (reviewed in Sapkota et al., 2022), and with thermodynamics (McBride, 1994), Mn IRIS paint removal occurred to a significantly greater extent compared to Fe IRIS paint removal in restored and created wetlands.

Similar to findings in natural wetlands (Rabenhorst et al., 2021), our data in restored wetlands support the development and use of IRIS paint removal thresholds that take into account soil temperature and the mineral composition (Fe or Mn) of the IRIS. Under cool soil conditions (<11°C), Fe reduction is slow enough that Fe IRIS paint removal does not often meet the current HSTS threshold of 30% removal, and a threshold of 15% would seem more appropriate. In contrast, Mn reduction occurs at a higher rate than Fe reduction, and in cool conditions, a Mn IRIS threshold of 30% removal best documents anaerobic conditions and minimizes the likelihood of conflicting results (between saturation and IRIS). In warm soil conditions, the current HSTS threshold of 30% for Fe paint appears to be satisfactory and appropriate. Because of its greater reactivity, Mn IRIS may be less useful in documenting the presence of anaerobic conditions in warm soil temperatures. However, if used in tandem with Fe IRIS, Mn IRIS may provide additional insight into the redox status and processes in the soil. For example, some wetlands are constructed/restored, with the goal of reducing nitrate loads. As denitrification and Mn reduction occur at similar redox potentials, Mn IRIS films may potentially be a useful proxy for nitrate reduction and evaluate if such a goal is met. Further research is needed to validate this conceptual alternative application of IRIS. We have demonstrated that Mn IRIS films are more sensitive than Fe IRIS when documenting anaerobic conditions in cool soil conditions such as during the early growing season of temperate wetlands and wetlands in cold climatic regions.

Chapter 3: Effect of temperature and soil organic carbon on the reduction of soil Fe and Mn

3.1 INTRODUCTION

Reduction-oxidation (redox) reactions have long been of interest in soil science, particularly in wet soils, due to the importance of these reactions in the biogeochemical cycling of nutrients, the mobilization of contaminants, and the formation and identification of hydric soils (Lovley et al., 2004; Reddy et al., 2022). The reduced state of wetland and other waterlogged soils chemically sets these soils apart from better-drained soils. Prolonged inundation inhibits the exchange of atmospheric oxygen, and aerobic microbial respiration quickly depletes soil oxygen levels. Under low oxygen conditions, facultative and obligate anaerobes utilize inorganic compounds as alternative terminal electron acceptors to O_2 in order to oxidize organic matter during anaerobic respiration. The alternative terminal electron acceptors, listed here in order of decreasing redox potential (Eh) and increasing Gibb's free energy, are NO_3^-, Mn oxides, Fe oxides, SO_4^{2-}, and CO_2 (Ponnamperuma, 1972). Insoluble oxides of Mn(III,IV) and Fe(III) are reduced to soluble Mn^{2+} and Fe^{2+} by metal-reducing microorganisms (e.g., *Geobacter* or *Shewanella*) when more energetically favorable electron acceptors (O_2 and NO_3^-) are not readily available (Lovley, 1991; Lovley et al., 2004; McBride, 1994).

Fe and Mn oxides, hydroxides, and oxyhydroxides (referred to as "oxides" for the remainder of the chapter) are ubiquitous soil minerals with Fe (2-550 g/kg of soil) more abundant than Mn (0.02-10 g/kg) (Essington, 2015). These redox-sensitive minerals are potent pigments in the soil; the presence of colorful Fe and Mn redoximorphic features (i.e., concentrations and depletions) visually represents the long-term redox conditions in a soil. Indicator of Reduction in Soils

(IRIS) devices utilize the change in the color of orange Fe oxides and brown Mn oxides to colorless and soluble Fe^{2+} and Mn^{2+} phases to document the presence of anaerobic and reducing soil conditions (Sapkota et al., 2022).

The rate and intensity of soil reduction are regulated by the duration of saturation, temperature, quantity and quality of organic carbon, pH, and the quantity and nature of terminal electron acceptors (McBride, 1994; Ponnamperuma, 1972). Many of these environmental drivers are also dependent on one another. For example, the time needed to induce Mn or Fe reduction under saturation depends on the status of the other drivers, especially temperature and organic carbon (Vepraskas & Vaughan, 2016). Since microbial activity is sensitive to temperature, the rate of reduction is greatly impacted by the soil temperature (Lovley, 1991). Cold temperatures have been found to decrease the reduction of Fe and Mn both in the field and the lab when measuring redox potential (Cogger & Kennedy, 1992; Vaughan et al., 2009), IRIS paint removal (Dorau et al., 2016, 2018; Rabenhorst et al., 2021; Rabenhorst & Castenson, 2005; Stiles et al., 2010), and porewater concentrations of aqueous Fe and Mn (Ponnamperuma, 1984, as cited in Reddy et al., 2022, p. 452; Sparrow & Uren, 2014; Weber et al., 2010). As organic carbon is the primary energy source for microbial respiration, and thus the electron donor during the reduction of Fe(III) and Mn(IV) (Lovley, 1991; Lovley et al., 2004), increases in the total amount of OC have been shown to typically result in increased rates of Fe and Mn reduction (Cogger & Kennedy, 1992; Glinski et al., 1996; Magen et al., 2011; Ponnamperuma, 1972; Reddy et al., 2022; Roden & Wetzel, 2002). The nature and properties of the carbon source (e.g., molecular size, polarity, composition) also influence the biodegradability of the carbon (Marschner & Kalbitz, 2003; Straathof et al., 2014) and the reactivity of carbon for organo-mineral interactions (Li et al., 2021). The availability of terminal electron acceptors with higher reduction potentials can buffer the decrease in Eh and the reduction of other compounds. Most notably, Mn and Fe reduction are generally thought to occur sequentially based on thermodynamics, and as such, significant additions of Mn oxides have been shown to slow or diminish the reduction of Fe (Ponnamperuma et al., 1965; Yuan & Ponnamperuma, 1966; Hammann & Ottow, 1974; Ehlert et al., 2014, 2016). While the impact of various environmental drivers has been observed using Eh measurements, IRIS paint removal, or direct porewater analysis, a comparative study assessing the concentration of reduced Fe and Mn in soil porewater and coating removal from IRIS films has not been conducted.

The objectives of this microcosm study were: 1) to examine the effects of duration of saturation, quantity of soil organic carbon, and temperature on the reduction and mobilization of Mn and Fe into soil porewater and 2) to compare the mobilization of reduced Mn and Fe with the removal of Mn and Fe oxide paint from IRIS films.

3.2 MATERIALS AND METHODS

3.2.1 Soil collection and characterization

Three soils were sampled, representing three different soil series in Maryland, USA. The Codorus and Glenelg series are common within the Piedmont, and the Downer series is common within the Coastal Plain physiographic provinces of Maryland and the Mid-Atlantic region. Bulk samples (approximately 20 L) were collected from three horizons of each soil during May and June 2023. This sampling of multiple horizons from the same soil helped ensure there was a range in soil organic carbon content but minimal differences in other chemical and mineralogical properties across samples. Additionally, it allows us to perhaps make inferences about rates and processes as they occur within soil profiles. Bulk samples were air-dried, crushed, and sieved to pass a 2 mm sieve. Samples were homogenized and analyzed for SOC via high temperature combustion using a LECO CH analyzer (Nelson & Sommers, 1996). Total carbon was assumed to equal organic carbon in these samples as carbonate C is absent from these soils. Dissolved organic carbon (DOC) was measured using a Shimadzu TOC-L analyzer after a two-hour water extraction (Anderson et al., 2023). Total extractable Fe and Mn was determined using a modification of method 4G1 (dithionite-citrate extraction) (Soil Survey Staff, 2022) and then measured by flame atomic absorption (AA) spectrophotometry. Soil pH was determined on a 1:1 soil and DI water slurry using a glass electrode.

3.2.2 Microcosm experimental design

The microcosm experiments were performed from June to September 2024 using a mechanical vacuum extractor and 60 mL microcosms made from syringes (Holmgren et al., 1977). As microcosms were assembled, miniature dual (half Mn and half Fe) IRIS films were inserted to line the interior circumference of the microcosms (27 mm diameter by 135 mm high). IRIS films were painted with either Mn or Fe oxide paint (Rabenhorst & Burch, 2006; Rabenhorst & Persing, 2017) on 11” by 17” (27.94 cm by 43.18 cm) polyester sheets (5 Mil Waterproof Copy paper from TerraSlate Inc.). After painting, each Fe and Mn IRIS film was trimmed to size (40 mm wide by 102 mm long) and bound together on the unpainted side with a piece of vinyl tape. Once the IRIS films were in place, each microcosm was filled with a homogenized mixture of 30 g of soil (from one horizon) and 30 g of quartz fracking sand. The sand was added to accommodate an additional experiment, which utilized additions of Mn oxide-coated sands (Chapter 4). Filter pads were placed at the base to help retain the soil in the columns. Microcosms were placed in basins and saturated from below with DI water over a one-hour period to help exclude trapped air. The water level was maintained just above the soil surface to ensure saturation in the soil until extraction. The temperature of the water in the basins was recorded at 4-hour intervals throughout the experiment.

The microcosms were analyzed destructively at 10 specified time points. To extract the porewater, the microcosms were carefully transferred from the water basins to the extractor. The bottom syringes were quickly secured below and connected to the microcosms with a small piece of rubber tubing. Any excess ponded water above the soil surface was removed before the extraction started. The extraction was run for 2 hours, although essentially the entire volume of porewater extracted (which generally ranged from 4 to 15 mL) was usually collected within the first 20 minutes of the extraction. Analyses indicate that the extracted portion represents approximately 20–30% of the total porewater in the samples (data not shown). Extracted porewater was transferred to plastic tubes and acidified with 50 µL of 1 M HCl to keep metals of interest in solution. The concentrations of Mn and Fe were determined using flame AA spectrophotometry. Standards and wash were proportionally acidified with 1 M HCl to match the sample matrix.

Shortly following the porewater extraction, the columns were disassembled, and IRIS films were removed, rinsed with water, and air dried. The height of the soil surface was marked on each film upon retrieval. The films were then scanned to produce 300 dpi JPEG images, which were cropped to only include the area in contact with the soil.

In the initial experiment, the microcosms were maintained at laboratory temperature. The average water temperature of the saturation basins was 21.3 °C (ranged from 19.7 to 23.4 °C). The experiment continued for 8 weeks, during which time samples were collected and analyzed on days 0 (after 2 hours initial saturation), 1, 2, 4, 7, 14, 21, 28, 42, and 56. All three soil horizons from each of the three pedons were used for this experiment. Each combination of soil and horizon was run in duplicate for a total of 180 microcosms.

A second experiment was run to examine the effect of temperature by setting up the materials and apparatus within a refrigerated room. The average water temperature of the saturation basins was 4.1 °C (ranged from 3.9 to 4.5 °C). In anticipation that colder temperatures would slow down microbial activity, the experiment was extended to 12 weeks. Samples were collected and analyzed on days 0 (after 2 hours of initial saturation), 3, 7, 14, 21, 28, 42, 56, 70, and 84. In contrast to the initial experiment that used all three soil horizons, this experiment only included the top two horizons for each soil (the bottom horizons being excluded because they had relatively low SOC and thus would likely yield little information). Each combination of soil and horizon was duplicated for a total of 120 microcosms.

3.2.3 Statistical analysis

Multiple stepwise linear regressions were conducted to test the influence of SOC content, DOC content, soil Mn content, and soil Fe content on the concentration of Mn and Fe mobilized into the porewater. Analysis of variance (ANOVA) was conducted on each regression model to assess statistical significance. All analyses were conducted in Excel.

3.3 RESULTS AND DISCUSSION

3.3.1 Soil characterization

Properties of the three soils used in the experiments are presented in Table 3-1. The Glenelg soil (Fine-loamy, mixed, semiactive, mesic Typic Hapludults) was formed in residuum derived from crystalline micaceous schist and sampled in a broad-leaf forested area. The Codorus soil (Fine-loamy, mixed, active, mesic Fluvaquentic Dystrudepts) was sampled in a floodplain with grass vegetation (primarily tall fescue, *Festuca arundinacea*) and formed in alluvial deposits derived from upland soils (like Glenelg), which were weathered from metamorphic crystalline rocks. The Downer soil (Coarse-loamy, siliceous, semiactive, mesic Typic Hapludults) formed in a stable landscape from sandy coastal plain sediments in a forest setting of mainly Loblolly pine (*Pinus taeda*). In all three soils, the SOC levels are (as expected) highest in the surface (A) horizons and decrease regularly with depth. In the Downer and Glenelg soils, the SOC levels decrease more rapidly with depth (which is common on older mature soils with argillic horizons) such that the SOC in each successive horizon is between one half and one tenth of that in the horizon above. However, due to the alluvial nature of the Codorus soil (derived from eroded surface soil horizons, thought to be post-European settlement in age), there is more organic carbon in the subsoil horizons which are close to 1% SOC.

With Glenelg soils being derived from crystalline rocks and Codorus soils formed in alluvium eroded from Glenelg type landscapes, both are ultimately derived from Piedmont materials, and thus, they are both somewhat elevated in extractable Fe and Mn. In contrast, the Downer soil, derived from highly weathered, coarse-textured coastal plain sediments, has much lower levels of extractable Fe and Mn. Even so, the Mn content in the Downer A horizon is substantially higher than the deeper horizons, which is likely the result of biocycling of this essential plant nutrient (Herndon et al., 2015).

Table 3-1. Characteristics of the pedons used in microcosm experiments. Texture determined by feel in the field. pH measured on 1:1 soil-water slurry. Soil organic carbon content (SOC%) obtained via dry combustion and dissolved organic carbon content (DOC%) via water extraction. Fe and Mn content obtained via dithionite-citrate extraction.

Pedon	No.	Horizon	Depth (cm)	Texture	pH	SOC%	DOC%	DOC/SOC (%)	Fe%	Mn%	Fe:Mn
Codorus	1	A	0-10	SL	6.22	1.4	0.024	1.75	1.04	0.037	28
	2	Bw1	45-60	LS	5.75	1.2	0.012	0.97	2.40	0.078	31
	3	Bw2	80-95	LS	6.03	0.88	0.007	0.75	2.57	0.086	30
Downer	1	A	0-10	SL	4.08	2.1	0.031	1.49	0.39	0.013	30
	2	AB	10-20	SL	4.33	0.68	0.010	1.41	0.38	0.003	127
	3	Bt1	25-40	SL	4.44	0.25	0.007	2.87	0.44	0.001	440
Glenelg	1	A	0-10	L	5.69	3.3	0.044	1.36	2.84	0.19	15
	2	AE	10-23	L	5.01	1.4	0.010	0.72	2.86	0.15	19
	3	BC	80-100	L	4.88	0.11	0.002	1.58	4.71	0.12	39

3.3.2 Saturated microcosms under laboratory temperatures

3.3.2.1 General observations

The Mn and Fe concentrations measured across time for the three horizons of each pedon are displayed in Figure 3-1. Generally, more Mn and Fe are mobilized into the porewater through the course of the experiment. However, in the surface horizons which have more SOC, the total amount of these reduced metals seems to plateau between 4 and 6 weeks. Ponnamperuma et al. (1969) observed a plateau (with no-added OM) or decrease (with added OM) in porewater Mn concentrations during a 15-week greenhouse study (a rice seedling was planted in each pot). They attributed the plateau or decrease in Mn to the precipitation of $MnCO_3$ (although they had no definitive confirmation that this phase was present). When evaluating the coupling between Fe and arsenic (As) reduction, Weber et al. (2010) also observed that the rate of Fe reduction decreased after >20 days of saturation. They suggest multiple possible explanations, including the depletion of readily bioavailable Fe, increased adsorption of Fe^{2+} on the surface of Fe(III) oxides, and/or as the result of microbial toxicity with increased mobilization of Fe and As. It is reasonable that any of these potential processes might affect the concentrations in surface horizons more so than the subsoil horizons, as the A horizons were not carbon limited and thus resulted in faster reduction rates and higher metal concentrations (Table 3-2) compared to the subsoil horizons. Additionally, the potential causes of the plateau may have been exacerbated in the microcosm setup due to negligible water flow.

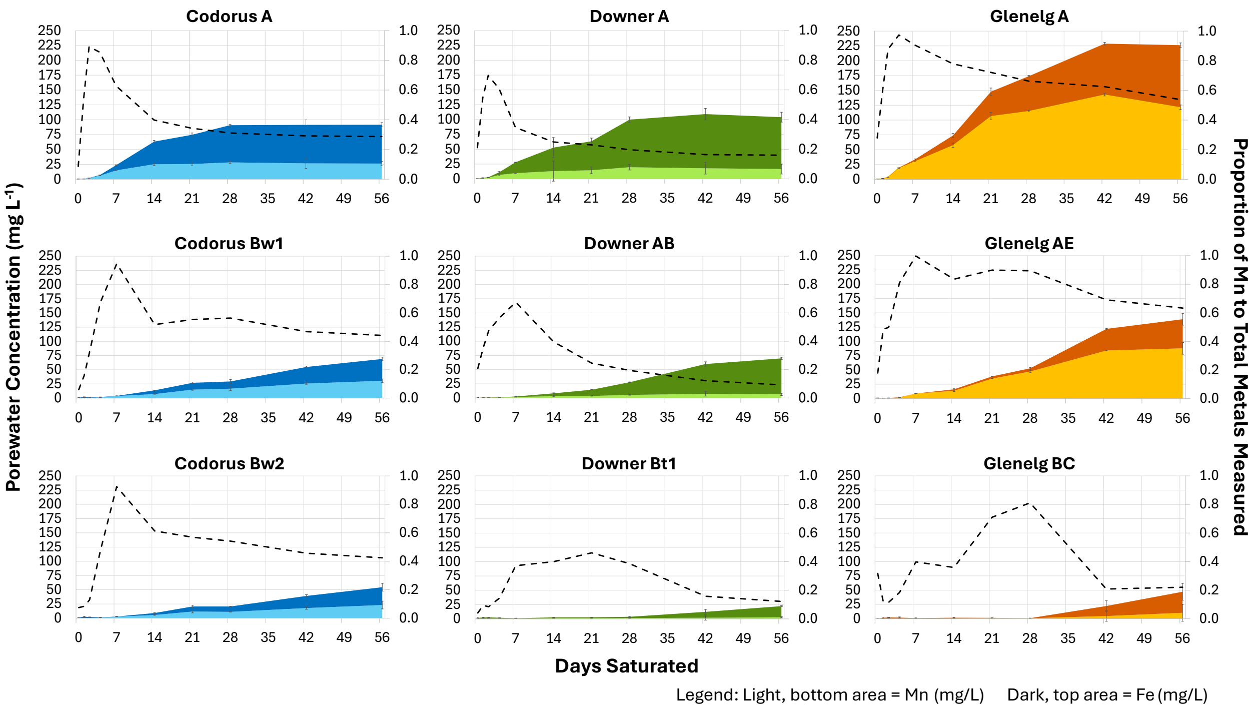

Figure 3-1. Stacked area graphs show the Mn and Fe porewater concentration (mg L-1, left axis) for warm temperature (mean of 21.3°C) experiment. [Mn] is displayed as the light shade (bottom) and [Fe] is the dark shade (top). The dashed line (right axis) represents the proportion of [Mn] in the porewater to the sum of [Mn] and [Fe] in the porewater. Overall, mobilization of reduced Mn and Fe decreases with soil depth (as SOC% decreases) and increases with time (longer saturation).

In nearly all soils and horizons, the initial reduction and mobilization of Mn seems to be substantially greater than Fe. This is illustrated by the dashed lines in Figure 3-1, which shows the proportion of [Mn] to [Mn+Fe] in solution. During the first few weeks of soil saturation, Mn remained dominant. However, as the reactions proceeded, the proportion of [Mn] to [Mn+Fe] in the porewater extracts decreased. This suggests that the anaerobic microorganisms, which initially favored the reduction of Mn, began to shift in favor of Fe reduction. The exact timing of when this shift occurs varies by horizon and by soil. The shift generally occurred the fastest in A horizons and more slowly in the subsoil horizons, as illustrated by the location of the peak (dashed line) representing the maximum [Mn] to [Mn+Fe] ratio. For a given soil, the peak appears to shift later (to the right) with deeper horizons, suggesting that this might be related to a decrease in availability of oxidizable carbon.

Table 3-2. The rate of Mn and Fe mobilization into the porewater under warm (mean of 21.3°C) temperatures, as shown by 1) the linear slope to either plateau or maximum concentration and 2) the number of days to reach a concentration of 3 mg L-1.

			Mn		Fe	
Pedon	**No**	**Horizon**	**Linear Slope to Plateau ($mg\ L^{-1} day^{-1}$)**	**Number of Days to 3 $mg\ L^{-1}$**	**Linear Slope to Plateau ($mg\ L^{-1} day^{-1}$)**	**Number of Days to 3 $mg\ L^{-1}$**
Codorus	1	A	1.91	2.5	2.57	5
	2	Bw1	0.56	6	0.78	10
	3	Bw2	0.42	8	0.63	13
Downer	1	A	1.37	2.5	3.16	3
	2	AB	0.17	14	1.39	11.5
	3	Bt1	0.05	56	0.62	29.5
Glenelg	1	A	5.44	2	2.07	7
	2	AE	2.16	4.5	1.62	16
	3	BC	0.34	35	1.31	30

The rates of Mn and Fe mobilization are reported in Table 3-2 in two ways: 1) as the linear slope ($mg\ L^{-1}\ day^{-1}$) to the plateau or maximum concentration, and 2) as the number of days required for porewater levels of Mn and Fe each to reach 3 $mg\ L^{-1}$. In all soils, the slope decreases and the number of days to the 3 $mg\ L^{-1}$ threshold increase in deeper horizons. This suggests that the rate is probably primarily a function of the amount of SOC present. As described earlier, for a given soil, the maximum porewater Mn and Fe are in the A horizon and they decrease with depth. The most straightforward explanation is that this is related to the availability of oxidizable OC. However, in the case of the Downer soil, where extractable Mn decreases dramatically with depth, the availability of Mn oxides may also affect the levels observed in the porewater.

3.3.2.2 Observations specific to soil series

Codorus

The reduction and mobilization of Mn in Codorus remained moderately high (23.1 to 30.5 mg L^{-1}) through all the horizons (Figure 3-1). The amount of porewater Fe also remained moderately high (31.3 to 65.4 mg L^{-1}) but did decrease by nearly half between the A horizon and subsoil horizons. The subtle decrease with depth in the combined porewater Mn and Fe is probably best explained by the SOC level, which decreases with depth (but not as dramatically as the other soils studied). Dissolved OC largely represents a more available or labile form of carbon (Bolan et al., 2011; Haynes, 2005), and the proportion of DOC is highest in the A surface horizon (Table 3-1). Thus, the nature of the organic carbon (as well as the quantity) may help explain the greater amount of mobilized Fe and Mn at the surface.

In Codorus, the rate of mobilization for both Mn and Fe slows down in deeper horizons (Table 3-2). When comparing total levels of Mn and Fe solubilized, the slopes for Fe are greater than Mn because the porewater Fe concentrations became higher than those for Mn. On the other hand, during the initial stages, Mn mobilization occurred faster than Fe in all horizons (as evidenced by the days required to reach 3 mg L^{-1}). This was expected based on the somewhat sequential nature of Mn oxides reducing before Fe oxides.

The patterns of IRIS paint removal (Figure 3-2) for Codorus show that Mn paint was generally removed sooner than Fe paint. It has been reported in both field (Rabenhorst et al., 2021) and lab (Dorau & Mansfeldt, 2015) studies that coatings are removed from Mn IRIS more rapidly than Fe coatings, which is also consistent with expectations based on Eh-pH diagrams (Takeno, 2005). Just as the rates of porewater Mn and Fe mobilization decreased with increasing horizon depth (Table 3-2), there was also a delay in the onset and decrease in the amount of removal of both Mn and Fe IRIS paint with increasing horizon depth. The difference in Mn and Fe reduction between the horizons, especially between Bw1 and Bw2 (Figure 3-2 C2 and C3), is more distinct in the IRIS images than in the porewater data. Mn paint removal is first observed in the Bw1 and Bw2 horizons on day 4, but there is complete paint removal from the Bw1 in 14 days, while in the Bw2, some Mn paint remains even after 56 days. Similarly, Fe paint removal in Bw1 can be seen within 14 days, while it takes 21 to 28 days to see the same thing in Bw2.

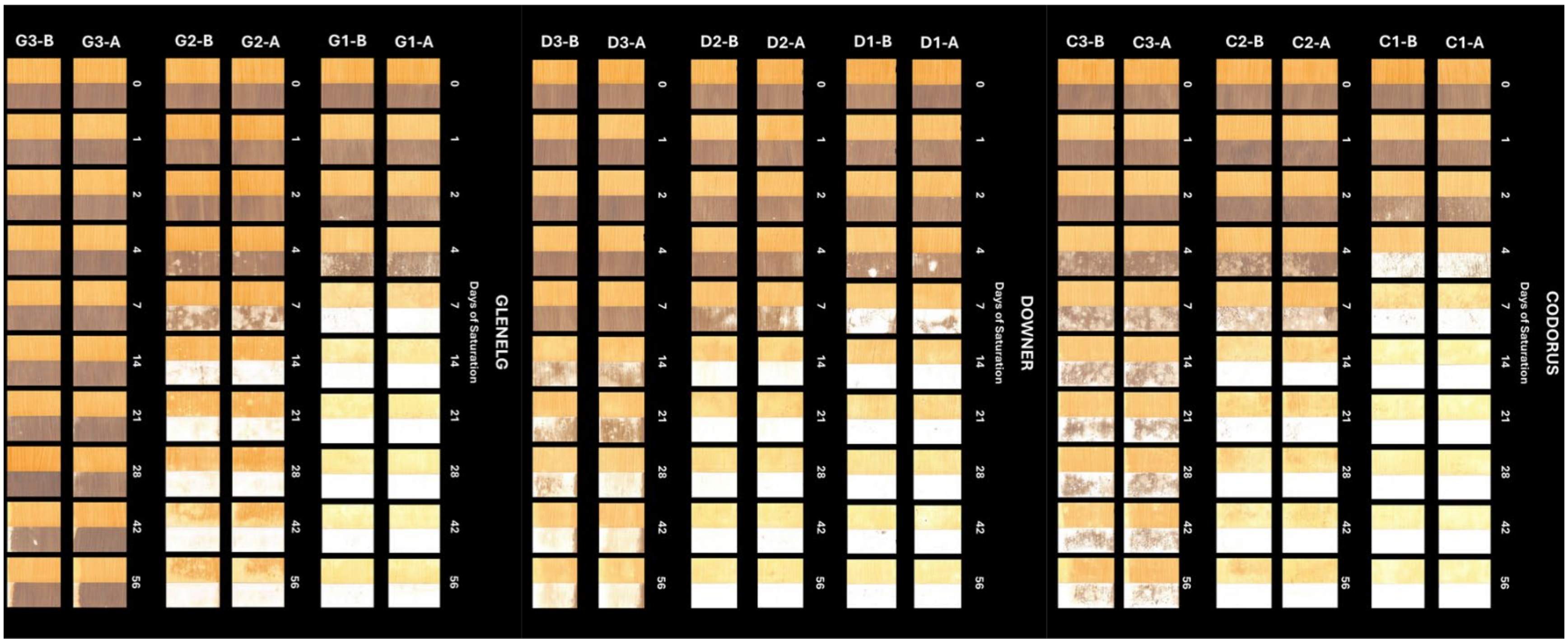

Figure 3-2. Scans of Indicator of Reduction in Soils (IRIS) films (left Fe, right Mn) for horizons 1, 2, and 3 for each of the three soils (Codorus, Downer, and Glenelg) under warm conditions (21°C). Films were removed at 10 sampling dates (days shown). Duplicates (A or B) shown in paired rows. IRIS paint removal (white or lighter colors) is the result of the reduction and dissolution of the Fe or Mn oxide minerals in the paint.

Downner

The total porewater concentration of Mn (2.7 to 19.6 mg L^{-1}) and Fe (19.5 to 91.3 mg L^{-1}) in the Downer soil steadily decreased with horizon depth (Figure 3-1), which is probably associated with the decrease in SOC with depth (Table 3-1). At the conclusion of the experiment, there was more Fe than Mn observed in the porewater in all horizons, and the proportion of [Mn] to [Mn+Fe] decreases with depth. The Downer soil has low levels of both extractable Fe and Mn compared to the other soils, and there is an especially dramatic decrease in extractable Mn with depth that is reflected in unusually high extractable Fe:Mn ratios (Table 3-1). Therefore, the low level of extractable Mn is likely the main reason why the Downer porewater Mn concentrations are so low. The much larger levels of porewater Fe compared to Mn in Downer may be related to the limited amount of Mn native to the soil, while the combined amount of Fe and Mn mobilized into each horizon may be related to the amount of SOC.

The rate of Fe and Mn mobilization in Downer decreased with horizon depth (Table 3-2). Similarly to Codorus, the slope of Fe mobilization for each horizon is higher than the slopes for Mn mobilization because there was much more porewater Fe mobilized compared to Mn. In contrast to Codorus, Mn mobilization rate (in terms of days to 3 mg L^{-1}) was slower than Fe mobilization, except in the A horizon. This is probably due to the extremely limited amount of extractable Mn in the soil.

The rate of IRIS paint removal for both Fe and Mn decreased with horizon depth (Figure 3-2), as did the rate of mobilization into the porewater (Table 3-2). The oxide paint was removed faster and more completely from Mn IRIS compared to Fe IRIS. This corresponds to the dashed line of Figure 3-1, which indicates proportionally more Mn was mobilized into the porewater than Fe within the first week or so of saturation. However, the more rapid removal of Mn paint than Fe paint contrasted with the mobilization rates shown in Table 3-2, where porewater Fe concentrations reached 3 mg L^{-1} more quickly than the Mn concentrations. Additionally, the difference in porewater metal concentrations between the A and AB horizons (Figure 3-2 D1 and D2) is less visually obvious for the Fe IRIS films but is more pronounced in the Mn IRIS paint removal that occurs between 4 to 14 days of saturation.

Glenelg

Compared to the other soils, the concentrations of porewater Mn in the Glenelg horizons are exceptionally high but show a steady decrease with depth (Figure 3-1). In the A and AE horizons, there was more Mn (87.9 to 143 mg L^{-1}) than Fe (50.9 to 104.5 mg L^{-1}) mobilized, which is most likely due to the very high SOC and the very high extractable Mn in these horizons (Table 3-1). In contrast, very little Mn (10.4 mg L^{-1}) was observed in the BC horizon porewater, even though the amount of extractable Mn in that horizon was quite high (0.12%). Thus, we might expect that the especially low SOC in this horizon (0.11%) is likely limiting Mn reductive dissolution. However, given the low SOC%, the porewater Fe was still surprisingly high (36.8 mg L^{-1}). It is possible that, given the very high levels of extractable Fe (4.7%), the Mn oxides in this horizon were (to some degree) occluded within the Fe oxide phases, and thus not readily accessible by microbial reduction, leading to far greater mobilization of Fe than Mn.

As with Codorus and Downer soils, the rate of Fe and Mn mobilization into the porewater decreased with horizon depth (Table 3-2). As the porewater Mn concentrations were higher than Fe, the slopes to the concentration plateau were higher for Mn than Fe (unlike Codorus and Downer). Porewater Mn concentrations reached 3 mg L^{-1} much faster than Fe in the A and AE horizons. However, the rate of Fe mobilization was slightly faster than Mn in the BC horizon, which is not surprising, as there was so little Mn mobilized.

The removal rate for both Mn and Fe IRIS paint decreased with depth in the Glenelg microcosms, corresponding to the decrease in SOC. The low porewater metal concentrations in the third horizon also corresponded to the paint removal patterns from the IRIS films, as there was essentially no Fe paint removal and very little Mn paint removal up to 42 days of saturation. An interesting difference observed on the Mn films on days 42 and 56 was the presence of the orange Fe oxide precipitation (most clearly seen at the bottom of G3-A and -B). This phenomenon is the result of Fe^{2+} in the porewater abiotically reducing Mn oxides and reprecipitating as Fe oxides in the same location as the now reduced Mn oxide (Dorau et al., 2016; Dorau & Mansfeldt, 2016; Limmer et al., 2023). This mechanism indicates that Fe reduction occurred in the soil and that some amount of Mn mobilized into the porewater (at least the portion from the Mn IRIS) was reduced abiotically rather than microbially.

3.3.2.3 Comparisons between soils

The observed differences in porewater concentrations between the three soils seem to be best explained by the differences in the level of extractable metals, especially Mn. When comparing the concentrations in the A horizons between Codorus and Glenelg, Glenelg has much higher porewater Mn, but the amount of porewater Fe is comparable. The Glenelg A horizon is higher in both SOC (2.4 times) and extractable Mn (5 times) than the Codorus A, so both variables may contribute to the higher concentration of porewater Mn in the Glenelg A horizon. In the second horizon, there is more than double the porewater Mn in the Glenelg than in Codorus, but the porewater Fe concentrations are similar. Unlike in the A horizons, the SOC in the Glenelg AE (1.4%) is similar to the amount in the Codorus Bw1 (1.2%), but the extractable Mn in the Glenelg is about 2 times higher than in the Codorus. The level of extractable Mn in the soil may also explain the dramatically lower concentrations in Downer compared to the other soils.

To further assess the effect of carbon and quantity of extractable Mn and Fe on the reduction and mobilization of Mn and Fe under warm temperatures, a stepwise linear regression was used to assess the effects of soil properties on concentrations of porewater Mn and Fe after 14 and 56 days of saturation. The earlier stage of reduction was represented by day 14 concentrations because 1) the shift from Mn to Fe mobilization generally started to occur around this time, and 2) the concentrations of Fe and Mn (each) were at least 1 mg L^{-1} in essentially all soil horizons (except the Glenelg Bt1 with only 0.63 mg L^{-1} Mn). The regression analysis indicated that the amount of SOC (%) had a significant positive effect (p-value = 0.001, adjusted R^2 = 0.78) on porewater Mn after 14 days of saturation. Running the same test using DOC in place of SOC yielded similar results (p-value = 0.0013, adjusted R^2 = 0.79). Adding extractable Mn as a variable (with SOC%) did not have a major impact on the regression (p-value = 0.004, adjusted R^2 = 0.79), but interestingly, when the model included DOC and extractable Mn, the strength of the regression improved (p-value = 0.0004, adjusted R^2 = 0.90). Using porewater data at the end of the experiment (56 days), both SOC and extractable Mn contributed significantly toward estimating porewater Mn (p-value = 0.001, adjusted R^2 = 0.86), and substituting DOC for SOC had a minimal effect. Overall, these regressions support our observations that the amount of oxidizable carbon (primarily) and extractable soil Mn (secondarily) both positively affect the reduction/mobilization of Mn.

When applying regression tools to assess which variables might significantly affect Fe reduction and mobilization, we found that extractable Fe level did not contribute significantly during either time period, likely because it is so readily abundant. When examining the porewater Fe concentrations at 14 days, a regression model that included both SOC and extractable Mn was significant (p-value = 0.049, adjusted R^2 = 0.51). However, the effect of extractable Mn on porewater Fe was negative, while it had been positive for porewater Mn. Similar to the 14-day Mn analysis, substituting DOC for SOC offered modest improvements to the regression (p-value = 0.027, adjusted R^2 = 0.60). When porewater Fe was examined at the end of the experiment (56 days), only the amount of organic carbon as SOC (p-value = 0.002, adjusted R^2 = 0.74) or DOC (p-value = 0.0007, adjusted R^2 = 0.80) was a significant variable. Thus, during the initial stages of the experiment (first two weeks of saturation), the microcosms seemed to be dominated by the reduction and mobilization of Mn, which is promoted by higher levels of extractable Mn, but seemed to inhibit Fe reduction. As the period of saturation extends from two to eight weeks, the microcosms have already shifted mostly to the reduction and mobilization of Fe, and thus, the impact of soil Mn became less influential.

These regression models indicate that the availability of reactive carbon is key to Mn and Fe reduction in the soil. This is expected as it has long been documented that the microorganisms conducting dissimilatory reduction in the soil utilize (and thus decompose) organic carbon compounds during respiration (Ehrlich et al., 2016; Ponnamperuma, 1972). Besides saturation, the presence of oxidizable carbon has been considered one of the most important factors in establishing soil reduction in general (not only of Mn and Fe) (Vepraskas et al., 2016). The regression analysis helps us explain that the shift from predominantly Mn reduction to Fe reduction (visualized by the timing and width of the dashed line peak in Figure 3-2) takes longer to occur in deeper soil horizons because there is less available organic carbon.

The presence and amount of Mn oxides in the soil is also important, especially in the early stages of soil reduction; as Mn oxides are reduced, they appear to inhibit or retard the reduction of Fe oxides. After 7 days of saturation, the porewater Mn concentrations in the A horizons (Glenelg 30.62 mg L^{-1} > Codorus 14.83 mg L^{-1} > Downer 9.69 mg L^{-1}) correspond closely to extractable soil Mn (Glenelg 1.90 mg/g > Codorus 0.37 mg/g > Downer 0.13 mg/g) whereas the porewater Fe content of the three soils rank in the opposite order (Downer 18.26 mg L^{-1} > Codorus 8.8 mg L^{-1} > Glenelg 3.22 mg L^{-1}). Because there are more Mn oxides present in the Glenelg horizons, which are more energetically favorable for microbes to utilize as a terminal electron acceptor, the shift to predominantly Fe reduction occurs much later (if at all) (Figure 3-1). Other laboratory studies have also observed how Mn oxides limit the reduction of Fe oxides and mobilization of Fe into soil porewater (Ponnamperuma et al., 1965; Yuan & Ponnamperuma, 1966; Hammann & Ottow, 1974; Ehlert et al., 2014, 2016).

3.3.3 Saturated microcosms under cold temperatures

The concentration of Mn and Fe in porewater from microcosms maintained under cold (4.1 °C) conditions is displayed in Figure 3-3. As expected, the porewater Mn and Fe concentrations were strikingly lower than when maintained under warm (21.3 °C) conditions. The colder temperatures slow microbial activity and thus impede microbially mediated Fe and Mn reduction (Lovley, 1991; Ponnamperuma, 1972). When directly comparing the two experiments, the cold temperature slows down the reduction and mobilization of Fe and Mn enough that the concentration levels after 84 days are at or below the concentration levels achieved in 14 days of saturation under warm conditions (Figure 3-4). It is worth noting that although the mean soil temperature during this experiment (4.1 °C) was below biological zero (5 °C), which is a somewhat simplistic soil temperature concept that describes the temperature below which mesophilic soil microbes are relatively inactive (Rabenhorst, 2005), we still observed the reduction of Mn and Fe within the span of 84 days at this low temperature, especially in the A horizons. Other laboratory microcosm studies also found measurable concentrations of reduced Fe and Mn in the porewater at temperatures ≤5 °C (Weber et al., 2010; Hofacker et al., 2013; Sparrow & Uren, 2014).

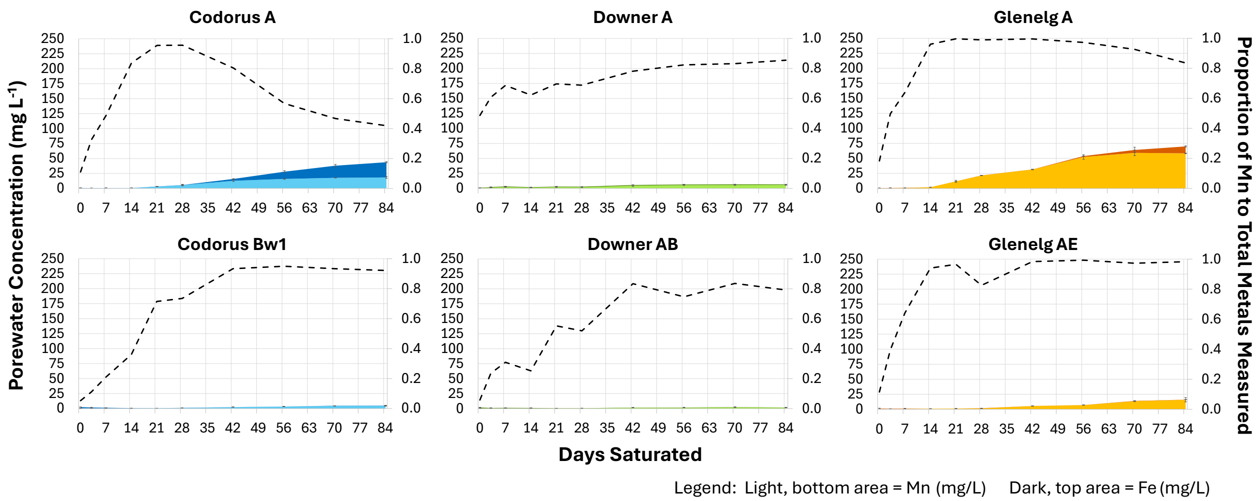

Figure 3-3. Stacked area graphs show the Mn and Fe porewater concentration (mg L^{-1}, left axis) for the cold temperature (mean of 4.1°C) experiment. [Mn] is displayed as the light shade (bottom), and [Fe] is the dark shade (top). The dashed line (right axis) represents the proportion of [Mn] in the porewater to the sum of [Mn] and [Fe] in the porewater. Overall, mobilization of reduced Mn and Fe decreases with soil depth (as SOC% decreases) and increases with time (longer saturation).

Table 3-3. The rate of Mn and Fe mobilization into the porewater under cold (mean of 4.1 °C) temperatures in terms of A) the linear slope to either plateau or maximum concentration and B) the number of days to reach a concentration of 3 mg L^{-1}. The rates of mobilization under cold temperatures were also compared to the rates under warm temperatures found in Table 3-2 as ratios. *Concentration levels did not reach 3 mg L^{-1} during the experiment period.

			Mn				Fe			
Pedon	**No**	**Horizon**	**Linear Slope to Plateau (mg L^{-1} day^{-1})**	Warm to Cold Ratio	**Days to 3 mg L^{-1}**	Cold to Warm Ratio	**Linear Slope to Plateau (mg L^{-1} day^{-1})**	Warm to Cold Ratio	**Days to 3 mg L^{-1}**	Cold to Warm Ratio
Codorus	1	A	0.44	4	21	8	0.45	6	42	8
	2	Bw1	0.08	7	56	9	0.01	78	*	
Downer	1	A	0.10	14	34	14	0.02	158	*	
	2	AB	0.03	6	*		0.002	659	*	
Glenelg	1	A	1.2	5	15	8	0.36	6	62.5	9
	2	AE	0.26	8	34	8	0.1	16	*	

As was also observed under warmer conditions, the A horizons with higher levels of SOC supported higher porewater Mn and Fe concentrations (Figure 3-3). When assessing the effect of soil properties via regression analysis, SOC had a positive and significant effect (p-value = 0.029, adjusted $R^2 = 0.67$) on Mn mobilization. Nevertheless, the drastically low levels of porewater Fe and Mn in the Downer A horizon, despite having higher SOC% than the Codorus A horizon, indicate that the extractable metal levels may also play a role in mobilization. Surprisingly, a model predicting porewater Mn that included both SOC and extractable Mn was not significant (p-value = 0.063, adjusted $R^2 = 0.74$), but when DOC was substituted for SOC (along with extractable Mn), the model was significant and explained the most variation (p-value = 0.028, adjusted $R^2 = 0.85$). DOC is generally considered a more accessible carbon pool for microbial degradation (Guo et al., 2020; Marschner & Kalbitz, 2003; Von Lützow et al., 2007) while total SOC would include less biodegradable forms. But since DOC and SOC strongly covary, both variables typically function largely the same. However, under these cold conditions where the microbes are far less active, this distinction between DOC and SOC might be more important. A similar improvement in the regression model after including both extractable Mn and DOC was also observed during the early stages (14 days) under warm conditions (Section 3.3.2.3). During further regression analysis, none of the variables appeared to contribute a significant effect on Fe reduction under cold temperatures. This may be due to the overall low concentrations of porewater Fe measured throughout the 84 days of saturation.

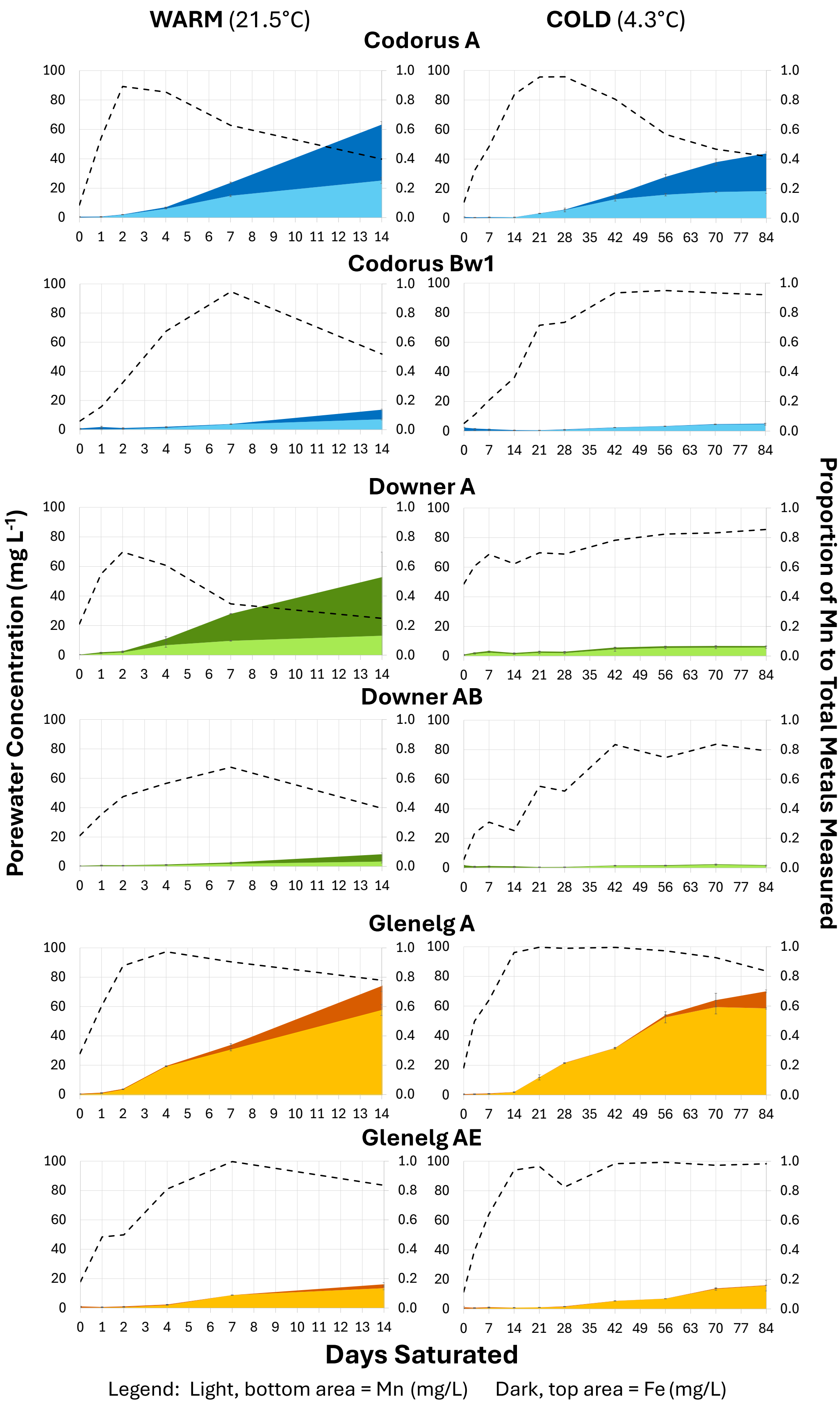

Figure 3-4. Stacked area graphs compare the Mn and Fe porewater concentration (mg L^{-1}, left axis) within 14 days of saturation under warm conditions (21.3°C, left column) and 84 days of saturation under cold conditions (4.1°C, right column). [Mn] is displayed as the light shade (bottom) and [Fe] is the dark shade (top). The dashed line (right axis) represents the proportion of [Mn] in the porewater to the sum of [Mn] and [Fe] in the porewater.

The effect of temperature on chemical and biological reactions has been known for a long time, and its initial recognition and documentation is generally attributed to Jacobus Henricus van't Hoff (E. A. Davidson & Janssens, 2006), who in his lectures on Physical Chemistry affirmed the generalization that "by far, the greater number of reactions double to treble their velocity for 10° rise in temperature" (van't Hoff, 1898). These ideas have been examined in a variety of ways and have been stated more recently using the concept of Q_{10}, a temperature coefficient which describes how much the rate of a biological or chemical reaction changes for each increase in 10 °C. While affirming that most published models use a simplified Q_{10} of 2, Meyer et al. (2018) measured Q_{10} values that ranged between 1.2 and 2.8, which seemed to be related to a variety of other soil properties. Others have also recognized that a Q_{10} of 2 is a generalization that is likely also affected by a variety of additional factors, such as soil moisture and the nature of the soil organic matter present (Conant et al., 2011; E. A. Davidson & Janssens, 2006). It is suggested by Kirschbaum (1995) that the Q_{10} for soil organic matter decomposition is itself temperature dependent, with observed Q_{10} values increasing at lower temperatures. His review of published work had Q_{10} at 0 °C averaging around 8, at 10 °C averaging around 4.5, and at 20 °C averaging around 2.5.

The number of days required for the porewater Mn and Fe to reach a threshold of 3 mg L^{-1} is shown in Table 3-3. The 17 °C difference between the warm and cold microcosms suggests that the Q_{10} value raised to the power of 1.7 should give us an approximation of the increase in reaction rates we might expect between the two treatments. Estimates of Q_{10} values by Kirschbaum (1995) for temperatures in the range of this study (2.5 to 6), lead one to expect that reaction rates under the warmer initial experiment would be somewhere between 5 and 20 fold greater than the rates in the colder second experiment.

Based on porewater Mn levels (3 mg L^{-1} ratio in Table 3-2), the Codorus and Glenelg soils (both horizons 1 and 2) experienced an 8 to 9 fold difference between the cold and warm microcosm reaction rates, and in the Downer soil (horizon 1), the difference was about 14 fold. As the simplified Q_{10} relationship represents a rough estimation, we conclude that these observations are in general agreement with expectations. The porewater Mn in Downer AB horizon did not reach the 3 mg L^{-1} threshold within the 84 days of the experiment under cold conditions. This was not surprising because under warm conditions, it required 14 days to reach this threshold, and a 9 or 14 fold difference would suggest that it might require 126 to 196 days to reach the threshold, which is longer than the duration of the experiment.

The porewater Fe data showed similar results, although, as mentioned earlier, the rates at which Fe mobilized to 3 mg L^{-1} are slower than for Mn. Surface horizons of the Codorus and Glenelg soils also showed an 8 to 9 fold difference in rates of Fe mobilization between the warm and cold conditions. The porewater Fe levels in the Downer surface horizon, however, did not reach the 3 mg L^{-1} threshold, which was surprising since using a 14-fold difference (as was observed for Mn in this horizon) would have predicted this would have occurred in approximately 42 days. The 3 mg L^{-1} threshold also was not observed for Fe in the second horizons of any of the three soils. This, however, was not surprising since the predicted times to reach the threshold (90, 161, and 144 days) are longer than the 84 days of the experiment.

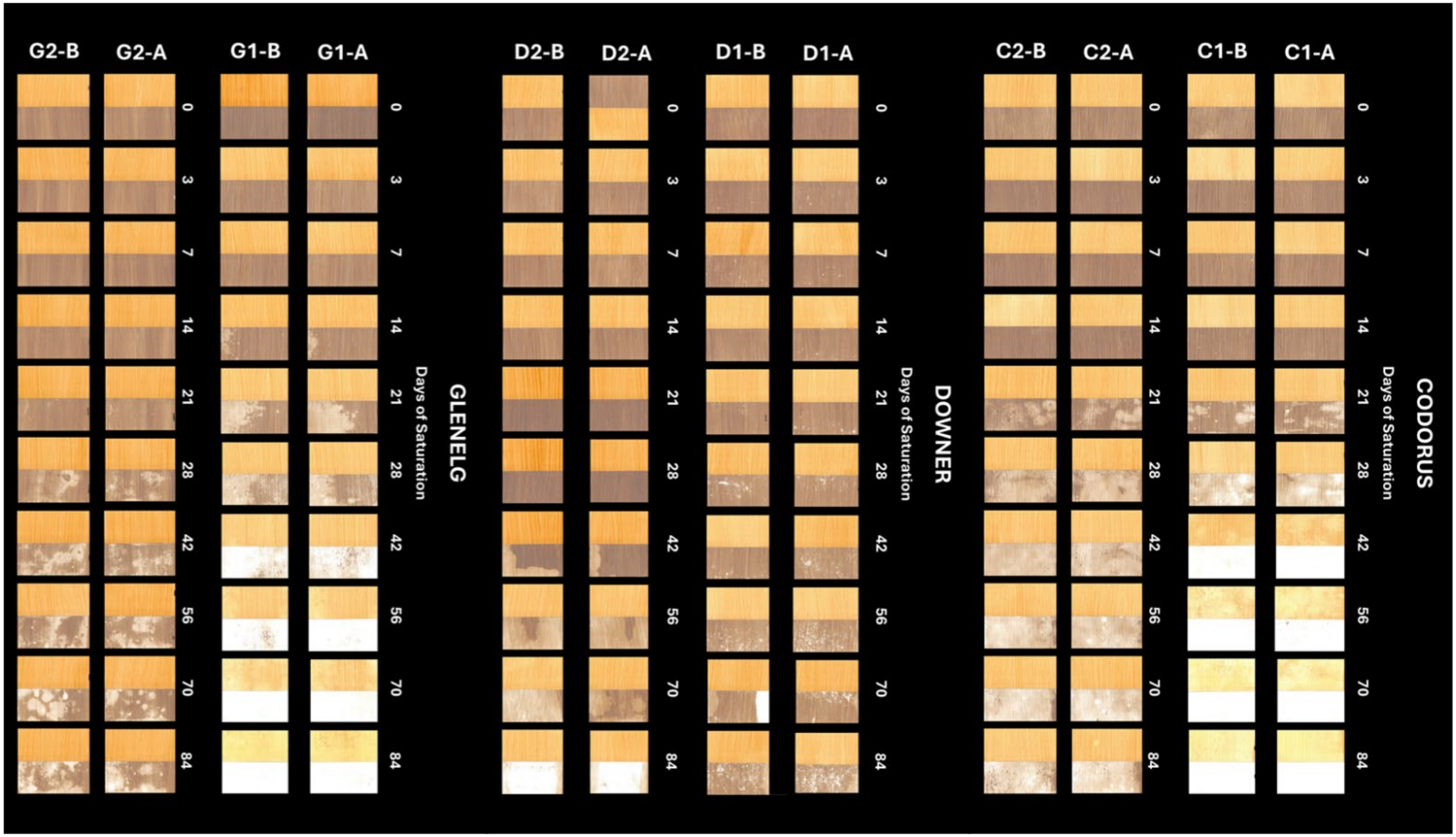

Figure 3-5. Scans of Indicator of Reduction in Soils (IRIS) films (left Fe, right Mn) for horizons 1 and 2 for each of the three soils (Codorus, Downer, and Glenelg) under cold conditions (4.1°C). Films were removed at 10 sampling dates (days shown). Duplicates (A or B) shown in paired rows. IRIS paint removal (white or lighter colors) is the result of the reduction and dissolution of the Fe or Mn oxide minerals in the paint.

Overall, Mn oxide paint removal under cold temperatures was delayed and/or diminished relative to warm conditions (Figure 3-3). This is consistent with the lower porewater Mn levels observed under cold conditions. Removal of Fe paint was even more limited than Mn, as noticeable paint removal only occurred in the Codorus and Glenelg A horizons. These horizons are also the only ones that had more than 3 mg L^{-1} of Fe mobilized into the porewater (25.5 and 11.5 mg L^{-1}, respectively) after 84 days of saturation (Table 3-3). The delay in IRIS paint removal, and the general decrease in paint removal under colder temperatures, especially for Fe, has also been observed in laboratory (Dorau et al., 2018) and field conditions (Chapter 2; Rabenhorst et al., 2021; Rabenhorst & Castenson, 2005).

There are a couple of instances where the patterns of paint removal in the Downer microcosms are a bit perplexing. It is surprising to see nearly complete removal of Mn paint for the AB horizon on day 84 (D2, Figure 3-5) since on day 84, porewater Mn was only 1.5 mg L^{-1} in this horizon. In contrast, the A horizon (D1), where the porewater concentration was 5.79 mg L^{-1}, had only minimal Mn paint removal. This unusual dissonance between the Mn paint removal and porewater concentrations may be due to the low Mn content of the Downer soil and possibly to differences in the nature of the Mn oxide phase in the soil and the birnessite on the IRIS films. Thus, the Mn of the birnessite paint seemed to be preferentially reduced over the soil Mn oxides.

3.3.4 Pedological Implications

In hydric soils, prolonged saturation must occur long enough in the upper part of the soil to form anaerobic conditions (Berkowitz et al., 2021). The upper part of the soil, particularly right near the surface, generally has the highest organic carbon content and is the most biologically active zone within the soil as it receives the most organic matter inputs from plant residues and other sources. As such, SOC and biological activity usually decrease with greater soil depth. The effect of available OC was highlighted in this study as porewater Fe and Mn concentrations for all three soils studied were the highest in the surface horizon and steadily decreased in deeper subsoil horizons. Thus, when fully saturated, surface horizons might have the highest capacity for soil reduction.

Saturation within a natural soil profile is also typically a function of depth, especially in soils that experience endosaturation. Longer periods of saturation generally occur deeper in the soil profile where there is less SOC. Therefore, even though the rate of reduction and mobilization of Fe and Mn is slower in deeper horizons due to less SOC, the development of anaerobic conditions, and thus, reduction of Fe and Mn may occur more often in this deeper part of the profile.

Soil temperature fluctuates with seasonal changes in air temperature across the year, and the rate of temperature change is quickest at the surface and decreases with soil depth. Additionally, global soil temperature also generally follows the distribution of global air temperature as it is highest around the equator and decreases towards the poles and with increased elevation. We saw the strong influence of temperature with the dramatic decrease in both porewater Mn and Fe concentrations in microcosm incubated under cold (4.1 °C) conditions. This indicates that in saturated soils, the intensity of soil reduction (as affected by temperature) may be seasonal, and may also be dependent on the geographic location. Furthermore, we observed that Fe reduction was suppressed far more than Mn reduction in cold soil conditions. As Fe reduction may be limited in wet soils located at high latitudes , in alpine environments, or in the early growing season, using Fe-reduction-based methods may not be the best way to document anaerobic conditions. Rather, Mn-reduction-based methods such as Mn IRIS may be a better option.

3.4 CONCLUSIONS

This microcosm study set out to assess the effects of the length of saturation, soil organic carbon content, and temperature on the rate and quantity of Mn and Fe reduction. Through the duration of the experiment, concentrations of metals increased in all soils and horizons. Higher rates of mobilization were observed in SOC-rich surface horizons, and the concentrations of both Mn and Fe were observed to be greater in horizons where SOC levels were higher. In the SOC-rich surface horizons, metal concentrations seemed to plateau and stabilize, while Mn and Fe concentrations in the deeper horizons continued to rise steadily through time. Several possible explanations for the plateau in metal concentrations in the surface horizons include a possible depletion of bioavailable forms of Mn and Fe oxides, the increased adsorption of Mn^{2+} and Fe^{2+} on surfaces of remaining oxides, or an induced microbial toxicity caused by high porewater levels of Mn and Fe. The stagnant nature of the saturated microcosms may have exacerbated these potential causes.

The availability of oxidizable carbon seems to strongly regulate the rate of porewater Mn and Fe mobilization. The decrease in SOC (and DOC) levels with greater depth corresponded to the decrease in Fe and Mn mobilized into the porewater. The larger quantity of SOC in the third horizon of Codorus (Bw2) likely contributed to the higher levels of porewater Fe and Mn than observed in the Downer and Glenelg microcosms. However, the differences in mobilization rates of Mn and Fe and differences in the concentrations of observed porewater Mn and Fe between soils are likely influenced not only by SOC but also by the amount of extractable Mn. The Glenelg A and AE horizons had some of the highest amounts of both SOC and extractable Mn, which resulted in high porewater metal concentrations compared to the other soils. Additionally, the quantity of Mn oxides present in the soil seems to be a key factor during the early stages of soil reduction and may affect the transition from Mn to Fe reduction. During the early stages of soil reduction (days 0–14), regression analysis suggests that both SOC and extractable Mn may govern Mn and Fe mobilization. However, as reduction processes proceed later in the experiment, extractable Mn no longer significantly affects Fe mobilization as the microbial community seems to have shifted to primarily Fe reduction.

The positive influence of warmer temperatures (average 21.3 °C) on the rates and magnitude of reduction processes was highlighted by the overall higher concentration of porewater Fe and Mn produced under warmer temperatures compared to colder temperatures (4.1 °C). Under cold temperatures, the lag time between the start of saturation and the onset of reducing conditions greatly increased, and the delay was especially seen in low Fe concentrations that in most cases did not reach 3 mg L^{-1} within 84 days. The delay in mobilization, as well as other trends in porewater chemistry, were also generally reflected in the resulting Fe and Mn paint removal patterns from IRIS films. IRIS films were shown to be useful in this experimental microcosm study to provide visual documentation of reducing soil conditions relative to Mn and Fe oxide phases. The removal of IRIS paint also seems sensitive to the same environmental drivers as the porewater concentrations.

While this study was limited to three soil series, the findings provide deeper insight into the influence of saturation, temperature, and SOC on reduction dynamics in soils by directly measuring Mn and Fe porewater concentrations coupled with observations of IRIS paint removal. The scientific community has become increasingly aware that Mn and Fe redox reactions are involved in or influence a complex web of reactions in the soil, water, biota, and atmosphere. The IRIS method has the potential to help researchers and practitioners better understand the role soil reduction plays in the cycling of nutrients, contaminants, and greenhouse gases.

Chapter 4: Effect of Mn oxide additions on soil Fe and Mn reduction

4.1 INTRODUCTION

Iron (Fe) and manganese (Mn) oxides are common in soils and can be dramatically altered by electron transfers during reduction-oxidation (redox) reactions in the environment. The redox sensitivity of Fe and Mn oxides makes these minerals especially influential in the biogeochemical cycles of carbon, various nutrients, and contaminants (Lovley et al., 2004; Reddy et al., 2022). During periods of prolonged soil saturation, anaerobic and reducing soil conditions commonly develop as the diffusion of O_2 into the soil is outpaced by the microbial consumption of O_2 during aerobic respiration. As O_2 is depleted, facultative and obligate anaerobic microorganisms utilize alternative terminal electron acceptors such as Mn(III/IV) and Fe(III) oxides when oxidizing organic carbon to carbon dioxide. The *redox ladder* or *sequence* represents the generalized and theoretical order in which these electron acceptors are utilized and become reduced, based on thermodynamics (McBride, 1994; Sapkota et al., 2022). Mn(IV) oxide reduction generally occurs after denitrification and before Fe(III) oxide reduction. Both insoluble Mn(IV) and Fe(III) oxides may be reduced to soluble Mn^{2+} and Fe^{2+} primarily by metal-reducing microorganisms (Reddy et al., 2022), although, abiotic processes can also be involved. Most notably, Fe^{2+} present in the soil solution can become oxidized while reducing Mn(III/IV) oxides (Loffredo et al., 2023; Lovley & Phillips, 1988).

The sequential nature of soil reduction, as predicted by thermodynamics, is largely based on the assumption of the soil system being in equilibrium. However, equilibrium is rarely achieved in natural environments. A number of studies have attempted to measure at what intensity of reduction (i.e., what soil redox potential, Eh) various electron acceptors, or other redox-sensitive compounds, are reduced (Gotoh & Patrick, 1972, 1974; McBride, 1994; Patrick, 1961, 1966; Patrick & Jugsujinda, 1992). These studies primarily measured and controlled the redox potentials of homogenized soil-water suspensions (reactors) to determine Eh thresholds for redox pairs. As described in McBride (1994), large discrepancies between theoretical and measured Eh thresholds for various redox pairs have been identified. While Mn oxides theoretically become reduced at much higher Eh than Fe oxides, the range of Eh values at which Mn and Fe oxides are observed to become reduced are much closer and even overlap, indicating that the reduction of Mn and Fe oxides in soil systems is not completely sequential (not all Mn oxides must be reduced before Fe oxides start to be reduced) (McBride, 1994). Nonetheless, Mn(III/IV) oxides generally do become reduced at substantially higher redox potentials (Eh) than Fe(III) oxides, and thus the reduction of Mn has been considered characteristic of "weakly reducing" conditions while the reduction of Fe is considered characteristic of "moderately reducing" conditions (Dorau & Mansfeldt, 2015; Sapkota et al., 2022).

The presence of more energetically favorable electron acceptors has been shown to inhibit the reduction of those less energetically favorable (Ponnamperuma, 1972). Even though Fe (2–550 g kg^{-1} of soil) is generally much more abundant than Mn (0.02–10 g kg^{-1}) (Essington, 2015), naturally higher concentrations of Mn oxides or added synthetic Mn oxides have been shown to impede the reduction of Fe oxides. The effect of Mn oxides on the reduction of Fe oxides has been explored in marine and freshwater sediments (Lovley & Phillips, 1988), as a remedy for physiologic disorders in rice (Ponnamperuma et al., 1965; Yuan & Ponnamperuma, 1966), and more recently, in moderating the release of heavy metals and contaminants such as arsenic (As) (Ehlert et al., 2014, 2016). In these studies, the synthesized Mn oxides used were directly mixed into the soil (birnessite - Ehlert et al., 2014, 2016; "MnO_2" - Ponnamperuma et al., 1965; Yuan & Ponnamperuma, 1966) or added as a slurry (Lovley & Phillips, 1988).

The redox chemistry of Fe and Mn is also important when assessing soil drainage and wetland soils. Fe and Mn oxides are strong pigments in the soil, with Fe oxides contributing yellow, orange, red, and brown colors while Mn oxides, when concentrated in masses, nodules, or concretions, contribute dark brown or black colors. The reduction of Fe and Mn oxides to soluble forms results in a visual change in the soil from these warm colors to gray as the underlying silicate clay minerals are exposed. This change in color following reduction and dissolution is the basis of the Indicator of Reduction in Soils (IRIS) technology. IRIS devices are usually constructed with a white substrate (i.e., PVC tube or sheet) and either an Fe oxide (ferrihydrite-goethite mixture) or Mn oxide (birnessite) "paint" is then applied. When the IRIS device is deployed in soils that develop reducing conditions strong enough to reduce Fe or Mn, the IRIS paint is "removed" via reductive dissolution (Sapkota et al., 2022). The amount and distribution of the oxide paint removal can be used to determine and document the presence of anaerobic conditions (Berkowitz et al., 2021). The removal of Mn paint from IRIS has been demonstrated to occur faster than Fe paint, as expected based on thermodynamics (Sapkota et al., 2022). The rate of IRIS paint removal has been studied in relation to the time saturated, temperature, soil pH, and soil organic carbon/matter content in laboratory and field studies. However, no studies (to the authors' knowledge) have looked at the effect of Mn oxide content on IRIS paint removal, nor in conjunction with measuring porewater Fe and Mn concentrations.

The objectives of this microcosm study are: 1) to assess the effects of Mn oxide content and duration of saturation on the reduction and mobilization of Fe and Mn into soil porewater, and 2) to compare the mobilization of reduced Fe and Mn in porewater with the removal of Fe and Mn IRIS paint.

4.2 MATERIALS AND METHODS

4.2.1 Soil collection and characterization

Approximately 20 L of the A horizon (0–10 cm depth) of three soil series were sampled in Maryland, USA (May and June 2023). Within Maryland and the greater Mid-Atlantic region, the Codorus and Glenelg series are common to the Piedmont, and the Downer series is common to the Coastal Plain, respective physiographic provinces. Bulk samples were air-dried, crushed, and sieved through a 2 mm sieve. To determine SOC, samples were homogenized and analyzed via high-temperature combustion using a LECO CH analyzer (Nelson & Sommers, 1996). As carbonate C is absent from these soils, total carbon was assumed to equal organic carbon. Total extractable Fe and Mn were determined using a modification of method 4G1 (dithionite-citrate extraction) (Soil Survey Staff, 2022) and then measured by flame atomic absorption (AA) spectrophotometry. Soil pH was determined on a 1:1 soil and DI water slurry using a glass electrode.

4.2.2 Mn oxide-coated sands

Mn oxide-coated sands were used as an amendment to increase the extractable Mn content (as birnessite) of the soils during the microcosm experiment. Using Mn oxide-coated sands better ensured that we enriched samples homogenously compared to when using small quantities of Mn oxide powders (Rabenhorst & Wardrup, 2024). The Mn-coated sands were synthesized using fine quartz fracking sand and 0.32 M $KMnO_4$ solution titrated to a ratio of 1.1 Na lactate: $KMnO_4$ according to Rabenhorst & Wardrup (2024). The Mn-coated sands contained 0.39% $HONH_2{\cdot}HCl$ extractable Mn.

4.2.3 Microcosm experimental design

The experiment consisted of 60 mL microcosms made from syringes designed to use with a mechanical vacuum extractor (Holmgren et al., 1977). Filter pads were placed at the base of the microcosms to retain the soil samples, and a miniature dual (half Mn and half Fe) IRIS film (80 mm wide by 102 mm long) was inserted to line the interior circumference of each microcosm (27 mm diameter by 135 mm high). IRIS films were painted with either Mn or Fe oxide paint (Rabenhorst & Burch, 2006; Rabenhorst & Persing, 2017) on 11” by 17” (27.94 cm by 43.18 cm) polyester sheets (5 Mil Waterproof Copy paper from TerraSlate Inc.). After painting, each Fe and Mn IRIS film was trimmed to size (40 mm wide by 102 mm long) and bound together on the unpainted side with a piece of vinyl tape.

Each microcosm was then filled with a homogenized mixture of 30 g of soil and 30 g of sand, which ranged in the proportion of uncoated and Mn-coated sand. The four treatments (uncoated sand: Mn-coated sand) included 30:0, 25:5, 15:15, and 0:30. Microcosms were saturated from below (to help exclude trapped air) over a one-hour period in basins of DI water. The water level in the basins was maintained just above the soil surface to ensure continued saturation. The microcosms were incubated at room temperature with an average temperature of 20.8 °C (ranging from 19.7 °C to 22.2 °C). Samples were analyzed destructively at 10 specified time points: day 0 (after 2 hours of saturation), and days 1, 2, 4, 7, 17, 21, 28, 42, and 56. Each combination of soil and treatment was run in duplicate for a total of 240 microcosms.

To collect the porewater, the saturated microcosms were transferred to the extractor and quickly connected to extracting syringes with a small piece of rubber tubing. Before the start of the extraction, any excess water ponded above the soil surface was removed. Extractions were run for 2 hours, although all the extractable porewater (which ranged from 4 to 11 mL) was usually collected within the first 20 minutes of the extraction. We estimated that this extracted portion represents approximately 20–30% of the total porewater (data not shown). The extracted porewater was acidified with 50 μL of 1 M HCl to keep metals of interest in solution. The porewater concentrations of Mn and Fe were determined using flame AA spectrometry. Standards and wash were proportionally acidified with 1 M HCl to match the sample matrix.

Immediately after the porewater extraction, the microcosms were disassembled, and the IRIS films were removed, rinsed with water, and air dried. Upon retrieval, the height of the soil surface was marked on each film. The films were then scanned to produce 300 dpi jpeg images, which were cropped to only include the area in contact with the soil.

4.3 RESULTS AND DISCUSSION

4.3.1 Soil and treatment characterization

Properties of the three soils used are shown in Table 4-1. The Glenelg soil (Fine-loamy, mixed, semiactive, mesic Typic Hapludults) was formed in residuum derived from crystalline micaceous schist and was sampled in a deciduous forested area. The Codorus soil (Fine-loamy, mixed, active, mesic Fluvaquentic Dystrudepts) was formed in alluvial deposits derived from upland soils (like Glenelg), which were weathered from metamorphic crystalline rocks. The Codorus soil was sampled in a floodplain under grass vegetation. The Downer soil (Coarse-loamy, siliceous, semiactive, mesic Typic Hapludults) formed in a stable landscape from sandy coastal plain sediments and was sampled in a forest setting of mainly Loblolly pine (*Pinus taeda*). With Glenelg soils being derived from crystalline rocks and Codorus soils formed in alluvium eroded from Glenelg-type landscapes, both are ultimately derived from Piedmont materials, and thus, they are both somewhat elevated in extractable Fe and Mn. In contrast, the Downer soil, derived from coarse-textured, highly weathered coastal plain sediments, has much lower levels of extractable Fe and Mn. The SOC content is higher in Downer and Glenelg compared to Codorus due to the forested vegetation.

Table 4-1. Characteristics of the soils used in microcosm experiments. Texture determined by feel in the field. pH measured on 1:1 soil-water slurry. Soil organic carbon content (SOC%) was obtained via dry combustion, and dissolved organic carbon content (DOC%) via water extraction. Fe and Mn content obtained via dithionite-citrate-bicarbonate extraction.

Pedon	Horizon	Depth (cm)	Texture	pH	SOC%	DOC%	DOC/SOC (%)	Fe%	Mn%	Fe:Mn
Codorus	A	0-10	SL	6.22	1.4	0.0243	1.75	1.04	0.037	28
Downer	A	0-10	SL	4.08	2.1	0.0313	1.49	0.39	0.013	30
Glenelg	A	0-10	L	5.69	3.3	0.0444	1.36	2.84	0.19	15

The amount of extractable Mn for each soil and treatment combination is presented in Figure 4-1. The figure also shows the percentile levels of Mn from 8000 surface soils analyzed at the USDA-NRCS Kellog Soil Survey Laboratory (Rabenhorst & Wardrup, 2024). The unamended Codorus, Downer, and Glenelg soils (that is, amended with only uncoated sand) were approximately equivalent to the 25th, 11th, and 78th percentiles, respectively. The addition of 5, 15, and 30 g of Mn-coated sand contributed 0.032%, 0.097%, and 0.195% Mn to the samples, respectively. Among the twelve soil-treatment combinations, three were below the median (50th percentile) and three were at or above the 95th percentile. The ratio of extractable Fe to Mn ranges from 30 to 1 across all soil-treatment combinations and decreases with larger additions of Mn-coated sand.

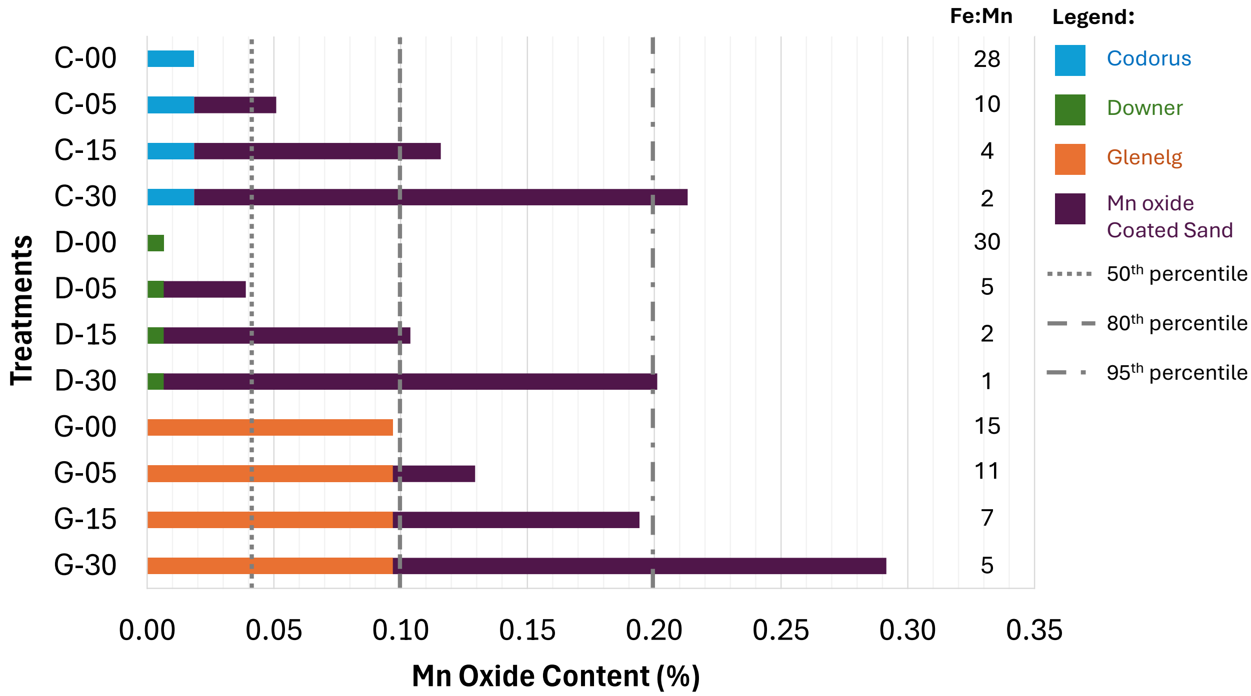

Figure 4-1. Mn oxide content (%) of the four treatment levels (0, 5, 15, and 30 g Mn-coated sand) for each soil (Codorus, Downer, and Glenelg). The amount of Mn oxide content contributed by the soil is shaded based on the pedon, and the amount contributed by the addition of Mn oxide-coated sands is shaded in dark purple. The Fe to Mn ratio for each treatment and soil is additionally listed on the right side of the graph. The 50th, 80th, and 95th percentiles calculated based on analysis of the dithionite-citrate-bicarbonate extractable Mn content of 8,000 soil surface samples from the USDA-NRCS Kellogg Soil Survey Laboratory (Rabenhorst & Wardrup, 2024).

4.3.2 Effect of Mn-coated sand on porewater Mn and Fe

4.3.2.1 Porewater Mn

The porewater Mn and Fe concentrations measured across time are displayed in Figure 4-2. For all soils, the concentration of porewater Mn is the lowest in the unamended treatment (0 g of Mn-coated sand added). The Glenelg soil (Figure 4-2 G-00), which contains the most extractable Mn and Fe (Table 4-1), had the highest concentration of porewater Mn (maximum of 117.9 mg L^{-1}) amongst the three soils. The Codorus soil (C-00), which has a moderate amount of extractable Mn and Fe, had much lower concentrations (23.7 mg L^{-1}) than Glenelg but the concentrations were slightly higher than those of Downer (D-00), which has a limited amount of extractable Mn and Fe and the lowest porewater Mn (17.2 mg L^{-1}). Thus, the differences in the levels of porewater Mn among the unamended soils seem, not surprisingly, to be related to the amount of extractable Mn naturally occurring in the soils.

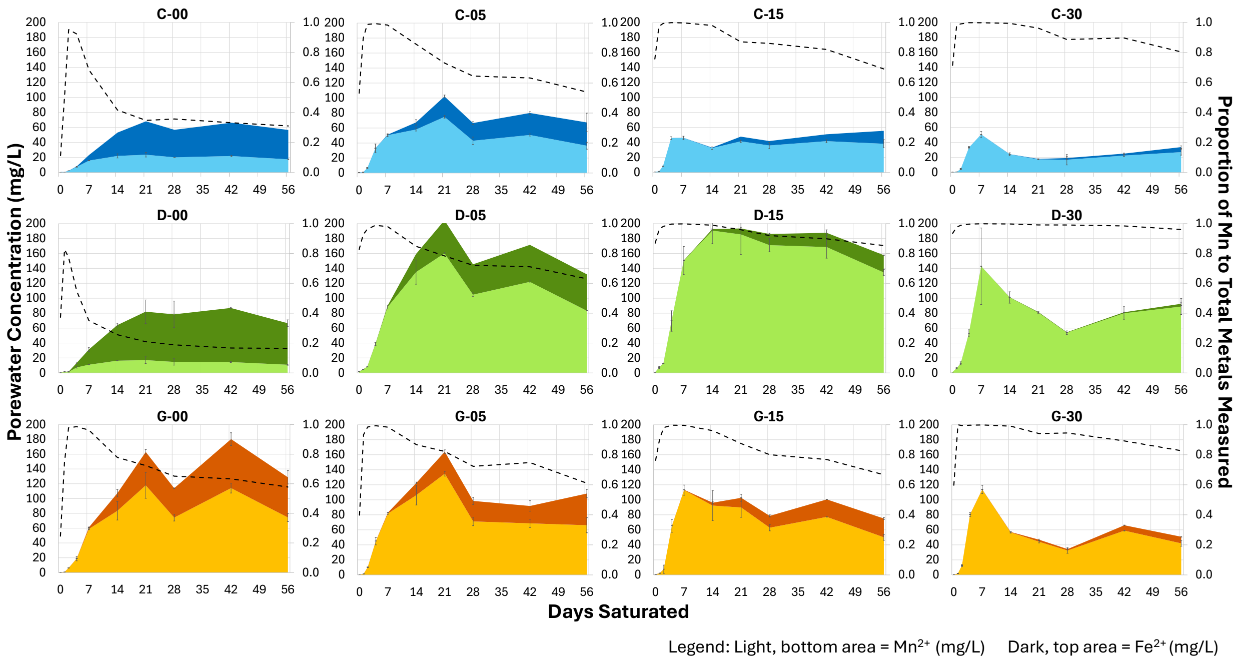

Figure 4-2. Stacked area graphs show the Mn and Fe concentrations (mg/L, left axis) in extracted porewater throughout the study period (56 days). [Mn] is displayed as the light shade (bottom) and [Fe] is the dak shade (top). Graphs are arranged by pedon (Codorus = top row, Downer = middle row, Glenelg = bottom row) and the amount of Mn oxide coated sand added (0, 5, 15, and 30 g columns). The dashed line (right axis) represents the proportion of [Mn] to the sum of [Mn] and [Fe] measured in the porewater throughout the study period.

When 5 g of Mn-coated sand was added, the maximum porewater Mn concentrations increased in all soils. The largest increase was seen in the Downer soil (D-05, 160.2 mg L^{-1}) while the Codorus soil had a modest increase (C-05, 74.9 mg L^{-1}), and the Glenelg soil had a minimal increase (G-05, 134.8 mg L^{-1}). The degree to which the 5 g of Mn-coated sand impacted the porewater Mn levels seems to be inversely related to the amount of extractable Mn in the soil. Interestingly, when 15 g of Mn-coated sand was added, the maximum Mn concentrations in the Codorus and Glenelg microcosms were somewhat diminished (C-15, 46.1 and G-15, 112.8 mg L^{-1}) while the Mn levels continued to increase in Downer (D-15, 190.6 mg L^{-1}). The maximum concentration recorded in the Downer soil is the highest Mn concentration measured in the entire study. When 30 g was added, the porewater Mn concentrations in all the soils were lower compared to those when 15 g was added. While the drop in porewater Mn in either the 15 or 30 g treatments was not anticipated, the maximum concentrations in these treatments (peak at 7 days of saturation) were still elevated compared to the unamended Mn concentrations found in Codorus and Downer or, for Glenelg, were comparable.

The rate of Mn mobilization is presented in Table 4-2, including rates at which porewater Mn levels are increasing during week 1 (slopes of lines relating concentrations with time), and the length of time (days) required for the porewater concentrations to reach/cross a threshold of 3 mg L^{-1}. The rate of Mn mobilization increased in all soils when 5 g of Mn-coated sand was added compared to the unamended soil as the slopes increased and the time required (days) to reach the 3 mg L^{-1} threshold decreased. The addition of higher levels (15 or 30 g) of coated sand generally resulted in rates within the first week that were similar to when 5 g was added. However, the peak in Mn concentration seems to occur earlier (Figure 4-2,) when more Mn-coated sand was added. In the unamended and 5 g treatment, the Mn porewater maximum generally occurred around day 21, but occurred by day 14 when 15 g was added and by day 7 when 30 g was added. Overall, the additions of reducible Mn oxides seem to promote the amount and rate of mobilization of Mn into the porewater within the first few weeks of saturation compared to the unamended soils.

Table 4-2. The rate of Mn and Fe mobilization into the porewater in terms of the linear slope (mg L-1 day-1) during the initial stages of reduction and the number of days to reach a concentration of 3 mg L-1.

Pedon	Mn-Coated Sand Added (mg)	Mn		Fe	
		Linear Slope (mg $L^{-1}day^{-1}$) days 1 to 7	Number of Days to reach 3 mg L^{-1}	Linear Slope (mg $L^{-1}day^{-1}$) days 7 to 21	Number of Days to reach 3 mg L^{-1}
Codorus	0	2.6	2.2	2.7	5
	5	8.3	1.4	1.9	9
	15	7.4	1.2	0.4	17
	30	8.3	1.5	0.04	43
Downer	0	1.6	2.6	3.2	3
	5	14.0	0.5	3.0	7.5
	15	23.9	0.3	0.5	15
	30	22.8	0.4	0.04	52
Glenelg	0	9.7	1.5	3.1	7
	5	13.4	1.3	2.0	8
	15	18.4	1.3	0.9	12
	30	18.6	1	0.2	31

Once the porewater Mn concentrations reached a maximum, in every treatment, concentrations either plateaued or decreased as the experiment continued. The concentrations in the unamended soils generally plateaued by day 21 (except Glenelg, where concentrations varied a bit more in the later part of the experiment compared to the other soils). In all soils, the additions of 5 and 15 g Mn-coated sand generally resulted in a steady decrease in porewater Mn after the peak. The addition of 30 g of coated sand resulted in a decrease after the 7-day peak but then, between 21 and 28 days, there began a steady increase during the second month of the experiment. The observed drop in porewater Mn levels could potentially be related to multiple processes. Birnessite, which is the mineral coating the sands, has a low point of zero charge (pH_{PZC} = 2.3–3.76) which describes the pH at which the net surface charge is zero. Thus, the Mn-coated sands have a net negative surface charge at a broad range of pHs and thus a greater ability to attract and retain cations (Essington, 2015, p. 398; Sparks et al., 2022, pp. 98–99). By adding more Mn-coated sand, we increased the affinity of soluble Mn to be sorbed to the remaining birnessite. Additionally, the pH in the microcosms likely increased throughout the experiment. Reduction reactions consume protons and thus generally raise the pH of more acidic soils (Ponnamperuma, 1972). Preliminary data suggests that the soil pH substantially increased within 14 days of saturation and remained high after 28 days (Appendix I). When 30 g of Mn-coated sand was added, within two weeks the pH in the Codorus, Downer, and Glenelg soils all increased by two full units, to 8.4, 6.9, and 7.8, respectively. After 28 days, the pH in the Codorus and Glenelg soil slightly decreased to 8.2 and 7.7, respectively, but the Downer soil continued to increase to 7.9. This significant increase in pH would increase the negative charge of minerals (like birnessite) carrying a pH-dependent charge and thus contribute to the increased sorption of cationic metals, organic matter, and microbial cells. Additionally, the significant rise in pH may have negatively affected the microbial community. Ehlert et al. (2016) found lower microbial activity with more birnessite additions in the soil, which they attributed to the rise in pH caused by the increased Mn concentrations caused by microbial Mn reduction in the soils with more birnessite.

The likely increased sorption of reduced Mn due to the rise in pH and the additions of Mn-coated sand might be masking the "true" amount of reduced Mn that was produced. When looking at the effect of redox potential on Mn fractions in soils, Patrick & Turner (1968) found the "easily reducible" Mn oxides decreased over a 40 day period of saturation and primarily converted to sorbed "exchangeable" Mn^{2+} (extracted 1 N ammonium acetate). However, the porewater Mn ("water soluble" fraction) did not increase and only made up a small fraction of the total Mn measured. As we did not conduct any additional extracts after collecting the porewater, we can only infer based on the porewater Mn and pH that there was likely exchangeable/sorbed Mn in these microcosms.

The development and effect of Mn toxicity to the metal-reducing microbial community may also contribute to the decrease in porewater Mn, especially in the highest additions (30 g) of Mn-coated sand. Mn is a required nutrient for microbes and can also be used to protect bacterial cells from oxidative stress (Waters, 2020). While we were unable to find Mn toxicity data for anaerobic microbes (which likely depends on the microbial strain), Mn^{2+} toxicity does reportedly occur in bacteria (Waters, 2020). Mn toxicity causes the mismetallation of enzymes and regulators, as well as generally disrupts the metal ion homeostasis in cells, which in severe excess is fatal to bacteria (Chandrangsu et al., 2017). When reviewing metal homeostasis in bacteria, Chandrangsu et al. (2017) also described that the metal uptake systems in metal-starved bacterium may become overactive and thus lead to metal toxicity when encountering a metal-rich environment. Also, the adsorption or precipitation of Mn^{2+} may negatively affect the microbial reduction of Mn oxides. The authors were not able to find any literature on the effect of Mn^{2+} adsorption on the dissimilatory reduction of Mn, but there is evidence of Mn^{2+} sorption onto Mn(II)-oxidizing bacteria (Vázquez-Ortega & Fein, 2017) and Fe(III)- and Mn(IV)-reducing species (Chubar et al., 2013). However, it has been suggested that Fe(II) compounds on Fe(III) oxides and bacteria cell surfaces may control the ability of Fe-reducing bacteria to enzymatically reduce Fe(III) oxides (Roden & Urrutia, 1999, 2002) but likely only occur at high concentrations (Hyacinthe et al., 2008).

When Ponnamperuma et al. (1969) saw porewater Mn concentrations plateau (when no OM was added) or decrease (with added OM) during a 105 day incubation, they attributed the plateau/decrease mainly to the precipitation of $MnCO_3$ (rhodochrosite). The accumulation of dissolved CO_2 from microbial respiration forms (bi)carbonate and, in the presence of Mn^{2+}, can lead to the precipitation of $MnCO_3$, especially at alkaline pHs (Ponnamperuma et al., 1969). The precipitation of $MnCO_3$ on birnessite was observed within 140 hours in an anaerobic Donnan reactor (Ying et al., 2011) and $MnCO_3$ was also precipitated on a novel synthetic amorphous Mn oxide in a pot study held at 80% water holding capacity (Ettler et al., 2014). In contrast, Ehlert et al. (2016) did not detect rhodochrosite with X-ray absorption spectroscopy (XAS) nor x-ray diffraction (XRD) analysis even though the formation was thermodynamically favorable, which they attribute to slow precipitation kinetics. While we have no means to confirm the presence of $MnCO_3$, the unexpected elevation in pH above 7 after 14 days (Appendix I) suggests this is another potential mechanism for the decrease in porewater Mn concentrations seen throughout the experiment. Furthermore, the influence of these possible processes on the plateau/decrease in porewater Mn may be exacerbated by the negligible water flow within the saturation basins. Roden & Urrutia (1999) found that advective removal of aqueous Fe^{2+} in semicontinuous cultures resulted in a significant increase in the amount of cumulative Fe^{2+} produced via microbial reduction compared to batches with no removal.

4.3.2.2 Porewater Fe

In all three soils, the unamended treatment produced the highest concentration of porewater Fe (Figure 4-2). Surprisingly, the Downer soil (D-00), which has a limited amount of extractable Mn and Fe (Table 4-1) and had the lowest porewater Mn concentrations, produced the highest concentration of porewater Fe (maximum of 72.5 mg L^{-1}) compared to the other soils. The Glenelg soil (G-00), which has the most extractable Mn and Fe and had the highest porewater Mn concentration, had slightly lower but comparable concentrations (66.2 mg L^{-1}) to the Downer soil while the Codorus soil (C-00) had the lowest concentration (44.6 mg L^{-1}).

The difference in porewater Fe concentrations between the unamended soils may be related to both the amount of extractable Mn and SOC content. The sharpness of the peak of the dashed line showing the proportion of [Mn] to [Mn+Fe] (Figure 4-2) may help interpret how quickly the microbial community shifted from primarily Mn reduction to Fe reduction in the microcosms. This peak for the unamended Downer soil (at day 1) is much narrower than the peak in the Codorus soil (days 2–7) and especially in the Glenelg soil (days 2–14). Additionally, the Downer soil reached 3 mg L^{-1} Fe in fewer days than the unamended Codorus and Glenelg soils (Table 4-2). This suggests that the Downer soil shifted from Mn to Fe reduction sooner than the other soils. Thus, there was more time during the experiment for Fe to be reduced and become mobilized into the porewater in the Downer soil compared to the other soils. If higher Mn oxide content in the soil has a negative effect on soluble Fe levels, then the low amount of extractable Mn in the unamended Downer soil would help explain why there are much higher porewater Fe concentrations than porewater Mn concentrations in Downer. The unamended Glenelg soil, which has nearly 15 times the amount of Mn and approximately 7 times the amount of Fe compared to the Downer soil (Table 4-1), was the slowest to reach porewater levels of 3 mg L^{-1} Fe and has a substantially broader peak of the [Mn] to [Mn+Fe] proportion line (Figure 4-2). This slight delay in the onset of Fe mobilization in the Glenelg soil could be explained by the high Mn content of the soil. However, the Glenelg soil still produced moderately high porewater Fe concentrations (compared to the Downer soil), even though it took more time for substantial Fe mobilization to occur, and the Mn oxide content is much higher in the unamended Glenelg compared to other soils. This suggests that Mn oxide content alone might not explain the differences in the porewater Fe concentrations between the soils. As discussed previously, SOC content, as the energy source for the microorganisms mediating these reactions, has been shown to be an important driver in soil redox reactions. The unamended Glenelg soil has the highest SOC% among the three soils (Table 4-1), and thus, may have enhanced Fe reduction and mobilization, even though it has such high Mn oxide content. The unamended Codorus soil has the lowest porewater Fe concentrations, even though it reached 3 mg L^{-1} Fe before the Glenelg soil. However, the Codorus soil has the lowest SOC% among all the soils and a moderate amount of Mn oxides, which together may have slowed Fe reduction and mobilization. The porewater trends in the unamended soils therefore suggest that higher levels of occurring naturally Mn oxides might deter the reduction of Fe, but this may also be mediated by other soil properties such as the SOC content.

When 5 g of Mn-coated sand was added to the microcosms, the porewater Fe concentrations decreased in all soils and continued to steadily decrease with further Mn oxide additions. Similarly, the rate of Fe mobilization decreased with more Mn oxides in all soils (Table 4-2). Hence, the lowest Fe concentrations for each soil were observed when 30 g Mn-coated sand was added. The strong and positive correlation between the amount of extractable Mn (%) present and the number of days required for the porewater Fe concentrations to reach 3 mg L^{-1} (Figure 4-3) further demonstrates the suppressive nature of Mn oxides on Fe reduction observed in unamended soil.

Our results are in line with previous laboratory studies, which explored the effect of Mn oxides on Fe reduction in soil. Using nutrient solutions containing suspensions of hematite and two strains of Fe-reducing bacteria, Hammann and Ottow (1974) observed that additions of MnO_2 almost completely suppressed Fe reduction. While exploring possible remedies for physiological disorders in rice caused by strongly reducing soil conditions, Ponnamperuma et al. (1965) and Yuan and Ponnamperuma (1966) noted that additions of MnO_2 delayed the decrease in Eh and lowered soluble Fe levels in the soil solution enough to improve rice growth. Ehlert et al. (2016) also observed a delay in the increase of aqueous Fe in extracted effluents when birnessite was added to contaminated soil in an attempt to limit As mobilization. These studies broadly support our observations that Mn oxides act as a negative control on the reductive dissolution of Fe oxides.

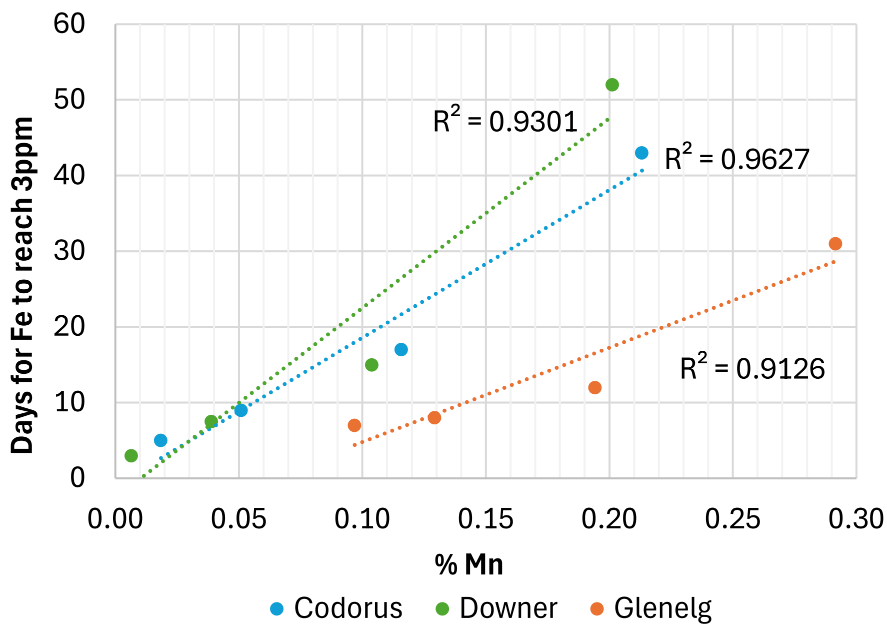

Figure 4-3. Scatter plot of the length of time (days) required for the porewater Fe concentrations to reach/cross a threshold of 3 mg L-1 (ppm) by the amount of extractable Mn (%) in each soil and treatment combination. The linear regression and corresponding R2 value were plotted for each soil.

In contrast to porewater Mn concentrations, the porewater Fe concentrations generally do not decrease over the course of the experiment. In the unamended soils, the Fe concentrations generally plateaued by day 28 (similar to the porewater Mn concentrations). However, even though there was a delay in the onset of Fe mobilization, and the maximum Fe concentration became lower as more Mn-coated sand was added in all soils, the amount of porewater Fe generally continued to increase with time for the duration of the experiment (clearer in Appendices H and J than Figure 4-2). This is rather surprising because the same reasons previously discussed regarding the decrease in porewater Mn concentrations (namely, the increased sorption due to more Mn oxides and higher pH and the microbial toxicity) would be expected to also affect porewater Fe concentrations in a similar manner. The reason for this discrepancy is not clear. It may be that the low levels of porewater Fe, especially in the 15 and 30 g treatment microcosms, are potentially low enough that we do not observe the effect of these other factors.

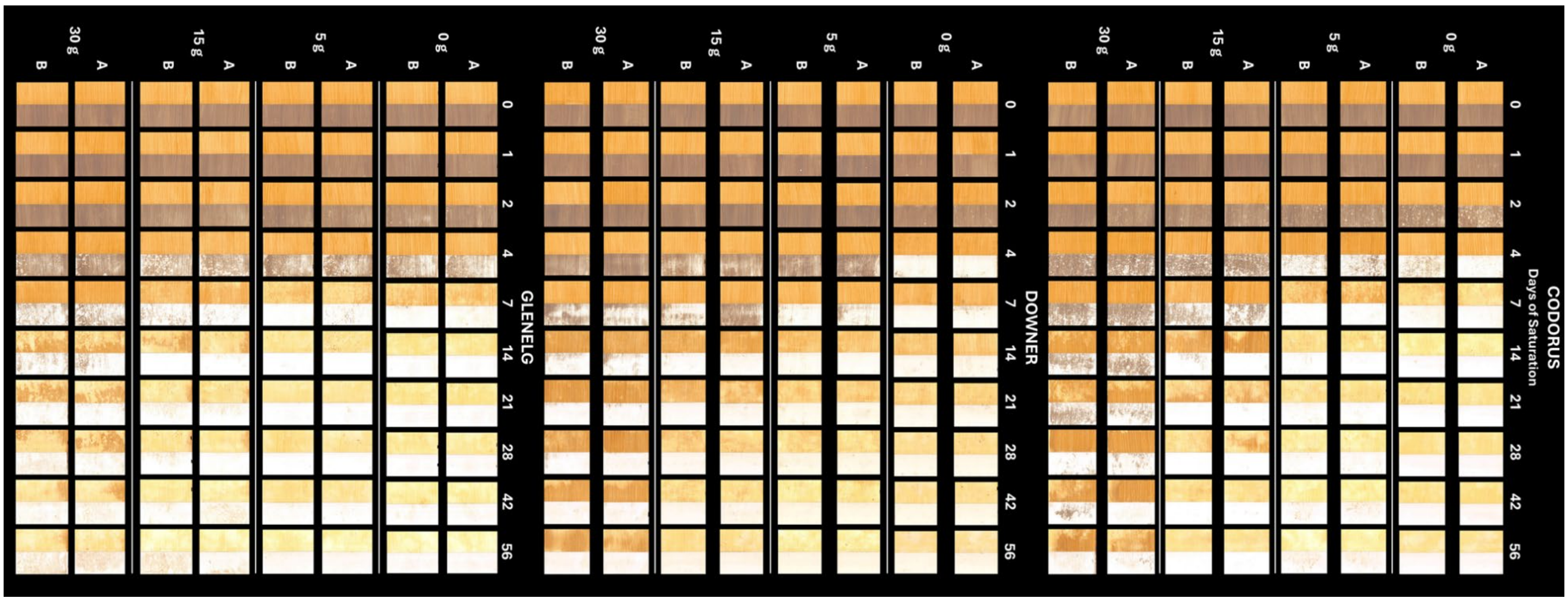

Figure 4-4. Scans of mini pairs of Indicator of Reduction in Soils (IRIS) films (left Fe, right Mn) for microcosms across time and separated by soil (Codorus, Downer, and Glenelg) and the amount of Mn oxide coated sand added (0, 5, 15, and 30 g). Duplicates are labeled as replicate A or B and paired in rows. IRIS paint removal (white or lighter colors) is the result of the reduction of the Fe or Mn oxide minerals of the IRIS paint.

4.3.3 Effect of Mn oxide additions of IRIS paint removal

Scans of the IRIS films from all microcosms are presented in Figure 4-4. When the Mn or Fe oxides in the IRIS paint are reduced, the paint dissolves, and this results in the paint color lightening or revealing the underlying film substrate. The Mn IRIS paint is generally removed entirely (exposing the white background), but on the Fe IRIS films, a lighter yellow color was persistent for the duration of the 56 days. The Fe IRIS paint is a suspension of both ferrihydrite and goethite (30–60% goethite) (Rabenhorst & Burch, 2006; Rabenhorst, 2013). Ferrihydrite, which has a redder hue, is reduced at slightly higher redox potentials than goethite, so the remaining lighter and yellower paint color may indicate that a small amount of goethite may persist even when the ferrihydrite (and some of the goethite) has been reduced (Rabenhorst et al., 2008; Schwertmann, 1993; Vepraskas et al., 2016). Also, there were a few instances of the development of an orange color on the Mn IRIS films. This orange color is the precipitation of Fe oxides caused by the simultaneous chemical reduction of Mn oxides and oxidation of porewater Fe^{2+} in solution (Limmer et al., 2023). Because the presence of Fe^{2+} demonstrates soil reduction, the formation of the Fe oxides (orange color) on Mn IRIS films is still indicative of soil reduction.

Overall, similar trends in IRIS paint removal were seen among all three soils. We observed that substantial Mn paint was generally removed after 4 to 7 days of saturation in the unamended soils. On the other hand, we began to observe the removal of Fe paint after 14 days of saturation in the unamended soils. Thus, the removal of Mn IRIS paint occurred earlier than the removal of Fe paint, as expected based on the thermodynamics of Mn and Fe reduction. Compared to the unamended soils, additions of Mn oxides to the microcosms resulted in some delay in the removal of the IRIS paint. The length of the delay was positively related to the magnitude of the Mn oxide additions, with the longest delay occurring under the highest level of Mn oxide added. When the soils were amended with 30 g of Mn-coated sands, the Mn paint started to be removed after 4 to 7 days, but nearly complete removal didn't occur until 14 to 28 days of saturation (depending on the soil). Therefore, compared to the unamended, substantial Mn paint removal was delayed on average by two weeks. The removal of Fe paint was more variable amongst the soils in the highest Mn treatment level. Visible Fe paint removal started after 14 days in the Codorus and Glenelg soil but 42 days in the Downer. Nearly complete Fe paint removal did not occur in any soil. The Glenelg and Codorus soils had substantial Fe removal after 42 and 56 days, respectively, while Downer did not within the 56-day period. Compared to the unamended soil, substantial Fe paint removal was delayed on average by five weeks. Overall, the removal of Fe paint was delayed and diminished to a much larger degree than the Mn paint.

When comparing the IRIS (Figure 4-4) and porewater (Figure 4-2) data, increased additions of Mn oxides resulted in an incremental delay and decrease in both the removal of Fe paint and the mobilization of Fe into the porewater. However, this is not true when looking at Mn reduction. The rate of porewater Mn mobilization during the first week of saturation (Table 4-2) is higher when Mn oxides are added, but in contrast, Mn paint removal is incrementally delayed. The delay in Mn IRIS paint removal was likely due to the soil microbes preferentially utilizing the increased amount of reactive Mn oxide material available within the amended soil, rather than the paint. Additionally, as IRIS paint removal is a cumulative measurement of soil reduction, the decrease in porewater Mn concentration throughout the experiment is not evident on the IRIS films. Therefore, the influence of birnessite additions on Fe IRIS paint removal parallels the influence on corresponding porewater concentrations more so than Mn IRIS paint removal.

The disconnect between Mn paint removal and porewater Mn mobilization in this study would likely not affect the interpretation of Mn IRIS films in the field, because Mn content in most soils is generally much lower than the levels tested in this project. Also, after 28 days of saturation, our results show there was complete (or nearly complete) removal of the Mn paint in all soil-treatment combinations. As the standard deployment period for IRIS films in the field is one month, the delay in Mn paint removal would likely not be evident.

4.4 CONCLUSIONS

Previous laboratory studies, which used either homogenized soils or diluted aqueous suspensions of soil or aquatic sediments, have shown that alternative terminal electron acceptors were generally reduced sequentially by microbes. Therefore, less energetically favorable compounds are generally reduced only once the more energetically favorable ones have been fully reduced. While the reduction of Mn oxides and Fe oxides can occur simultaneously, higher Mn oxide content (both natural and added) has also been observed to hinder the reduction of Fe oxides. In agreement with previous work, we found that increasing additions of reducible Mn oxide delayed the onset of Fe reduction and resulted in lower concentrations of porewater Fe in all three soils studied. However, even in microcosms with the highest amounts of added Mn oxides, the reduction and mobilization of Fe was not completely extinguished, and at least 3 mg L^{-1} porewater Fe was mobilized within 56 days of saturation.

Increased Mn oxide content seemed to promote the initial mobilization of Mn into the porewater. Moderate additions of birnessite resulted in higher concentrations of porewater Mn, especially within the first 21 days of saturation. However, with larger additions of Mn oxides, the measured concentrations of porewater Mn were generally lower than when amended with a moderate amount, but still higher than in the unamended soil. Furthermore, following an initial rise in porewater Mn levels during the first 1 to 3 weeks, the concentration of porewater Mn either plateaued or decreased over time in all soils. This phenomenon may be due to a rising pH during soil reduction. The high pH may have increased the affinity of soil solids (such as Mn and Fe oxides) to sorb aqueous Mn or possibly caused precipitation of a $MnCO_3$ phase. Additionally, a potential decrease in microbial activity, possibly due to unsuitable pH conditions or Mn toxicity, may have contributed to the plateau or fall of porewater Mn concentrations.

Fe and Mn IRIS films provided a visual and cumulative understanding of how the redox status of the soil was influenced by the presence of Mn oxides in this microcosm study. Mn oxide additions delayed and diminished the removal of IRIS paint, with the delay in Fe paint removal much more substantial than the delay in Mn paint removal. The delay and decrease in Fe paint removal when more birnessite was added closely resembled the delay and decrease in porewater Fe concentrations observed throughout the study. In contrast, additions of Mn oxides resulted in a moderate delay in Mn IRIS paint removal, while the additions had more dramatic and positive effects on porewater Mn concentrations during the first week of saturation. Thus, the trends in porewater concentrations were generally better reflected by Fe IRIS paint removal than that of Mn IRIS.

Natural variation in the proportion of Mn oxides and Fe oxides in the unamended soils seemed to have a dramatic effect on the dynamics between Mn and Fe reduction. While the Mn oxide content in some of the amended treatments may have been unrealistically high for natural soils, the additions of birnessite enabled us to better explore and illustrate effects of Mn oxides on soil reduction observed in natural soils. In summary, it is the amount of Mn oxides available for microbial reduction in the soil that may impact the degree to which Fe reduction and mobilization from soil and IRIS paint is impeded. As a result, Mn oxides may function to buffer or slow down the release of various compounds that may be sorbed to Fe oxides in the soil, and thus potentially have large impacts on soil and water quality as well as nutrient cycling.

Thesis Summary and Conclusions

The biogeochemistry and redox dynamics of Fe and Mn are often used to identify, delineate, and investigate soils characterized by prolonged saturation. First developed by Jenkinson (2002), Indicator of Reduction in Soils (IRIS) devices are an innovative way to visually document the reduction of Fe oxides, and more recently, Mn oxides as well as provide evidence of anaerobic soil conditions. While these redox-sensitive minerals tend to reduce sequentially (Mn before Fe) based on redox potential (Eh) and thermodynamics of each reaction, various environmental factors and soil properties have been shown to influence Mn and Fe reduction.

In Chapter 2, to evaluate the impact of saturation, soil temperature, and soil organic carbon content, Fe and Mn IRIS films were deployed in 11 mitigation wetlands in Maryland, USA, during the early to mid-growing season. Significantly more IRIS oxide paint was removed under longer saturation, warmer soil temperatures, and when more SOC was present. As expected, Mn paint removal was more sensitive to these drivers than Fe paint removal. Similar to previous work done in natural wetlands (Rabenhorst et al., 2021), our findings support implementing IRIS paint removal thresholds that incorporate soil temperature and the mineral compositions (Fe or Mn) of the IRIS. Under cool conditions (<11 °C), our data suggests that a Mn paint removal threshold of 30% can confirm the presence of reducing soil conditions, while the current HSTS threshold of 30% Fe removal is too conservative. However, we found lowering the Fe paint removal threshold to 15% minimized the likelihood of conflicting results (between saturation and IRIS). In warm soil conditions (≥ 11 °C), Mn IRIS paint removal occurs so rapidly that it is less informative and should not be used alone to document the presence of anaerobic conditions for HSTS investigations. Rather, the current HSTS removal threshold of 30% for Fe IRIS seems most appropriate in warmer soil conditions.

In Chapter 3, porewater extractions and IRIS films were used to assess the influence of saturation, temperature, and SOC on the rate and quantity of Mn and Fe reduction and mobilization in a laboratory microcosm study. Similar to the findings of Chapter 2, these environmental drivers had a significant and positive effect on porewater metal concentrations and oxide paint removal. Soils saturated at warm laboratory temperatures (approximately 21 °C) produced dramatically higher concentrations of porewater Fe and Mn at a faster rate compared to those under cold refrigerated temperatures (approximately 4 °C). IRIS oxide paint removal under cold conditions was significantly delayed or completely extinguished, especially for the Fe paint. Under both warm and cold experiments, surface horizons rich in SOC mobilized Fe and Mn faster and consequently, resulted in higher porewater concentrations compared to deeper horizons. The mobilization of Mn into the porewater occurred before Fe in all soils. In addition to SOC, the amount of Mn oxides present in the soil seemed to strongly influence the early stages of soil reduction and the transition from primarily Mn reduction to Fe reduction.

In Chapter 4, we further explored Mn-Fe interactions by testing the effect of birnessite additions on soil reduction in another laboratory microcosm experiment. Moderate additions of Mn oxides increased the quantity and rate of porewater Mn mobilization within the first few weeks of saturation. However, the porewater Mn concentrations in soils amended with larger amounts of Mn oxides were lower than those amended with less, and the porewater Mn concentrations either plateaued or decreased throughout the study. The decrease in porewater Mn may be due to Mn toxicity inhibiting microbial respiration, or the rise in pH could have increased the sorption of aqueous Mn to mineral soils or possibly promoting the precipitation of $MnCO_3$.

Furthermore, we found that increased Mn oxide content suppressed Fe reduction as the mobilization of porewater Fe and the removal of Fe paint was substantially delayed and resulted in lower concentration of porewater Fe in all soils studied.

In both field and laboratory studies, temperature, organic carbon, and saturation, were found to strongly regulate the rate and magnitude of both Fe and Mn reduction. Additionally, Mn oxides present in the soil inhibited Fe reduction in microcosm experiments. Our results affirm that IRIS films are sensitive to these environmental drivers of soil reduction and can provide a window into soil redox processes by offering the ability to visualize the reduction of Mn and Fe oxides. Most notably, Mn IRIS films may better document anaerobic conditions in cool, early growing season conditions than Fe IRIS.

Current and predicted global shifts in temperature and precipitation will likely influence the distribution of wetlands and hydric soils, as well as impact soil reduction processes. Increased temperatures may extend the growing season and thus promote the reduction of soil Mn and Fe in wet soils. Changes in precipitation patterns may shrink or expand wetlands and therefore redistributing where and when soil reduction may occur. Furthering our knowledge about soil redox dynamics may help us better understand how soils may change in the future especially under the influence of changing climate.

This thesis has provided deeper examination of the impact of these environmental drivers on Mn and Fe reduction and also on their interactions. Hence, this work will help researchers and practitioners better use and interpret IRIS devices in a wide range of settings, including in colder regions, early growing season conditions, and highly disturbed environments such as mitigation wetlands.

Appendix A. Mitigation wetland site soil descriptions

Abbreviations used in the tables are as follows:
Texture:

- L – loam
- SCL – sandy clay loam
- CL – clay loam
- SiL – silt loam
- SL – sandy loam
- SiCL – silty clay loam
- LS – loamy sand
- F – indicates fine sand within texture
- Co – indicated coarse sand within texture

Redoximorphic Features:
Written as “Color (Abundance %, Contrast)”

- Contrast:
  - F – faint
  - D – distinct
  - P – prominent

Pedon/Site: Bishop **SHA Code**: WO-04

Describers: GMB, MCR, JW

Date: 1/11/2023 **Time**: 12:00 PM

Weather: Overcast

Mapping Unit: Fallsington sandy loams, 0 to 2%, Northern Tidewater Area (Typic Endoaquults)

Taxonomic Classification: Typic Umbraquult

State: MD **County**: Worcester

Latitude: 38.41858326 **Longitude**: -75.21612407

Site Group: Outer Coaster Plain

Dominant Vegetation: Loblolly pine, sweet gum, willow oak

Mitigation: Construction completed in 2001. Excavation (1 to 3 feet) and blockage of onsite drainage ditches. Tree and shrub planting.

Remarks: Location of plot likely was graded very little as the pedon seemed undisturbed.

Horizon	Lower Boundary (cm)	Textural Class	Clay %	Hue	Value	Chroma	Redoximorphic Features		%OC	pH	Notes
							Concentrations	Depletions			
A	17	L	15	10YR	2	1	-	-	2.16	4.27	
Btg1	34	SCL	23	10YR	3	1	7.5YR 3/3 (5%, D)	-	0.61	4.46	
Btg2	46	CL	30	10YR	3	1	7.5YR 3/3 (5%, D)	-	0.47	4.35	
BCg	67	FSL	18	2.5Y	5	1	7.5YR 5/6 (5%, P)	-	0.26	4.44	
CBg	83	LFS	5	2.5Y	5	2	-	-	0.06	5.17	
B'Cg	98	FSL	11	2.5Y	6	1	10YR 6/4 (25%, P); 7.5YR 5/6 (10%, P)	-	0.08	4.66	
Cg	120+	LFS	5	2.5Y	6	1	2.5Y 6/2 (20%, F)	-	0.05	5.28	

Pedon/Site: Bounds **SHA Code**: WO-03

Describers: GMB, MCR, JW

Date: 1/11/2023 **Time**: 2:00 PM

Weather: Overcast

Mapping Unit: Othello silt loams, 0 to 2% slopes, Northern Tidewater Area (Typic Endoaquults)

Taxonomic Classification: Typic Endoaquult

State: MD **County**: Worcester

Latitude: 38.34074882 **Longitude**: -75.30095092

Site Group: Outer Coaster Plain

Dominant Vegetation: Loblolly pine

Mitigation: Constructed completed in 2003. Drainage ditches plugged. Site was plowed instead of excavated to create furrows and undulating microtopography. Subsequent planting occurred after construction.

Remarks:

Horizon	Lower Boundary (cm)	Textural Class	Clay %	Hue	Value	Chroma	Redoximorphic Features		%OC	pH	Notes
							Concentrations	Depletions			
Ap	12	SiL	13	10YR	3	2	7.5YR 3/2 (1%, D)	-	3.02	4.19	
Eg	33	SiL	10	10YR	4	1.5	7.5YR 3/3 (3%, D)	-	0.97	5.30	
Btg1	53	SiL	16	10YR	4	1	10YR 4/4 (15%, D)	-	0.44	5.52	
Btg2	104	SiL	22	5Y	5	1	10YR 5/6 (20%, P)	-	0.12	4.35	
2BCg	120+	SL	12	5Y	6	1	10YR 5/4 (10%, P); 10YR 5/6 (10%, P)	-	0.05	4.84	

Pedon/Site: Buckingham A **SHA Code**: AA-22

Describers: GMB, MCR, AQ

Date: 1/12/2023 **Time**: 10:30 AM

Weather: Overcast

Mapping Unit: In: Patapsco-Fort Mott-Urban land complex, 0-5% slopes (Grossarenic Paleudults); Next to: Fallsington sandy loams, 0 to 2 % slopes, northern coastal plain (Typic Endoaquults)

Taxonomic Classification: Anthropic Udorthent

State: MD **County**: Anne Arundel

Latitude: 39.15007569 **Longitude**: -76.69444907

Site Group: Inner Coaster Plain

Dominant Vegetation: Virgina pine, Loblolly pine, Sweetgum

Mitigation: Constructed completed in 1997. Excavated and created tiered wetlands (3 elevations) in the floodplain fo Stony Run. Likely excavated down to 2Cg horizon then filled with sandy materials and topped with amended topsoil.

Remarks: Plot located on middle tier.

Horizon	Lower Boundary (cm)	Textural Class	Clay %	Hue	Value	Chroma	Redoximorphic Features		%OC	pH	Notes
							Concentrations	Depletions			
^A1	7	SL	10	10YR	3	2	-	-	6.68	3.98	Anthropic epipedon
^A2	16	LS	8	10YR	3	3	-	-	1.22	4.83	
^A3	31	LS	6	10YR	2	2	-	-	1.15	4.95	
^C1	72	SL	18	10YR	5	4	5YR 5/6 (15%, P)	-	0.16	4.98	
^C2	86	SL	16	10YR	6	4	-	-	0.09	4.72	
2Cg	98	SCL	22	10YR	7	1	5YR 5/6 (15%, P)	-	0.05	4.68	
2C	118+	SCL	23	10YR	6	4	10YR 6/6 (35%, D); 5YR 5/6 (5%, P)	10YR 7/1 (20%, D)	0.05	4.25	

Pedon/Site: Churchview **SHA Code**: n/a
Describers: GMB, MCR, AQ, GJ
Date: 1/12/2023 **Time**: 1:00 PM
Weather: Overcast

Mapping Unit: Collington-Wist complex, 2 to 5% slopes (85% Typic Hapludults, 15% Aquic Hapludults)

Taxonomic Classification: Aquic Hapludult

State: MD **County**: Anne Arundel
Latitude: 39.05170141 **Longitude**: 39.05170141
Site Group: Inner Coaster Plain
Dominant Vegetation: Broomsedge, slender rush, sweetgum, swamp white oak
Mitigation: Construction completed in 2015. Soil excavated down an average of 2 feet which removed original topsoil and the upper part of the original argillic horizon. Either stockpiled or amended organic-rich topsoil added. Planted with woody species.

Remarks: Private mitigation site.

Horizon	Lower Boundary (cm)	Textural Class	Clay %	Hue	Value	Chroma	Redoximorphic Features		%OC	pH	Notes
							Concentrations	Depletions			
^A	2	L	11	10YR	3	2	-	-	5.39	4.80	
^Ap	11	L	14	2.5Y	4	2.5	5YR 4/4 (15%, D)	-	0.97	4.60	
Bt	28	CL	29	10YR	4	4	7.5YR 4/6 (30%, D)	10YR 5/2 (15%, D)	0.25	4.03	
BC1	54	L	15	10YR	4	4	7.5YR 4/6 (25%, D); 5YR 4/6 (5%, P)	10YR 4/2 (10%, D)	0.20	3.90	
BC2	75	L or FSL	12	10YR	4	4	7.5YR 4/6 (30%, D)	10YR 4.5/2 (15%, D)	0.18	3.85	
BC3	120+	L/FSL	15	10YR	4	4	7.5YR 5/6 (30%, D)	10YR 4/2 (5%, D)	0.18	3.76	

Pedon/Site: Firehouse **SHA Code**: WO-05

Describers: GMB, MCR, JW

Date: 1/11/2023 **Time**: 10:40 AM

Weather: Overcast

Mapping Unit: Nassawango fine sandy loam 0 to 2% (Typic Hapludults)

Taxonomic Classification: Anthrodensic Dystrudept?

State: MD **County**: Worcester

Latitude: 38.39912063 **Longitude**: -75.20447981

Site Group: Outer Coaster Plain

Dominant Vegetation: Broom sedge, foxtail, bald cypress, loblolly pine, deer tongue grass

Mitigation: Construction completed in 2004. Excavated to have three tiers of elevation to have both shallow marsh and forested wetland areas. Pedon taken from middle terrace in transitional area between low lying bald cypress pond and surrounding upland.

Remarks: Soil was extremely dense and difficult to insert IRIS films, especially when it started to dry out.

Horizon	Lower Boundary (cm)	Textural Class	Clay %	Hue	Value	Chroma	Redoximorphic Features		%OC	pH	Notes
							Concentrations	Depletions			
^Ap	25	FSL	7	10YR	2	2	-	-	1.00	5.91	
^(?)Bw	42	SL	8	10YR	5	6	-	10YR 7/3 (25%, D)	0.12	5.80	
C	60	SL	8	2.5Y	7	2.5	10YR 7/4 (25%, D); 7.5YR 5/6 (5%, P)	-	0.04	6.16	
Cg1	73	LS	8	2.5Y	7	2.5	7.5YR 5/6 (5%, P)	-	0.03	5.73	
Cg2	88	LFS	10	5Y	8	2	-	-	0.05	5.51	
Cg3	101	SL	7	5Y	7	2	2.5Y 7/4 (50%, D)	-	0.04	5.42	
Cg4	124+	LFS	5	5Y	8	1	2.5Y 7/2 (35%, D); 10YR 7/4 (15%, P)	-	0.03	5.35	

Pedon/Site: Holly Neck **SHA Code**: BA-11
Describers: GMB, MCR, AQ
Date: 1/12/2023 **Time**: 8:40 AM
Weather: Overcast
Mapping Unit: Mattapex silt loam, 0 to 2% (Aquic Hapludults)

Taxonomic Classification: Aquic Hapludult

State: MD **County**: Baltimore
Latitude: 39.27505698 **Longitude**: -76.42606327
Site Group: Inner Coaster Plain
Dominant Vegetation: Sweetgum, Black Willow
Mitigation: Construction completed in 2006. Excavated to create depressions/vernal pools as well as preserve areas of existing wetland and upland forest.
Remarks: Pedon/plot located a bit west of the depressions, so does not seem greatly disturbed by construction.

Horizon	Lower Boundary (cm)	Textural Class	Clay %	Hue	Value	Chroma	Redoximorphic Features		%OC	pH	Notes
							Concentrations	Depletions			
A	13	SiL	11	10YR	4	3	-	-	2.01	5.38	
Ap	34	SiL	14	10YR	5	3	7.5YR 4/4 (10%, F)	-	0.95	5.66	
Bt1	65	SiL	23	7.5YR	4.5	6	-	10YR 5/2 (8%, P)	0.17	4.98	10YR 5/4 (25%, D) but not RMF
Bt2	92	SiCL	28	10YR	5	6	7.5 YR 4/4 (3%, D)	10YR 5/2 (5%, P)	0.12	4.61	
Bt3	120+	SiCL	32	10YR	5	6	-	10YR 5/2 (3%, P)	0.11	4.74	10YR 5/4 (25%, D) but not RMF

Pedon/Site: Nixon **SHA Code**: HO-16

Describers: GMB, MCR, JK

Date: 1/16/2023 **Time**: 2:50 PM

Weather: Colors described in full sun (photos shaded)

Mapping Unit: Codorus and Hatboro silt loams, 0 to 3% (Fluvaquentic Dystrudepts; Fluvaquentic Endoaquepts)

Taxonomic Classification: Typic Endoaquept

State: MD **County**: Howard

Latitude: 39.28907838 **Longitude**: -76.96073826

Site Group: Piedmont

Dominant Vegetation: Black willow, Sycamore, Japanese stilt grass, small carpet grass

Mitigation: Construction completed in 2010. Shallow berms and depressions excavated, and small tributary channel was plugged & redirected to improve hydrology across floodplain.

Remarks: Pedon/plot was within enhanced pre-existing farmed wetland area that was not directly impacted by construction efforts.

Horizon	Lower Boundary (cm)	Textural Class	Clay %	Hue	Value	Chroma	Redoximorphic Features		%OC	pH	Notes
							Concentrations	Depletions			
A	6	SiL	13	10YR	3	2	5YR 3/4 (5%, P)	-	3.48	4.84	
Ap	20	SiL	16	10YR	4	2	5YR 3/4 (10%, P)	-	1.62	4.64	
Bg1	48	SiL	23	2.5Y	5.5	2	10YR 5/6 (10%, P); 7.5YR 5/6 (10%, P)	-	0.39	4.86	
Bg2	85	L	25	5Y	6	1	7.5YR 5/6 (15%, P)	-	0.18	4.89	
BC	115+	SL	14	5Y	6.5	1	7.5YR 5/6 (3%, P)	-	0.10	5.15	

Pedon/Site: Northwest Branch **SHA Code**: NW-128

Describers: GMB, MCR, JK

Date: 1/16/2023 **Time**: 8:35 AM

Weather: Colors described in full sun (photos shaded)

State: MD **County**: Montgomery

Latitude: 39.09473659 **Longitude**: -77.034815

Site Group: Piedmont

Dominant Vegetation: Sycamore, Black willow, Small carpetgrass, other grasses and sedges

Mapping Unit: Hatboro silt loam, 0 to 3 % slopes, frequently flooded (Fluvaquentic Endoaquepts)

Mitigation: Construction completed in 2007. Soil was excavated down approximately 4 feet and then approximately 6 inches of stockpiled topsoil added.

Taxonomic Classification: Aeric Endoaquept

Remarks:

Horizon	Lower Boundary (cm)	Textural Class	Clay %	Hue	Value	Chroma	Redoximorphic Features		%OC	pH	Notes
							Concentrations	Depletions			
^A	6	L	15	10YR	3	2	-	-	5.53	5.77	Many roots
^Ap	20	L	18	10YR	4	2	5YR 4/6 (10%, P)	-	1.17	5.69	
Bg	40	CL	32	2.5YR	5	1	10YR 5/4 (30%, P); 7.5YR 5/6 (5%, P)	-	0.21	6.42	
Cg	69	SL	10	5GY	5	1	7.5YR 4/4 (3%, P)	10Y 5/1 (47%, F)	0.11	7.02	
C1	95	LS	7	5YR	4	6	7.5YR 5/6 (35%, F); 10YR 5/4 (25%, P)	-	0.06	6.78	Colors extremely mixed
C2	115+	LS	8	10YR	5	4	5YR 5/6 (10%, P); 10YR 5/2 (40%, D)	-	0.06	6.78	

Pedon/Site: Pilchard **SHA Code**: WI-03

Describers: GMB, MCR, JW

Date: 1/11/2023 **Time**: 3:45 PM

Weather: Overcast

Mapping Unit: Pepperbox-Rockawalkin complex, 0 to 2% (50% Aquic Arenic Paleudults, 30% Aquic Arenic Hapludults)

Taxonomic Classification: Aquic Hapludult

State: MD **County**: Wicomico

Latitude: 38.40634994 **Longitude**: -75.63746526

Site Group: Outer Coastal Plain

Dominant Vegetation: Button bush, soft rush, sedges, wool grass

Mitigation: Construction completed in early 2000's. Originally a borrow pit, but due to excess hydrology reforestation planting was abandoned. Then converted into a Bald cypress forested wetland.

Remarks: Observed short and perched hydrology in the early growing season.

Horizon	Lower Boundary (cm)	Textural Class	Clay %	Hue	Value	Chroma	Redoximorphic Features		%OC	pH	Notes
							Concentrations	Depletions			
^Ap	18	LS	6	2.5Y	3	3	-	-	0.70	7.01	Anthropic epipedon
^A/C	39	SL (A) / SCL (C)	12 / 33	10YR / 2.5Y	2 / 4	2 / 3	-	-	1.00	7.48	OC% for A = 1.46% and C = 0.35%
2^Cg	47	LS	3	2.5Y	4	2	-	-	0.42	7.54	
3Bt	72	SCL	45	10YR	5	4	5YR 5/6 (4%, P)	2.5Y 6/1 (5%,P)	0.09	6.94	
3Btg	92	CL	35	2.5Y	6	2	10YR 6/4 (30%, D); 5YR 5/6 (8%, P)	-	0.08	5.33	
4C	122+	LCoS	9	10YR	6	4	7.5YR 5/6 (25%, D)	-	0.06	4.71	

Pedon/Site: Goshen Branch **SHA Code**: SC-02
Describers: GMB, MCR, JK
Date: 1/16/2023 **Time**: 11:00 AM
Weather: Colors described in full sun (photos shaded)

Mapping Unit: Codorus silt loam, 0 to 3%, occasionally flooded (Fluvaquentic Dystrudepts)

Taxonomic Classification: Aquic Dystrudept

State: MD **County**: Montgomery
Latitude: 39.20682794 **Longitude**: -77.18769702
Site Group: Piedmont
Dominant Vegetation: Black willow, sycamore, reed canary grass, red and silver maple, silky dogwood, soft rush, and other sedges/ushes/grasses

Mitigation: Construction completed in 2012 with subsequent tree and shrub planting in 2017. Wetland creation, enhancement, and restoration along a portion of Goshen Branch which included excavation of the floodplain to intercept groundwater and adjustments were made to the groundwater and surface water flow patterns.

Remarks: Augur refusal at 90 cm due to excess gravels.

Horizon	Lower Boundary (cm)	Textural Class	Clay %	Hue	Value	Chroma	Redoximorphic Features		%OC	pH	Notes
							Concentrations	Depletions			
^A	8	SiL	14	10YR	3	2	-	-	5.35	6.70	Either transported or highly altered during construction
BA	22	L	25	10YR	5	3	7.5YR 4/4 (15%, D)	-	0.54	6.19	
Bw1	40	CL	28	10YR	5	6	7.5YR 5/6 (20%, F);	10YR 6/2 (5%, P)	0.36	5.95	
Bw2	60	SiCL	28	10YR	5	6	10YR 6/6 (30%, F)	5Y 6/2 (20%, P)	0.36	6.08	
2BC1	75	CL	28	2.5Y	5	3	10YR 6/6 (30%, P)	2.5Y 6/2 (30%, F)	0.32	6.20	
2BC2	90+	SCL	28	10YR	6	8	10YR 5/6 (15%, D)	10YR 5/2 (3%, P)	0.28	6.12	

Pedon/Site: SC-19 **SHA Code**: SC-19

Describers: GMB, MCR, JK

Date: 1/16/2023 **Time**: 1:00 PM

Weather: Colors described in full sun (photos shaded)

Mapping Unit: Codorus silt loam, 0 to 3%, occasionally flooded (Fluvaquentic Dystrudepts)

Taxonomic Classification: Aquic Dystrudept

State: MD **County**: Montgomery

Latitude: 39.23298009 **Longitude**: -77.18089499

Site Group: Piedmont

Dominant Vegetation: Cattails, soft rush, Japanese stilt grass, Arrow-leaved tearthumb, River birch

Mitigation: Construction completed in 2013. Wetland creation/enhancement along Great Seneca Creek with streambank restoration.

Remarks: Based on construction plans, plot likely experienced some amount of grading and replacement with salvaged or amended topsoil.

Horizon	Lower Boundary (cm)	Textural Class	Clay %	Hue	Value	Chroma	Redoximorphic Features		%OC	pH	Notes
							Concentrations	Depletions			
^A	7	SiL	12	10YR	2	2	-	-	6.64	6.79	
^Ap	20	SiL	16	10YR	4	4	5YR 3/3 (15%, D)	-	2.04	6.72	
2Bg	36	L	21	2.5Y	5	1	5YR 3/3 (5%, P)	-	0.66	6.77	Other color: N2 (2%)
2Bw	62	L	24	10YR	5	3	7.5YR 5/6 (33%, P)	2.5Y 6/1 (33%, D)	0.44	6.06	5% gravels, Colors of equal distribution (33%)
3BC1	85	L	18	10YR	5	3	7.5YR 5/6 (33%, P)	2.5Y 6/1 (33%)	0.32	6.01	15% gravels, Colors of equal distribution (33%)
3BC2	115+	SL	15	10YR	5	4	7.5YR 5/6 (5%, D)	5Y 5/1 (40%, P); 5Y 4/2 (10%, P)	0.28	6.36	

Appendix B. WETS Data for Analysis of Precipitation Normality

Graphs displaying monthly precipitation and three-month weighted mean, as well as 30-year average (WETS) data for 30th and 70th percentiles. Note the light green shading shows the period of this study. Data sourced from National Weather Service stations.

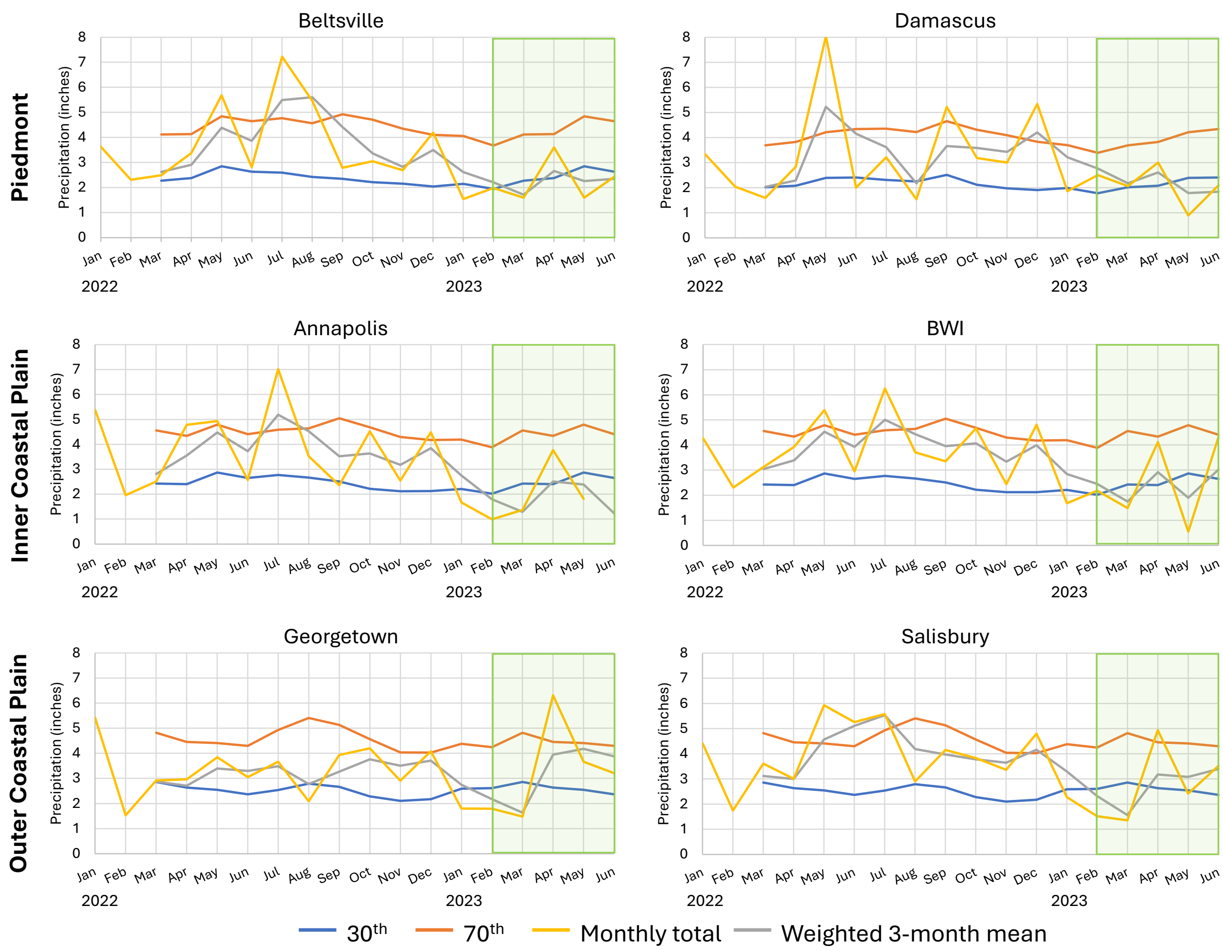

Appendix C: IRIS paint removal data from mitigation wetland sites

Indicator of Reduction in Soils (IRIS) paint removal and environmental data for each deployment period (batch #) at every study site is shown below. IRIS paint removal (%) for both Fe and Mn IRIS were determined in two ways. Firstly, following guidance from the Hydric Soil Technical Standard (HSTS), the 15 cm contiguous zone within the upper 30 cm of the IRIS film that had the maximum paint removal was determined for each of the five replicate films. The median value of the five replicate films is listed under "15 Median." Secondly, the mean paint removal from 10 cm zones (0–10, 10–20, and 20–30 cm) of 5 replicate films is displayed. Average soil temperature (ST) for each deployment period was recorded at a depth of 25 cm. The total number of days as well as the maximum number of consecutive days the water table was at or shallower than 25 cm is separately listed. If the water table was at or shallower than 25 cm for 14 or more consecutive days, then the batch at a given site met the HSTS saturation requirement.

Study Site	Batch #	Fe IRIS Paint Removal (%)				Mn IRIS Paint Removal (%)				Mean ST	Total Days WT ≥25 cm	Max Cons. Days WT ≥25 cm	HSTS Sat. Reqmt. Met?
		15 Median	0-10 Mean	10-20 Mean	20-30 Mean	15 Median	0-10 Mean	10-20 Mean	20-30 Mean				
Bishop	1	38.2	42.2	36.8	23.2	100	99.0	97.4	91.7	8.8	28.0	28.0	Y
Bishop	2	52.8	51.4	29.0	11.1	100	97.8	99.2	97.3	8.1	27.0	27.0	Y
Bishop	3	15.7	13.7	10.2	12.4	100	75.3	85.4	88.5	9.4	27.3	20.0	Y
Bishop	4	10.0	13.1	4.8	8.4	69.5	50.2	49.7	70.3	12.0	21.5	7.8	N
Bishop	5	54.9	30.9	33.3	50.0	100	79.0	94.5	84.8	13.2	20.5	8.8	N
Bishop	6	47.3	36.5	40.4	53.7	99.9	95.0	99.8	99.7	14.0	24.8	19.8	Y
Bishop	7	45.9	13.2	15.6	47.2	99.5	60.0	89.4	99.5	15.0	16.3	11.0	N
Bounds	1	14.5	4.1	20.9	6.9	77.4	36.5	65.2	69.5	8.6	24.5	13.5	N
Bounds	2	20.3	2.1	14.9	17.4	54.6	16.4	48.2	64.3	7.9	18.3	18.0	Y
Bounds	3	4.2	2.0	1.1	3.4	11.6	11.3	5.8	24.8	9.2	6.3	4.5	N
Bounds	4	7.1	5.6	4.1	3.3	31.0	11.8	7.4	44.7	11.9	2.5	2.5	N

Bounds	5	38.9	3.5	6.7	39.5	78.2	32.7	49.0	79.4	13.3	6.0	5.0	N
Bounds	6	61.8	10.8	36.2	70.6	96.8	70.7	85.8	99.2	14.2	5.0	5.0	N
Bounds	7	5.4	3.4	3.7	9.5	12.5	30.1	23.2	41.5	15.2	0.0	0.0	N
Buckingham A	1	22.2	22.2	32.0	19.0	94.7	61.9	71.6	64.0	7.4	28.0	28.0	Y
Buckingham A	2	26.5	10.2	25.0	19.7	86.2	59.8	79.1	77.5	7.1	30.0	30.0	Y
Buckingham A	3	53.6	21.2	41.2	25.7	91.3	44.0	90.4	87.0	8.4	30.0	30.0	Y
Buckingham A	4	41.4	20.7	37.9	27.1	95.4	50.9	88.9	79.9	11.4	26.0	26.0	Y
Buckingham A	5	66.6	58.2	48.4	37.4	100	69.8	95.1	99.1	12.7	26.0	26.0	Y
Buckingham A	6	84.3	55.1	59.7	33.9	99.8	72.5	96.2	98.0	13.5	20.0	19.0	Y
Buckingham A	7	16.3	21.8	26.9	28.3	82.9	49.3	73.6	87.6	14.8	6.0	5.0	N
Churchview	1	19.3	37.9	16.5	9.7	39.3	47.4	7.0	5.2	7.2	28.0	28.0	Y
Churchview	2	28.7	44.2	11.7	4.8	31.3	53.3	16.5	22.3	7.5	22.8	20.0	Y
Churchview	3	5.9	13.4	7.7	1.6	43.7	52.0	19.2	15.6	9.3	19.5	7.5	N
Churchview	4	12.8	20.7	3.1	2.7	33.5	41.2	20.2	21.0	12.8	11.8	5.3	N
Churchview	5	25.8	31.6	8.6	2.9	36.6	50.1	15.9	6.1	14.6	10.3	7.3	N
Churchview	6	35.7	38.3	10.9	1.8	40.9	56.2	26.7	3.9	15.7	13.3	10.5	N
Churchview	7	15.9	25.4	1.3	1.5	25.5	41.6	14.2	10.5	17.6	4.0	3.3	N
Firehouse	1	3.3	2.8	5.1	5.1	14.0	6.2	11.6	6.0	9.3	12.5	6.3	N
Firehouse	2	1.0	0.2	0.5	0.8	11.1	8.6	11.0	1.6	9.1	7.8	6.3	N
Firehouse	3	0.6	0.2	0.5	0.9	1.5	0.3	0.6	1.1	11.4	3.0	1.5	N
Firehouse	4	0.2	0.2	0.1	0.9	0.5	0.4	0.4	0.1	15.4	1.5	1.5	N

Firehouse	5	4.3	2.0	1.8	5.2	12.9	9.4	9.9	7.8	17.3	5.3	4.3	N
Firehouse	6	0.0	1.0	0.3	0.2	0.0	6.3	4.2	8.6	18.3	6.0	4.3	N
Firehouse	7	0.4	0.4	0.2	0.4	2.0	1.1	2.1	3.8	19.7	1.5	0.5	N
Hollyneck	1	60.1	62.4	46.1	44.3	81.4	76.2	77.7	61.1	6.6	28.0	28.0	Y
Hollyneck	2	86.3	50.8	80.3	79.7	96.0	80.1	92.5	83.8	6.9	23.5	22.8	Y
Hollyneck	3	59.9	56.2	50.5	60.5	77.8	70.6	69.8	75.8	9.2	24.3	13.8	N
Hollyneck	4	87.8	62.7	72.2	64.5	97.8	69.2	92.4	98.7	12.8	16.0	13.0	N
Hollyneck	5	24.9	33.7	28.9	34.3	39.9	38.8	24.9	20.5	15.0	7.8	6.5	N
Hollyneck	6	50.8	48.8	41.1	38.8	88.7	67.1	76.8	84.4	16.1	6.5	6.5	N
Hollyneck	7	3.5	5.1	1.8	0.7	11.1	8.8	6.1	15.1	18.1	0.0	0.0	N
Nixon	1	19.5	20.5	19.0	9.7	45.4	45.3	32.1	10.9	6.9	28.0	28.0	Y
Nixon	2	21.7	24.5	14.9	9.3	57.5	51.6	45.0	32.4	7.0	28.0	28.0	Y
Nixon	3	23.5	28.2	23.6	21.5	89.0	79.3	83.0	47.3	8.9	28.0	28.0	Y
Nixon	4	28.3	17.7	19.9	7.9	46.7	37.0	40.2	21.6	12.5	21.3	18.5	Y
Nixon	5	21.6	26.1	16.2	23.4	53.7	34.3	43.6	59.5	13.6	19.3	9.3	N
Nixon	6	24.5	32.9	22.8	21.4	80.7	64.2	68.0	64.4	14.1	16.3	12.0	N
Nixon	7	5.7	8.2	2.7	10.4	22.4	25.9	11.9	22.2	15.5	4.3	2.8	N
NW Branch	1	66.8	60.9	46.2	28.5	64.8	59.9	59.9	36.8	7.0	28.0	28.0	Y
NW Branch	2	66.5	65.7	51.4	28.4	72.0	66.4	61.9	72.8	7.4	28.0	28.0	Y
NW Branch	3	90.8	86.0	67.8	48.4	94.4	94.2	86.6	72.4	9.7	28.0	28.0	Y
NW Branch	4	89.9	90.8	74.4	47.4	97.8	90.4	87.2	52.1	13.5	28.0	28.0	Y

NW Branch	5	95.5	82.6	77.1	75.5	100	88.7	99.9	97.7	14.9	28.0	28.0	Y
NW Branch	6	98.0	92.1	87.7	86.3	99.8	95.7	96.5	84.6	15.9	28.0	28.0	Y
NW Branch	7	92.2	81.9	77.8	77.5	99.9	89.8	96.6	97.3	18.1	15.3	15.0	Y
Pilchard	1	8.5	4.2	11.0	4.8	17.7	6.4	15.9	25.6	8.3	16.0	7.8	N
Pilchard	2	16.6	4.0	3.9	21.0	38.5	11.1	14.2	43.0	8.0	9.3	7.8	N
Pilchard	3	4.8	1.9	2.7	7.7	7.4	2.1	6.0	7.0	10.2	3.3	1.8	N
Pilchard	4	1.0	1.1	1.6	1.7	16.9	4.6	6.6	24.2	14.1	2.5	2.0	N
Pilchard	5	81.3	65.7	58.5	52.1	75.2	57.3	51.4	54.1	16.2	8.8	8.0	N
Pilchard	6	81.2	53.5	61.8	61.9	82.6	63.6	46.0	53.1	17.8	16.0	13.5	N
Pilchard	7	94.7	45.1	73.1	80.8	97.8	84.1	88.9	92.8	19.6	9.0	5.5	N
Goshen Branch	1	8.3	6.6	6.2	16.1	37.1	21.1	20.5	26.0	6.6	28.0	28.0	Y
Goshen Branch	2	7.7	18.8	20.6	28.3	23.4	17.2	31.5	23.1	7.0	28.0	28.0	Y
Goshen Branch	3	29.3	33.5	21.2	21.7	12.5	18.8	12.1	15.5	8.9	28.0	28.0	Y
Goshen Branch	4	3.8	14.9	18.8	20.2	9.5	12.5	9.7	5.5	12.4	14.8	14.3	Y
Goshen Branch	5	20.4	9.9	11.1	13.0	39.9	19.8	41.1	37.2	14.0	9.8	9.0	N
Goshen Branch	6	34.0	29.4	29.3	48.5	78.7	73.6	63.4	73.6	15.4	12.0	12.0	N
Goshen Branch	7	5.1	5.1	4.6	4.2	12.1	14.9	3.3	6.8	17.9	3.0	3.0	N
SC-19	1	3.2	1.8	4.0	4.8	6.9	1.5	3.2	7.9	6.4	25.5	12.5	N
SC-19	2	13.5	5.1	9.6	18.7	15.7	5.7	12.3	15.2	6.7	18.0	9.3	N
SC-19	3	25.1	16.2	14.6	31.6	26.1	20.7	15.7	30.5	8.6	11.0	5.8	N

SC-19	4	3.0	3.4	0.4	5.1	7.6	8.3	8.3	6.8	12.1	6.0	3.3	N
SC-19	5	5.2	9.3	2.5	10.2	28.6	18.6	21.3	35.0	13.5	7.8	6.5	N
SC-19	6	4.2	6.4	2.5	6.0	11.8	21.9	12.4	13.6	14.7	6.8	6.5	N
SC-19	7	5.1	5.1	4.6	4.2	12.1	14.9	3.3	6.8	17.0	0.0	0.0	N

Appendix D. Soil organic carbon level determination

The soil organic carbon (SOC) content for each 10 cm zone (0-10, 10-20, and 20-30 cm) within a pedon was determined by calculating a weighted average based on the SOC% measured for each horizon (descending order). All A horizons were considered to have “high” SOC content, so if the majority of a 10 cm zone corresponded to the depths of surface (A) horizons, then the SOC was designated as “high.”

Site-Section	Weighted Average SOC%	SOC Level
SC-19 0-10	5.263	High
BuckinghamA 0-10	5.045	High
Goshen Branch 0-10	4.390	High
Northwest Branch 0-10	3.787	High
Bounds 0-10	3.015	High
Nixon 0-10	2.734	High
Bishop 0-10	2.164	High
SC-19 10-20	2.040	High
Hollyneck 0-10	2.013	High
Churchview 0-10	1.850	High
Bishop 10-20	1.698	High
Nixon 10-20	1.620	High
Bounds 10-20	1.379	High
Hollyneck 10-20	1.270	High
BuckinghamA 10-20	1.193	High
Northwest Branch 10-20	1.173	High
BuckinghamA 20-30	1.152	High
Firehouse 0-10	1.002	High
Firehouse 10-20	1.002	High
Pilchard 20-30	0.998	High
Bounds 20-30	0.970	High
Hollyneck 20-30	0.952	High
Pilchard 10-20	0.757	High
Pilchard 0-10	0.697	High
SC-19 20-30	0.656	Low
Bishop 20-30	0.609	Low
Goshen Branch 10-20	0.536	Low
Firehouse 20-30	0.470	Low
Goshen Branch 20-30	0.393	Low
Nixon 20-30	0.387	Low
Churchview 10-20	0.326	Low
Churchview 20-30	0.243	Low
Northwest Branch 20-30	0.207	Low

	Mean SOC%	Median SOC%	Standard Deviation
High Level	2.01	1.50	1.35
Low Level	0.43	0.39	0.16
All	1.58	1.15	1.35

Appendix E. Churchview site IRIS paint removal

Picture of the augured pedon from the Churchview study site and the corresponding organic carbon (%OC) levels within each soil horizon. Scans of three Fe IRIS (left) and Mn IRIS (right) films deployed at the Churchview study site which showcase that IRIS paint removal usually occurred in zones with relatively high amounts of OC.

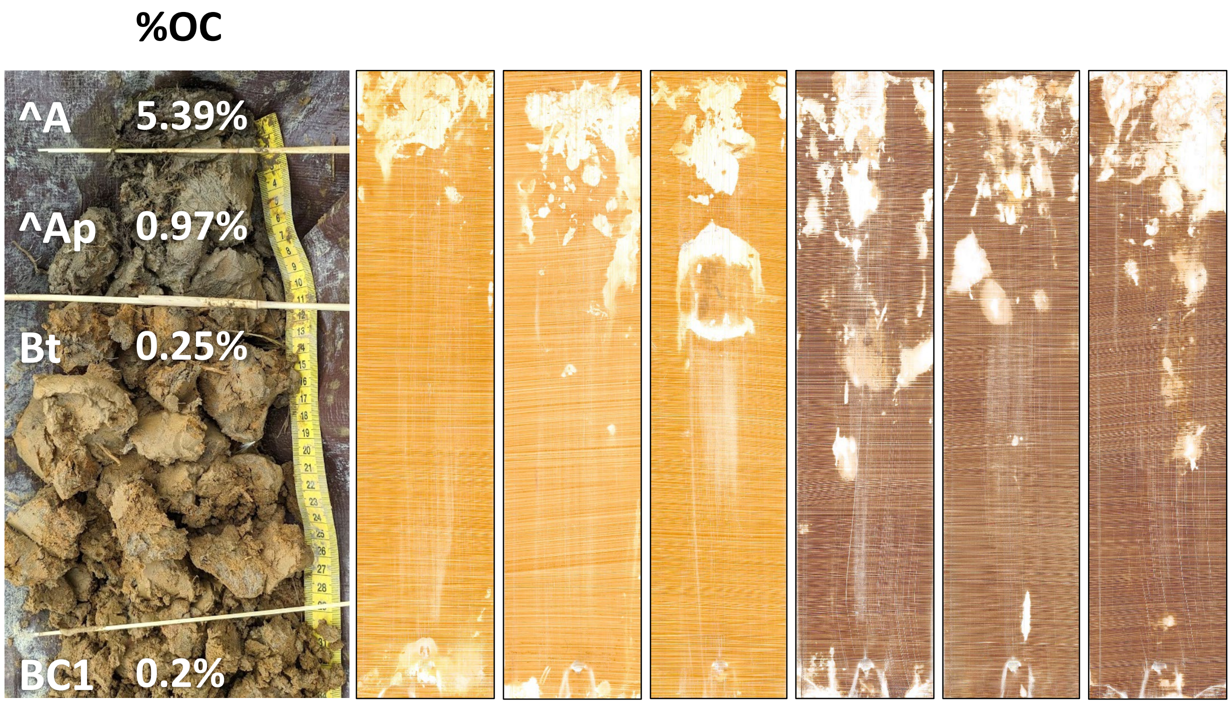

Appendix F. Porewater concentrations of Mn and Fe in microcosms under laboratory temperatures

Average concentrations of Mn and Fe in the extracted porewater from microcosms under warm conditions (21.3 °C). Data are arranged in rows by each pedon (Codorus, Downer, and Glenelg) and horizon (1, 2, and 3) combination and in columns by the sampling times (in terms of days of saturation).

Average Mn Concentration (mg L^{-1})

	0	1	2	4	7	14	21	28	42	56	Maximum
C1	0.05	0.39	1.91	6.03	14.83	25.19	25.57	28.27	26.62	26.31	28.27
C2	0.05	0.29	0.37	1.34	3.69	7.11	14.92	16.59	25.69	30.48	30.48
C3	0.07	0.22	0.25	0.63	2.71	5.52	11.68	11.14	17.80	23.06	23.06
D1	0.07	1.08	1.85	6.73	9.69	13.13	14.52	19.62	17.89	16.64	19.62
D2	0.09	0.29	0.38	0.71	1.80	3.27	3.60	5.41	7.29	6.46	7.29
D3	0.08	0.22	0.22	0.29	0.43	1.05	1.26	1.40	1.94	2.71	2.71
G1	0.16	0.77	3.39	19.02	30.62	57.64	106.67	115.24	143.01	121.70	143.01
G2	0.19	0.33	0.54	1.93	8.79	13.51	34.93	47.35	84.15	87.87	87.87
G3	0.09	0.21	0.26	0.38	0.43	0.63	1.11	0.82	4.64	10.39	10.39

Average Fe Concentration (mg L^{-1})

	0	1	2	4	7	14	21	28	42	56	Maximum
C1	0.58	0.33	0.23	1.03	8.80	38.08	49.14	62.61	64.74	65.36	65.36
C2	0.82	1.56	0.76	0.64	0.21	6.61	12.02	12.81	29.15	38.48	38.48
C3	0.86	2.45	1.73	0.70	0.22	3.48	8.85	9.43	21.20	31.29	31.29
D1	0.26	0.89	0.80	4.35	18.26	39.65	48.82	80.20	91.28	87.40	91.28
D2	0.35	0.53	0.41	0.55	0.87	5.01	11.03	22.42	52.55	63.42	63.42
D3	1.75	2.10	2.36	1.70	0.72	1.57	1.47	2.22	10.34	19.53	19.53
G1	0.40	0.51	0.47	0.52	3.22	16.37	41.17	58.78	85.79	104.53	104.53
G2	0.89	0.35	0.54	0.45	0.03	2.66	3.93	5.60	37.72	50.92	50.92
G3	0.20	1.51	2.04	1.68	0.65	1.12	0.45	0.19	17.65	36.76	36.76

Appendix G. Porewater concentrations of Mn and Fe in microcosms under cold temperatures

Average concentrations of Mn and Fe in the extracted porewater from microcosms under warm conditions (4.1 °C). Data are arranged in rows by each pedon (Codorus, Downer, and Glenelg) and horizon (1, 2, and 3) combination and in columns by the sampling times (in terms of days of saturation).

Average Mn Concentration (mg L^{-1})

	0	3	7	14	21	28	42	56	70	84	Max
C1	0.09	0.19	0.35	0.57	3.15	5.55	12.80	15.86	17.71	18.36	18.36
C2	0.12	0.19	0.28	0.23	0.39	0.83	2.29	3.19	4.38	4.60	4.60
D1	0.49	1.40	2.32	1.29	2.18	2.03	4.50	5.46	5.64	5.79	5.79
D2	0.10	0.26	0.40	0.26	0.33	0.34	1.42	1.38	2.12	1.50	2.12
G1	0.11	0.42	0.68	1.96	11.90	21.50	31.58	52.37	59.29	58.45	59.29
G2	0.13	0.32	0.74	0.81	1.04	1.42	5.34	6.94	13.49	15.75	15.75

Average Fe Concentration (mg L^{-1})

	0	3	7	14	21	28	42	56	70	84	Max
C1	0.71	0.39	0.37	0.11	0.15	0.25	3.11	12.09	20.22	25.45	25.45
C2	2.25	1.53	1.04	0.41	0.16	0.30	0.16	0.17	0.31	0.39	2.25
D1	0.51	0.90	1.06	0.78	0.95	0.92	1.26	1.17	1.14	0.98	1.26
D2	1.71	0.84	0.89	0.78	0.26	0.31	0.28	0.47	0.42	0.39	1.71
G1	0.49	0.42	0.38	0.08	0.05	0.23	0.15	1.51	4.73	11.50	11.50
G2	1.00	0.49	0.41	0.05	0.04	0.30	0.09	0.05	0.38	0.28	1.00

Appendix H. Porewater concentrations of Mn and Fe in microcosms with Mn oxide additions

Average concentrations of Mn and Fe in the extracted porewater from microcosms under warm conditions (4.1 °C). Data are arranged in rows by each pedon (Codorus, Downer, and Glenelg) and treatment (0, 5, 15, and 30 g Mn oxide-coated sand) combination and in columns by the sampling times (in terms of days of saturation).

Mean Porewater Mn Concentration (mg L^{-1})

	0	1	2	4	7	14	21	28	42	56	Max
C00	0.09	0.33	2.35	7.70	15.95	22.16	23.72	20.29	22.02	17.60	23.72
C05	0.39	0.91	6.64	32.98	50.46	57.99	74.90	43.08	50.76	36.43	74.90
C15	0.85	1.44	8.44	45.85	46.12	32.54	41.63	36.08	41.80	38.35	46.12
C30	0.31	0.86	4.61	33.16	50.66	24.30	17.52	17.06	22.62	27.22	50.66
D00	0.13	1.36	1.29	7.34	11.00	16.37	17.15	14.73	14.51	10.94	17.15
D05	1.61	4.49	8.09	38.57	88.23	135.01	160.19	104.77	121.96	83.27	160.19
D15	0.90	7.20	12.68	69.52	150.45	190.62	185.51	171.13	168.56	134.55	190.62
D30	1.09	6.20	12.88	53.05	142.82	101.07	80.86	53.94	79.91	88.89	142.82
G00	0.09	0.54	6.16	18.83	58.88	83.41	117.86	74.28	114.15	74.38	117.86
G05	0.16	1.40	10.14	44.83	81.68	106.28	134.79	71.21	68.65	66.14	134.79
G15	0.57	2.18	7.56	65.33	112.84	92.29	89.74	62.84	77.21	50.07	112.84
G30	0.29	2.01	12.53	80.33	113.73	56.63	44.15	32.46	58.95	42.03	113.73

Mean Porewater Fe Concentration (mg L^{-1})

	0	1	2	4	7	14	21	28	42	56	Max
C00	0.72	0.31	0.12	0.65	7.42	31.09	44.56	36.61	44.35	39.10	44.56
C05	0.34	0.10	0.06	0.14	0.68	9.52	27.24	23.53	29.31	31.04	31.04
C15	0.27	0.04	0.06	0.09	0.15	0.68	6.20	5.87	9.19	17.22	17.22
C30	0.13	0.02	0.05	0.07	0.12	0.16	0.70	2.19	2.62	6.65	6.65
D00	0.22	0.28	0.38	6.03	20.40	47.59	64.88	63.65	72.46	55.65	72.46
D05	0.34	0.36	0.32	0.45	1.81	24.25	44.20	40.63	49.60	48.83	49.60
D15	0.14	0.26	0.24	0.24	0.29	2.07	7.98	14.99	19.11	23.17	23.17
D30	0.08	0.15	0.15	0.20	0.16	0.27	0.74	0.51	1.28	3.65	3.65
G00	0.29	0.18	0.14	0.27	2.27	23.79	45.17	39.74	66.17	54.31	66.17
G05	0.24	0.10	0.16	0.32	1.36	16.26	29.24	27.33	23.14	42.16	42.16
G15	0.18	0.22	0.15	0.22	0.46	3.82	12.93	15.71	23.29	25.03	25.03
G30	0.20	0.00	0.07	0.27	0.19	0.55	2.77	1.90	7.16	8.80	8.80

Appendix I. Results of pH study

To elucidate the results of the Mn addition microcosm experiment (Chapter 4), a follow up microcosm study is being conducted to record the change in pH over time. The microcosms (same soil-treatment combinations used in Chapter 4) are saturating for a total of 56 days. Microcosms will be destructive sampled on days 0, 14, 28, and 56. So far, days 0, 14, and 28 have been sampled as shown below. The pH of the extracted porewater (not acidified with 1 M HCl) and of a 1:1 soil-water slurry was measured. Due to supply limitations, there was only one replicate for soil-treatment combination for each sampling date (total of 48 microcosms).

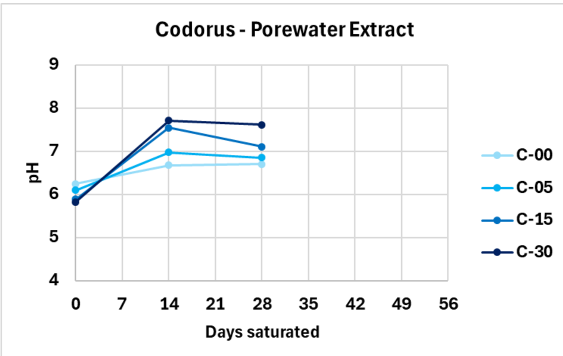

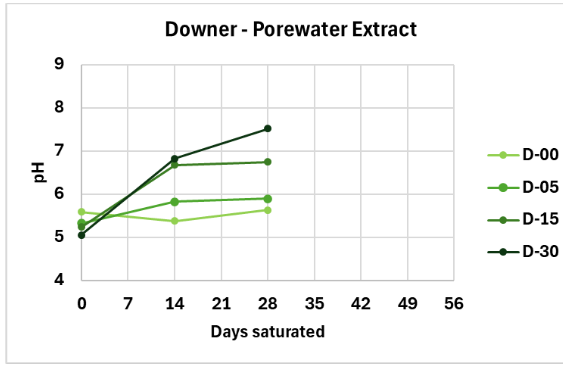

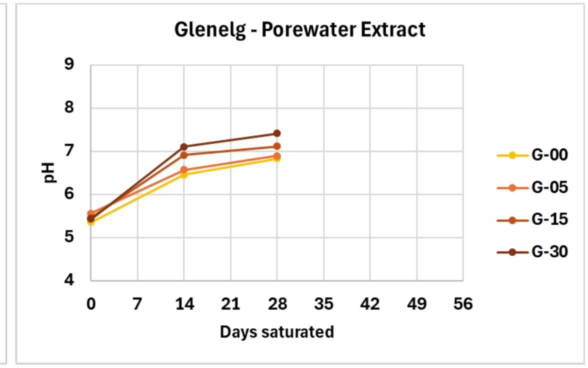

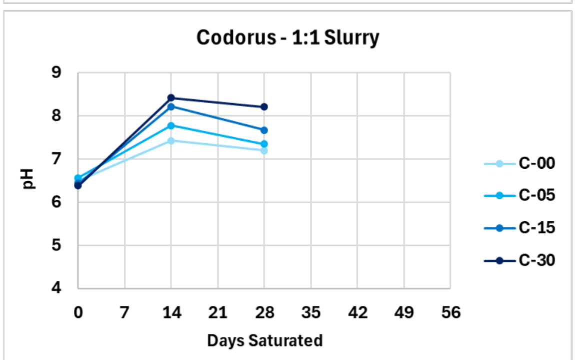

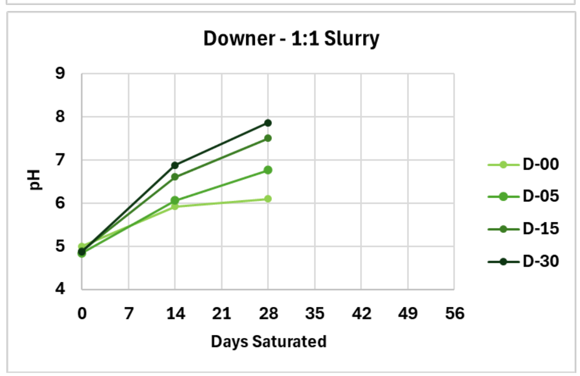

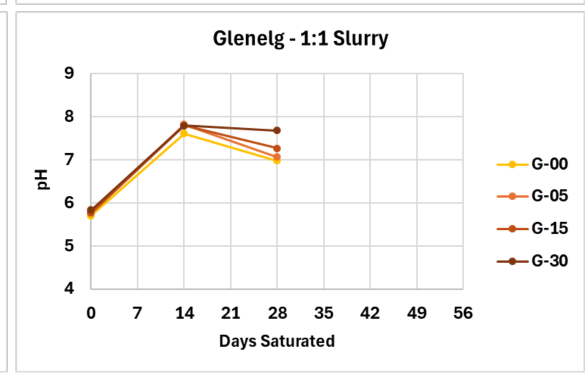

Appendix J. Chapter 4 porewater Fe concentrations

Concentration of Fe (mg L^{-1}) in extracted porewater throughout the study period (56 days) for each soil. Treatment levels (0, 5, 15, and 30 g of Mn oxide-coated sands) shown in each graph.

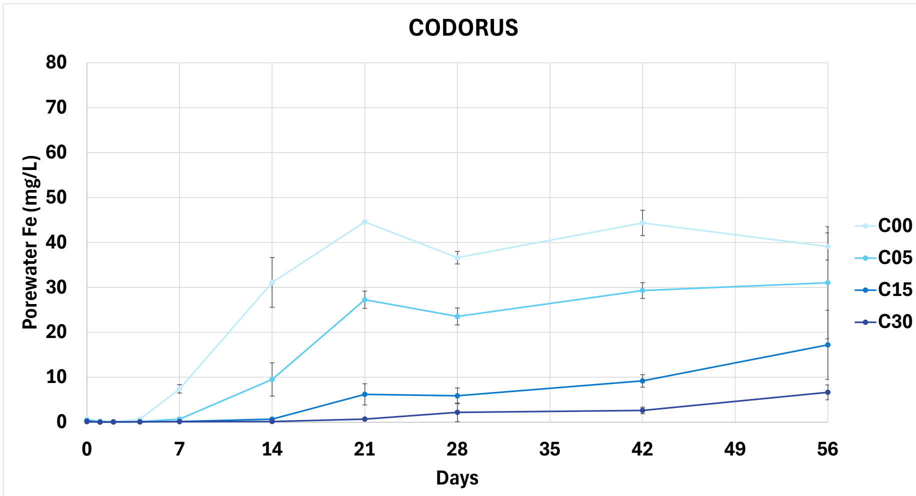

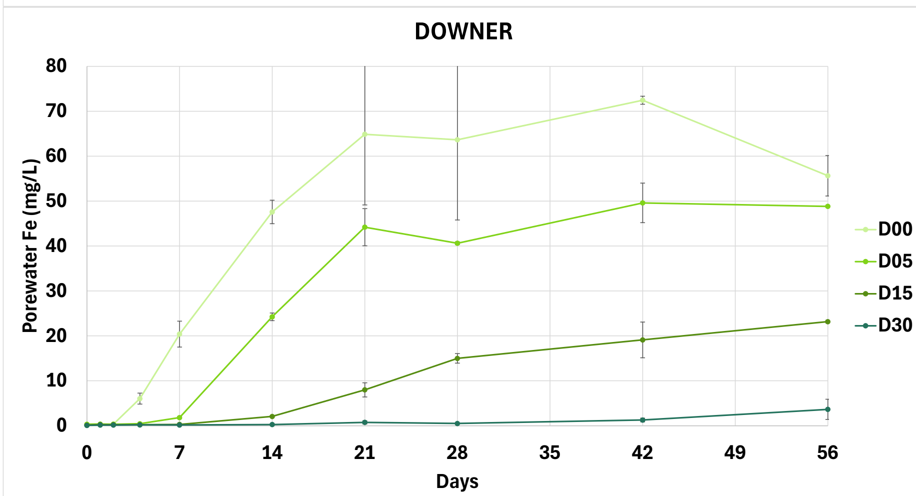

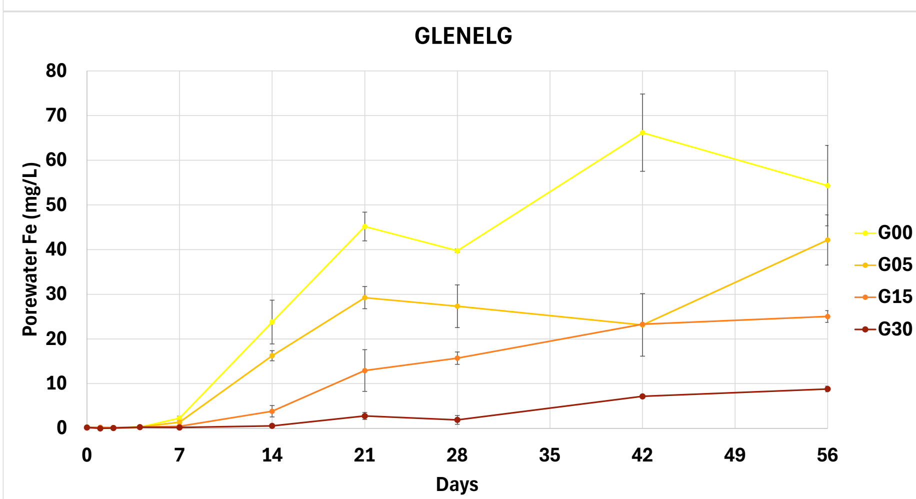

Bibliography

Anderson, C. G., Goebel, G. M., Tfaily, M. M., Fox, P. M., Nico, P. S., Fendorf, S., & Keiluweit, M. (2023). Molecular Nature of Mineral-Organic Associations within Redox-Active Mountainous Floodplain Sediments. *ACS Earth and Space Chemistry*, *7*(9), 1623–1634. https://doi.org/10.1021/acsearthspacechem.3c00037

Berkowitz, J. F., VanZomeren, C. M., Currie, S. J., & Vasilas, L. (2017). Application of α,α’-dipyridyl dye for hydric soil identification. *Soil Science Society of America Journal*, *81*(3), 654–658. https://doi.org/10.2136/sssaj2016.12.0431

Berkowitz, J. F., Vepraskas, M. J., Vaughan, K. L., & Vasilas, L. M. (2021). Development and application of the Hydric Soil Technical Standard. *Soil Science Society of America Journal*, *85*(3), 469–487. https://doi.org/10.1002/saj2.20202

Bigham, J. M., Fitzpatrick, R. W., & Schulze, D. G. (2002). Iron Oxides. In J. B. Dixon & D. G. Schulze (Eds.), *SSSA Book Series* (pp. 323–366). Soil Science Society of America. https://doi.org/10.2136/sssabookser7.c10

Bolan, N. S., Adriano, D. C., Kunhikrishnan, A., James, T., McDowell, R., & Senesi, N. (2011). Dissolved Organic Matter: Biogeochemistry, Dynamics, and Environmental Significance in Soils. In D. L. Sparks (Ed.), *Advances in Agronomy* (Vol. 110, pp. 1–75). Academic Press. https://doi.org/10.1016/B978-0-12-385531-2.00001-3

Burdt, A. C., Galbraith, J. M., & Daniels, W. L. (2005). Season Length Indicators and Land-Use Effects in Southeast Virginia Wet Flats. *Soil Science Society of America Journal*, *69*(5), 1551–1558. https://doi.org/10.2136/sssaj2004.0124

Campbell, E., Marks, R., & Conn, C. (2018). *Accounting for Maryland’s Ecosystem Services: Integrating the value of nature into decision making Accounting for Maryland’s Ecosystem Services*. State of Maryland. http://rgdoi.net/10.13140/RG.2.2.13136.97286

Castenson, K. L., & Rabenhorst, M. C. (2006). Indicator of Reduction in Soil (IRIS). *Soil Science Society of America Journal*, *70*(4), 1222–1226. https://doi.org/10.2136/sssaj2005.0130

Chandrangsu, P., Rensing, C., & Helmann, J. D. (2017). Metal homeostasis and resistance in bacteria. *Nature Reviews Microbiology*, *15*(6), 338–350. https://doi.org/10.1038/nrmicro.2017.15

Changes in Hydric Soils of the United States, 59 Federal Register (1994). https://www.federalregister.gov/d/94-16835

Chubar, N., Visser, T., Avramut, C., & De Waard, H. (2013). Sorption and precipitation of Mn2+ by viable and autoclaved Shewanella putrefaciens: Effect of contact time. *Geochimica et Cosmochimica Acta*, *100*, 232–250. https://doi.org/10.1016/j.gca.2012.09.051

Coffin, C. A. (2012). *Indicators of Reduction in Soils (IRIS) in Various Conditions of Saturation in South Florida Marl* [Master's Thesis, University of Flordia]. University of Florida Digital Collections. https://ufdc.ufl.edu/UFE0044806/00001/pdf

Cogger, C. G., & Kennedy, P. E. (1992). Seasonally Saturated Soils in the Puget Lowland I. Saturation, Reduction, and Color Patterns. *Soil Science*, *153*(6), 421–433. https://doi.org/10.1097/00010694-199206000-00001

Conant, R. T., Ryan, M. G., Ågren, G. I., Birge, H. E., Davidson, E. A., Eliasson, P. E., Evans, S. E., Frey, S. D., Giardina, C. P., Hopkins, F. M., Hyvönen, R., Kirschbaum, M. U. F., Lavallee, J. M., Leifeld, J., Parton, W. J., Megan Steinweg, J., Wallenstein, M. D., Martin Wetterstedt, J. Å., & Bradford, M. A. (2011). Temperature and soil organic matter decomposition rates—Synthesis of current knowledge and a way forward. *Global Change Biology*, *17*(11), 3392–3404. https://doi.org/10.1111/j.1365-2486.2011.02496.x

Dahl, T. E., & Allord, G. J. (1996). History of Wetlands in the Conterminous United States. In *National Water Summary on Wetland Resources* (Vol. 19, p. 8). U.S. Government Printing Office. https://www.fws.gov/wetlands/documents/History-of-Wetlands-in-the-Conterminous-United-States.pdf

Davidson, E. A., & Janssens, I. A. (2006). Temperature sensitivity of soil carbon decomposition and feedbacks to climate change. *Nature*, *440*(7081), 165–173. https://doi.org/10.1038/nature04514

Davidson, N. C., van Dam, A. A., Finlayson, C. M., & McInnes, R. J. (2019). Worth of wetlands: Revised global monetary values of coastal and inland wetland ecosystem services. *Marine and Freshwater Research*, *70*(8), 1189. https://doi.org/10.1071/MF18391

Dixon, J. B., & White, G. N. (2002). Manganese Oxides. In J. B. Dixon & D. G. Schulze (Eds.), *Soil Mineralogy with Environmental Applications* (pp. 367–388). Soil Science Society of America. https://doi.org/10.2136/sssabookser7.c11

Dorau, K., Eickmeier, M., & Mansfeldt, T. (2016). Comparison of Manganese and Iron Oxide-Coated Redox Bars for Characterization of the Redox Status in Wetland Soils. *Wetlands*, *36*(1), 133–141. https://doi.org/10.1007/s13157-015-0724-5

Dorau, K., & Mansfeldt, T. (2015). Manganese-Oxide-Coated Redox Bars as an Indicator of Reducing Conditions in Soils. *Journal of Environmental Quality*, *44*(2), 696–703. https://doi.org/10.2134/jeq2014.03.0140

Dorau, K., & Mansfeldt, T. (2016). Manganese and iron oxide-coated redox bars as a tool to in situ study the element sorption in wet soils. *Journal of Soils and Sediments*, *16*(3), 976–986. https://doi.org/10.1007/s11368-015-1300-6

Dorau, K., Papenfuß, S., & Mansfeldt, T. (2018). Temperature-dependent oxide removal from manganese- and iron oxide-coated soil redox bars. *Journal of Soils and Sediments*, *18*(3), 680–687. https://doi.org/10.1007/s11368-017-1812-3

Dorau, K., Zanger, T., Bolten, A., & Mansfeldt, T. (2024). Soil redox maps: Assessment of small field-scale redox zonation by Mn and Fe oxide-coated IRIS films. *Journal of Soils and Sediments*, *24*(3), 1206–1219. https://doi.org/10.1007/s11368-023-03705-6

Duball, C., Vaughan, K., Berkowitz, J. F., Rabenhorst, M. C., & VanZomeren, C. M. (2020). Iron monosulfide identification: Field techniques to provide evidence of reducing conditions in soils. *Soil Science Society of America Journal*, *84*(2), 303–313. https://doi.org/10.1002/saj2.20044

Ehlert, K., Mikutta, C., & Kretzschmar, R. (2014). Impact of Birnessite on Arsenic and Iron Speciation during Microbial Reduction of Arsenic-Bearing Ferrihydrite. *Environmental Science & Technology*, *48*(19), 11320–11329. https://doi.org/10.1021/es5031323

Ehlert, K., Mikutta, C., & Kretzschmar, R. (2016). Effects of Manganese Oxide on Arsenic Reduction and Leaching from Contaminated Floodplain Soil. *Environmental Science & Technology*, *50*(17), 9251–9261. https://doi.org/10.1021/acs.est.6b01767

Ehrlich, H. L., Newman, D. K., & Kappler, A. (2016). *Ehrlich's geomicrobiology* (Sixth edition). CRC Press, Taylor & Francis Group.

Essington, M. E. (2015). *Soil and Water Chemistry: An Integrative Approach, Second Edition*. CRC Press.

Ettler, V., Knytl, V., Komárek, M., Puppa, L. D., Bordas, F., Mihaljevič, M., Klementová, M., & Šebek, O. (2014). Stability of a novel synthetic amorphous manganese oxide in contrasting soils. *Geoderma*, *214–215*, 2–9. https://doi.org/10.1016/j.geoderma.2013.10.011

Evans, A. E., Limmer, M. A., & Seyfferth, A. L. (2021). Indicator of redox in soil (IRIS) films as a water management tool for rice farmers. *Journal of Environmental Management*, *294*, 112920. https://doi.org/10.1016/j.jenvman.2021.112920

Fiola, J. C., Rabenhorst, M. C., Scaduto, E., Seitz, C. R., & Rankin, K. M. S. (2020). Soil biogeochemistry of the capillary fringe in laboratory mesocosms with contrasting soil textures. *Soil Science Society of America Journal*, *84*(3), 1011–1021. https://doi.org/10.1002/saj2.20076

Fluet-Chouinard, E., Stocker, B. D., Zhang, Z., Malhotra, A., Melton, J. R., Poulter, B., Kaplan, J. O., Goldewijk, K. K., Siebert, S., Minayeva, T., Hugelius, G., Joosten, H., Barthelmes, A., Prigent, C., Aires, F., Hoyt, A. M., Davidson, N., Finlayson, C. M., Lehner, B., … McIntyre, P. B. (2023). Extensive global wetland loss over the past three centuries. *Nature*, *614*(7947), Article 7947. https://doi.org/10.1038/s41586-022-05572-6

Glinski, J., Stahr, K., Stepniewska, Z., & Brzezinska, M. (1996). Changes of redox and pH conditions in a flooded soil amended with glucose and manganese oxide or iron oxide under laboratory conditions. *Zeitschrift Für Pflanzenernährung Und Bodenkunde*, *159*(3), 297–304. https://doi.org/10.1002/jpln.1996.3581590311

Gotoh, S., & Patrick, W. H. (1972). Transformation of Manganese in a Waterlogged Soil as Affected by Redox Potential and pH. *Soil Science Society of America Journal*, *36*(5), 738–742. https://doi.org/10.2136/sssaj1972.03615995003600050018x

Gotoh, S., & Patrick, W. H. (1974). Transformation of Iron in a Waterlogged Soil as Influenced by Redox Potential and pH. *Soil Science Society of America Journal*, *38*(1), 66–71. https://doi.org/10.2136/sssaj1974.03615995003800010024x

Guo, Z., Wang, Y., Wan, Z., Zuo, Y., He, L., Li, D., Yuan, F., Wang, N., Liu, J., Song, Y., Song, C., & Xu, X. (2020). Soil dissolved organic carbon in terrestrial ecosystems: Global budget, spatial distribution and controls. *Global Ecology and Biogeography*, *29*(12), 2159–2175. https://doi.org/10.1111/geb.13186

Hammann, R., & Ottow, J. (1974). Reductive Dissolution of Fe2O3 by Saccharolytic Clostridia and Bacillus polymyxa under anaerobic Conditions. *Journal of Plant Nutrition and Soil Science*, *137*(2), 108–115. https://doi.org/10.1002/jpln.19741370205

Hansel, C. M. (2017). Manganese in Marine Microbiology. In R. K. Poole (Ed.), *Advances in Microbial Physiology* (Vol. 70, pp. 37–83). Academic Press. https://doi.org/10.1016/bs.ampbs.2017.01.005

Haynes, R. J. (2005). Labile Organic Matter Fractions as Central Components of the Quality of Agricultural Soils: An Overview. In *Advances in Agronomy* (Vol. 85, pp. 221–268). Elsevier. https://doi.org/10.1016/S0065-2113(04)85005-3

Heimlich, R. E., Wiebe, K. D., Claassen, R., Gadsby, D., & House, R. M. (1998). Federal Wetland Policies and National Trends. In *Wetlands and agriculture: Private interests and public benefits*. US Department of Agriculture, Economic Research Service.

Herndon, E. M., Jin, L., Andrews, D. M., Eissenstat, D. M., & Brantley, S. L. (2015). Importance of vegetation for manganese cycling in temperate forested watersheds. *Global Biogeochemical Cycles*, *29*(2), 160–174. https://doi.org/10.1002/2014GB004858

Hino, K. C., Romero, J., Loffredo, J. L., Stolt, M., Amador, J., Moseman-Valtierra, S., Wigand, C., & Pellock, B. J. (2023). Birnessite films are sensitive indicators of microbial manganese reduction in soil. *Soil Science Society of America Journal*, *87*(1), 196–201. https://doi.org/10.1002/saj2.20468

Hofacker, A. F., Voegelin, A., Kaegi, R., Weber, F.-A., & Kretzschmar, R. (2013). Temperature-dependent formation of metallic copper and metal sulfide nanoparticles during flooding of a contaminated soil. *Geochimica et Cosmochimica Acta*, *103*, 316–332. https://doi.org/10.1016/j.gca.2012.10.053

Holmgren, G. G. S., Juve, R. L., & Geschwender, R. C. (1977). A Mechanically Controlled Variable Rate Leaching Device. *Soil Science Society of America Journal*, *41*(6), 1207–1208. https://doi.org/10.2136/sssaj1977.03615995004100060041x

Hyacinthe, C., Bonneville, S., & Van Cappellen, P. (2008). Effect of Sorbed Fe(II) on the Initial Reduction Kinetics of 6-Line Ferrihydrite and Amorphous Ferric Phosphate by Shewanella putrefaciens. *Geomicrobiology Journal*, *25*(3–4), 181–192. https://doi.org/10.1080/01490450802081911

Hychka, K. C., Brooks, R. P., & Cole, C. A. (2013). Hydrology of Mid-Atlantic Freshwater Wetlands. In R. P. Brooks & D. H. Wardrop (Eds.), *Mid-Atlantic Freshwater Wetlands: Advances in Wetlands Science, Management, Policy, and Practice* (pp. 109–127). Springer New York. https://doi.org/10.1007/978-1-4614-5596-7_4

Jenkinson, B. (2002). *Indicators of Reduction in Soils (IRIS): A visual method for the identification of hydric soils* [Doctoral Dissertation]. Purdue University.

Jenkinson, B. J., & Franzmeier, D. P. (2006). Development and Evaluation of Iron-Coated Tubes that Indicate Reduction in Soils. *Soil Science Society of America Journal*, *70*(1), 183–191. https://doi.org/10.2136/sssaj2004.0323

Kappler, A., Bryce, C., Mansor, M., Lueder, U., Byrne, J. M., & Swanner, E. D. (2021). An evolving view on biogeochemical cycling of iron. *Nature Reviews Microbiology*, *19*(6), 360–374. https://doi.org/10.1038/s41579-020-00502-7

King, M., Vaughan, K. L., Clause, K., & Mattke, D. (2019). Limitations to Redoximorphic Feature Development in Highly Calcareous Hydric Soils. *Soil Science Society of America Journal*, *83*(5), 1585–1594. https://doi.org/10.2136/sssaj2019.04.0108

Kirschbaum, M. U. F. (1995). The temperature dependence of soil organic matter decomposition, and the effect of global warming on soil organic C storage. *Soil Biology and Biochemistry*, *27*(6), 753–760. https://doi.org/10.1016/0038-0717(94)00242-S

Li, H., Santos, F., Butler, K., & Herndon, E. (2021). A Critical Review on the Multiple Roles of Manganese in Stabilizing and Destabilizing Soil Organic Matter. *Environmental Science & Technology*, *55*(18), 12136–12152. https://doi.org/10.1021/acs.est.1c00299

Limmer, M. A., Linam, F. A., Evans, A. E., & Seyfferth, A. L. (2023). Unraveling the Mechanisms of Fe Oxidation and Mn Reduction on Mn Indicators of Reduction in Soil (IRIS) Films. *Environmental Science & Technology*, *57*(16), 6530–6539. https://doi.org/10.1021/acs.est.3c00161

Loffredo, J. A., Rabenhorst, M. C., Stolt, M. H., & Amador, J. A. (2023). Potential interference of organic acids and ferrous iron in the interpretation of Fe and Mn indicators of reduction in soil. *Soil Science Society of America Journal*, *87*(5), 1165–1173. https://doi.org/10.1002/saj2.20560

Lovley, D. R. (1991). Dissimilatory Fe(III) and Mn(IV) reduction. *Microbiological Reviews*, 259–287. https://doi.org/10.1128/mr.55.2.259-287.1991

Lovley, D. R., Holmes, D. E., & Nevin, K. P. (2004). Dissimilatory Fe(III) and Mn(IV) Reduction. *Advances in Microbial Physiology*, *49*, 219–286. https://doi.org/10.1016/S0065-2911(04)49005-5

Lovley, D. R., & Phillips, E. J. P. (1988). Manganese inhibition of microbial iron reduction in anaerobic sediments. *Geomicrobiology Journal*, *6*(3–4), 145–155. https://doi.org/10.1080/01490458809377834

Mack, S. C., Rabenhorst, M. C., & Berkowitz, J. F. (2019). Understanding the Inhibition of Color Change in Problematic Red Parent Material Hydric Soils. *Soil Science Society of America Journal*, *83*, 838–847. https://doi.org/10.2136/sssaj2018.10.0390

Magen, C., Mucci, A., & Sundby, B. (2011). Reduction Rates of Sedimentary Mn and Fe Oxides: An Incubation Experiment with Arctic Ocean Sediments. *Aquatic Geochemistry*, *17*(4), 629–643. https://doi.org/10.1007/s10498-010-9117-9

Marschner, B., & Kalbitz, K. (2003). Controls of bioavailability and biodegradability of dissolved organic matter in soils. *Geoderma*, *113*(3–4), 211–235. https://doi.org/10.1016/S0016-7061(02)00362-2

McBride, M. B. (1994). *Environmental chemistry of soils*. Oxford University Press.

Megonigal, J. P., Faulkner, S. P., & Patrick, W. H. (1996). The Microbial Activity Season in Southeastern Hydric Soils. *Soil Science Society of America Journal*, *60*(4), 1263–1266. https://doi.org/10.2136/sssaj1996.03615995006000040043x

Meyer, N., Welp, G., & Amelung, W. (2018). The Temperature Sensitivity (Q10) of Soil Respiration: Controlling Factors and Spatial Prediction at Regional Scale Based on Environmental Soil Classes. *Global Biogeochemical Cycles*, *32*(2), 306–323. https://doi.org/10.1002/2017GB005644

Mitsch, W. J., & Gosselink, J. G. (2015). *Wetlands* (Fifth edition). John Wiley and Sons, Inc.

Musser, K. (Kmusser), & Pierce, E. (wapcaplet). (2012). *Map of USA MD.svg* [Digital]. Wikipedia Commons. https://commons.wikimedia.org/wiki/File:Map_of_USA_MD.svg

National Research Council. (1995). *Wetlands: Characteristics and Boundaries* (p. 4766). National Academies Press. https://doi.org/10.17226/4766

Nelson, D. W., & Sommers, L. E. (1996). Total Carbon, Organic Carbon, and Organic Matter. In *Methods of Soil Analysis* (pp. 961–1010). John Wiley & Sons, Ltd. https://doi.org/10.2136/sssabookser5.3.c34

Patrick, W. H. (1961). Nitrate reduction rates in a submerged soil as affected by redox potential. In *Transactions of 7th International Congress of Soil Science: Madison, Wiconsin, 1960* (Vol. 2, pp. 494–500). Elsevier or International Society of Soil Science.

Patrick, W. H. (1966). Apparatus for controlling the Oxidation-reduction Potential of Waterlogged Soils. *Nature*, *212*(5067), 1278–1279. https://doi.org/10.1038/2121278a0

Patrick, W. H., & Jugsujinda, A. (1992). Sequential Reduction and Oxidation of Inorganic Nitrogen, Manganese, and Iron in Flooded Soil. *Soil Science Society of America Journal*, *56*(4), 1071–1073. https://doi.org/10.2136/sssaj1992.03615995005600040011x

Patrick, Wm. H., & Turner, F. T. (1968). Effect of Redox Potential on Manganese Transformation in Waterlogged Soil. *Nature*, *220*(5166), 476–478. https://doi.org/10.1038/220476a0

Ponnamperuma, F. N. (1972). The Chemistry of Submerged Soils. In *Advances in Agronomy* (Vol. 24, pp. 29–96). Elsevier. https://doi.org/10.1016/S0065-2113(08)60633-1

Ponnamperuma, F. N. (1984). Effects of flooding on soils. In *Flooding and plant growth* (pp. 9–45). Academic Press.

Ponnamperuma, F. N., Loy, T. A., & Tianco, E. M. (1969). Redox equilibria in flooded soils: II. the manganese oxide systems. *Soil Science*, *108*(1), 48–57.

Ponnamperuma, F. N., Yuan, W. L., & Nhung, M. T. M. (1965). Manganese Dioxide as a Remedy for a Physiological Disease of Rice associated with Reduction of the Soil. *Nature*, *207*(5001), 1103–1104. https://doi.org/10.1038/2071103a0

Post, J. E. (1999). Manganese oxide minerals: Crystal structures and economic and environmental significance. *Proceedings of the National Academy of Sciences*, *96*(7), 3447–3454. https://doi.org/10.1073/pnas.96.7.3447

Rabenhorst, M., Buchanan, A., Morozov, E., Shay, J., & Mack, S. (2020). Field test for identifying problematic red parent materials. *Soil Science Society of America Journal*, *84*(3), 1006–1010. https://doi.org/10.1002/saj2.20066

Rabenhorst, M. C. (2005). Biologic zero: A soil temperature concept. *Wetlands*, *25*(3), 616–621. https://doi.org/10.1672/0277-5212(2005)025[0616:BZASTC]2.0.CO;2

Rabenhorst, M. C. (2008). Protocol for Using and Interpreting IRIS Tubes. *Soil Survey Horizons*, *49*(3), 74–77. https://doi.org/10.2136/sh2008.3.0074

Rabenhorst, M. c. (2013). Using Synthesized Iron Oxides as an Indicator of Reduction in Soils. In *Methods in Biogeochemistry of Wetlands* (pp. 723–740). John Wiley & Sons, Ltd. https://doi.org/10.2136/sssabookser10.c37

Rabenhorst, M. C. (2018). A System for Making and Deploying Oxide-Coated Plastic Films for Environmental Assessment of Soils. *Soil Science Society of America Journal*, *82*, 1301–1307. https://doi.org/10.2136/sssaj2018.05.0178

Rabenhorst, M. C., & Burch, S. N. (2006). Synthetic Iron Oxides as an Indicator of Reduction in Soils (IRIS). *Soil Science Society of America Journal*, *70*(4), 1227–1236. https://doi.org/10.2136/sssaj2005.0354

Rabenhorst, M. C., & Castenson, K. L. (2005). TEMPERATURE EFFECTS ON IRON REDUCTION IN A HYDRIC SOIL. *Soil Science*, *170*(9), 734–742. https://doi.org/10.1097/01.ss.0000185908.26083.53

Rabenhorst, M. C., Drohan, P. J., Galbraith, J. M., Moorberg, C., Spokas, L., Stolt, M. H., Thompson, J. A., Turk, J., Vasilas, B. L., & Vaughan, K. L. (2021). Manganese-coated IRIS to document reducing soil conditions. *Soil Science Society of America Journal*, *85*(6), 2201–2209. https://doi.org/10.1002/saj2.20301

Rabenhorst, M. C., Hively, W. D., & James, B. R. (2009). Measurements of Soil Redox Potential. *Soil Science Society of America Journal*, *73*(2), 668–674. https://doi.org/10.2136/sssaj2007.0443

Rabenhorst, M. C., Megonigal, J. P., & Keller, J. (2010). Synthetic Iron Oxides for Documenting Sulfide in Marsh Pore Water. *Soil Science Society of America Journal*, *74*(4), 1383–1388. https://doi.org/10.2136/sssaj2009.0435

Rabenhorst, M. C., Ming, D. W., Morris, R. V., & Golden, D. C. (2008). Synthesized iron oxides used as a tool for documenting reducing conditions in soils. *Soil Science*, *173*(6), 417–423. https://doi.org/10.1097/SS.0b013e31817751b17

Rabenhorst, M. C., & Persing, K. A. (2017). A Synthesized Manganese Oxide for Easily Making Durable Manganese-Coated IRIS Tubes. *Soil Science Society of America Journal*, *81*(1), 233–239. https://doi.org/10.2136/sssaj2016.10.0348n

Rabenhorst, M. C., & Wardrup, J. L. (2024). Advances in making Mn oxide-coated sands. *Soil Science Society of America Journal*, *88*(3), 921–929. https://doi.org/10.1002/saj2.20649

Rabenhorst, M. C., Wyss-Gallifent, J., Kim, J. D., Park, C. E., & Wessel, B. M. (2025). Advances in technology for using Indicator of Reduction in Soils (IRIS) to quantify porewater sulfide levels in the coastal zone. *Soil Science Society of America Journal*, *89*(2), e70035. https://doi.org/10.1002/saj2.70035

Reddy, K. R., DeLaune, R. D., & Inglett, P. W. (2022). *Biogeochemistry of Wetlands: Science and Applications* (2nd ed.). CRC Press. https://doi.org/10.1201/9780429155833

Richardson, C. J., Bruland, G. L., Hanchey, M. F., & Sutton-Grier, A. E. (2016). Soil Restoration: The Foundation of Successful Wetland Reestablishment. In M. J. Vepraskas & C. B. Craft (Eds.), *Wetland Soils* (0 ed., pp. 484–509). CRC Press. https://doi.org/10.1201/b18996-26

Roden, E. E., & Urrutia, M. M. (1999). Ferrous Iron Removal Promotes Microbial Reduction of Crystalline Iron(III) Oxides. *Environmental Science & Technology*, *33*(11), 1847–1853. https://doi.org/10.1021/es9809859

Roden, E. E., & Urrutia, M. M. (2002). Influence of Biogenic Fe(II) on Bacterial Crystalline Fe(III) Oxide Reduction. *Geomicrobiology Journal*, *19*(2), 209–251. https://doi.org/10.1080/01490450252864280

Roden, E. E., & Wetzel, R. G. (2002). Kinetics of microbial Fe(III) oxide reduction in freshwater wetland sediments. *Limnology and Oceanography*, *47*(1), 198–211. https://doi.org/10.4319/lo.2002.47.1.0198

Romero, J., Hino, K., Loffredo, J., Stolt, M., Moseman-Valtierra, S., Amador, J., & Pellock, B. (2021). Abiotic soil properties affecting interpretation of IRIS sensors in tidal and freshwater soils. *Soil Science Society of America Journal*, *85*(6), 2234–2239. https://doi.org/10.1002/saj2.20293

Sapkota, Y., Duball, C., Vaughan, K., Rabenhorst, M. C., & Berkowitz, J. F. (2022). Indicator of Reduction in Soil (IRIS) devices: A review. *Science of The Total Environment*, *852*, 158419. https://doi.org/10.1016/j.scitotenv.2022.158419

Schwertmann, U. (1993). Relations Between Iron Oxides, Soil Color, and Soil Formation. In *Soil Color* (pp. 51–69). John Wiley & Sons, Ltd. https://doi.org/10.2136/sssaspecpub31.c4

Scott, B., Baldwin, A. H., Ballantine, K., Palmer, M., & Yarwood, S. (2020). The role of organic amendments in wetland restorations. *Restoration Ecology*, *28*(4), 776–784. https://doi.org/10.1111/rec.13179

Seybold, C. A., Mersie, W., Huang, J., & McNamee, C. (2002). Soil redox, pH, temperature, and water-table patterns of a freshwater tidal wetland. *Wetlands*, *22*(1), 149–158. https://doi.org/10.1672/0277-5212(2002)022[0149:SRPTAW]2.0.CO;2

Soil Survey Staff. (2022). *Kellogg Soil Survey Laboratory Methods Manual* (Soil Survey Investigations Report Nos. 42, Version 6.0). U.S. Department of Agriculture, Natural Resources Conservation Service. https://www.nrcs.usda.gov/sites/default/files/2023-01/SSIR42.pdf

Sokolova, T. A. (2020). Low-Molecular-Weight Organic Acids in Soils: Sources, Composition, Concentrations, and Functions: A Review. *Eurasian Soil Science*, *53*(5), 580–594. https://doi.org/10.1134/S1064229320050154

Sparks, D. L., Singh, B., & Siebecker, M. G. (2022). *Environmental Soil Chemistry* (Third). Elsevier.

Sparrow, L., & Uren, N. (2014). Manganese oxidation and reduction in soils: Effects of temperature, water potential, pH and their interactions. *Soil Research*, *52*, 483. https://doi.org/10.1071/SR13159

Sprecher, S. W., & Warne, A. G. (2000). *Accessing and Using Meteorological Data to Evaluate Wetland Hydrology:* Defense Technical Information Center. https://doi.org/10.21236/ADA378910

Stiles, C. A., Dunkinson, E. T., Ping, C.-L., & Kidd, J. (2010). Initial Field Installation of Manganese Indicators of Reduction in Soils, Brooks Range, Alaska. *Soil Horizons*, *51*(4), 102. https://doi.org/10.2136/sh2010.4.0102

Straathof, A. L., Chincarini, R., Comans, R. N. J., & Hoffland, E. (2014). Dynamics of soil dissolved organic carbon pools reveal both hydrophobic and hydrophilic compounds sustain microbial respiration. *Soil Biology and Biochemistry*, *79*, 109–116. https://doi.org/10.1016/j.soilbio.2014.09.004

Sumner, J. P., Vepraskas, M. J., & Kolka, R. K. (2009). Methods to evaluate normal rainfall for short-term wetland hydrology assessment. *Wetlands*, *29*(3), 1049–1062. https://doi.org/10.1672/09-026D.1

Takeno, N. (2005). *Atlas of Eh_pH Diagrams: Intercomparison of Thermodynamic Databases.* (Geological Survey of Japan Open File Report No. 419). National Institute of Advance Industrial Science and Technology, Research Center for Deep Geological Environments. https://www.nrc.gov/docs/ML1808/ML18089A638.pdf

US EPA, O. (2013, January 29). *The Origins of EPA* [Collections and Lists]. EPA History. https://www.epa.gov/history/origins-epa

USACE, & MDE. (2023, September 14). *Ecological Performance Standards and Monitoring Protocol for Nontidal Wetland Mitigation Sites in Maryland*. U.S. Army Corps of Engineers. https://www.nab.usace.army.mil/Portals/63/IRT%20NT%20WetlBuffer%20Mon%20Prot%2020230914.pdf

USDA-NRCS. (2024). *Field Indicators of Hydric Soils in the United States, Version 9.0*. USDA-NRCS. https://www.nrcs.usda.gov/sites/default/files/2024-09/Field-Indicators-of-Hydric-Soils.pdf

Van't Hoff, J. H. (1898). *Lectures on Theoretical and Physical Chemistry. Part 1. Chemical Dynamics.* Edward Arnold.

Vaughan, K. L., Miller, F., Navarro, N., & Appel, C. (2016). Visual Assessment of Sulfate Reduction to Identify Hydric Soils. *Soil Science Society of America Journal*, *80*(4), 1114–1119. https://doi.org/10.2136/sssaj2016.02.0035

Vaughan, K. L., Rabenhorst, M. C., & Needelman, B. A. (2009). Saturation and Temperature Effects on the Development of Reducing Conditions in Soils. *Soil Science Society of America Journal*, *73*(2), 663–667. https://doi.org/10.2136/sssaj2007.0346

Vázquez-Ortega, A., & Fein, J. B. (2017). Thermodynamic modeling of Mn(II) adsorption onto manganese oxidizing bacteria. *Chemical Geology*, *464*, 147–154. https://doi.org/10.1016/j.chemgeo.2016.12.040

Vepraskas, M. J. (2016). History of the concept of hydric soil. In *Wetland Soils: Genesis, Hydrology, Landscapes, and Classification. CRC Press Lewis Publishers, Boca Raton*.

Vepraskas, M. J., Polizzotto, M. L., & Faulkner, S. P. (2016). Redox Chemsitry of Hydric Soils. In *Wetland Soils: Genesis, Hydrology, Landscapes, and Classification. CRC Press Lewis Publishers, Boca Raton*.

Vepraskas, M. J., & Vaughan, K. L. (2016). Morphological Features of Hydric and Reduced Soils. In *Wetland Soils*.

Von Lützow, M., Kögel-Knabner, I., Ekschmitt, K., Flessa, H., Guggenberger, G., Matzner, E., & Marschner, B. (2007). SOM fractionation methods: Relevance to functional pools and to stabilization mechanisms. *Soil Biology and Biochemistry*, *39*(9), 2183–2207. https://doi.org/10.1016/j.soilbio.2007.03.007

Walbeck, D., Clearwater, D., & Neff, K. (2011, January). *Maryland Nontidal Wetland Mitigation Guidance*. Maryland Department of Environment. https://mde.maryland.gov/programs/water/WetlandsandWaterways/AboutWetlands/Documents/www.mde.state.md.us/assets/document/wetlandswaterways/MITGUIDEfeb72011.pdf

Waters, L. S. (2020). Bacterial manganese sensing and homeostasis. *Current Opinion in Chemical Biology*, *55*, 96–102. https://doi.org/10.1016/j.cbpa.2020.01.003

Weber, F.-A., Hofacker, A. F., Voegelin, A., & Kretzschmar, R. (2010). Temperature Dependence and Coupling of Iron and Arsenic Reduction and Release during Flooding of a Contaminated Soil. *Environmental Science & Technology*, *44*(1), 116–122. https://doi.org/10.1021/es902100h

Xu, J.-X., Li, X.-M., Sun, G.-X., Cui, L., Ding, L.-J., He, C., Li, L.-G., Shi, Q., Smets, B. F., & Zhu, Y.-G. (2019). Fate of Labile Organic Carbon in Paddy Soil Is Regulated by Microbial Ferric Iron Reduction. *Environmental Science & Technology*, *53*(15), 8533–8542. https://doi.org/10.1021/acs.est.9b01323

Ying, S. C., Kocar, B. D., Griffis, S. D., & Fendorf, S. (2011). Competitive Microbially and Mn Oxide Mediated Redox Processes Controlling Arsenic Speciation and Partitioning. *Environmental Science & Technology*, *45*(13), 5572–5579. https://doi.org/10.1021/es200351m

Yuan, W. L., & Ponnamperuma, F. N. (1966). Chemical Retardation of the Reduction of Flooded Soils and the Growth of Rice. *Plant and Soil*, *25*(3), 347–360.